Chair of Drilling and Completion Engineering

Master's Thesis

Scoring Well Construction Process and Impact on Well Integrity

Andreas Thomas Liegenfeld, BSc

August 2019

EIDESSTATTLICHE ERKLÄRUNG

Ich erkläre an Eides statt, dass ich diese Arbeit selbständig verfasst, andere als die angegebenen Quellen und Hilfsmittel nicht benutzt, und mich auch sonst keiner unerlaubten Hilfsmittel bedient habe.

Ich erkläre, dass ich die Richtlinien des Senats der Montanuniversität Leoben zu "Gute wissenschaftliche Praxis" gelesen, verstanden und befolgt habe.

Weiters erkläre ich, dass die elektronische und gedruckte Version der eingereichten wissenschaftlichen Abschlussarbeit formal und inhaltlich identisch sind.

Datum 01.09.2019

Unterschrift Verfasser/in
Andreas Thomas, Liegenfeld
Matrikelnummer: 01335189

Abstract

Maintaining the integrity of a well throughout its whole life cycle is very crucial in well construction and operation. Many risks are waiting along that chain of events to threaten the well's integrity. Recent studies and research have long tried to link well integrity events to constraints in the well operation phase, with emphasis on stresses and their limits in the cement sheath.

However, this thesis aims to have a closer look at the well construction process and how it might impact well integrity events. Through a simple performance assessment of the well construction process, a score between 0 and 100 is assigned to each casing/liner section to asses wellbore quality. Responses and parameters during drilling, final BHA pull, casing-running and cementing were used as input for the scoring process. The performance assessment output of the scorecard is precious in detecting shortcomings in the well construction process to help determine root causes of well integrity events. The scoring results of 29 casing/liner sections on 11 OMV Vienna Basin wells already indicate the tool's effectiveness in detecting problematic well sections. The lowest-scoring ones face incidents like failing casing pressure tests, proven lack of zonal isolation or cementing losses during cementing. Furthermore, the scorecard's ability to trouble-shoot problematic well sections has been proved with actual and expected/calculated casing pressure test bleed-off volumes. Gaining knowledge about the performance of the well construction process helps to enhance wellbore quality and avoid future well integrity events.

The proposed wellbore scorecard tool only covers and captures what is happening in the well construction process, but to study and understand well integrity along the whole life cycle of the well, a more holistic approach will be necessary. Therefore, a stress model is proposed to understand the impact of well operations on the cement sheath in terms of stresses and failure of the cement. Manufacturing a test cell according to the proposed design to verify the stress model is highly recommended.

This piece of work covers one essential part of the holistic approach to better understand well integrity events and aims towards a more environmental-friendly, safer and cost-effective way to operate hydrocarbon wells.

Zusammenfassung

Der Erhalt der Integrität eines Bohrlochs während seines gesamten Lebenszyklus ist ein entscheidender Faktor in der Konstruktion und im Betrieb von Bohrlöchern. Viele Risiken mit potenziell negativen Auswirkungen auf die Integrität können jederzeit auftreten. Studien in der Vergangenheit haben lange versucht Ursachen für Vorfälle, die zum Verlust der Integrität des Bohrlochs führen im Überschreiten der Spannungsgrenzen im Zementmantel während der Fluidproduktion und Injektion zu finden.

Dahingegen beschäftigt sich diese Arbeit mit dem Prozess zur Bohrlochkonstruktion und wie dieser negative Vorfälle, die zum Verlust der Bohrlochintegrität führen, beeinflussen kann. Durch eine einfache Leistungsbeurteilung des Prozesses der Bohrlochkonstruktion wird jeder Casing/Liner Sektion eine qualitative Bewertung des Bohrlochs auf einer Skala zwischen 0 und 100 zugewiesen. Hierzu wurden Reaktionen und Parameter aus dem Bohrprozess, dem Ziehen des letzten Bohrstranges, dem Einführen des Casings und des Zementationsprozess als Beitrag für die Bewertung herangezogen. Das Ergebnis der Leistungsbeurteilung des Bewertungstools hilft Mängel und Defizite im Prozess der Bohrlochkonstruktion zu ermitteln und so potenzielle Ursachen für den Verlust der Bohrlochintegrität zu finden. Es wurden insgesamt 29 Casing/Liner Sektionen in 11 OMV-Bohrungen aus dem Wiener Becken untersucht. Die Resultate zeigen bereits die Effektivität des Tools, problematische Bohrlochsektionen zu ermitteln. Sektionen mit der niedrigsten Bewertung weisen verschiedene Probleme wie gescheiterte Casing-Drucktests, Fehlen von Zonenabdichtung, oder Verluste beim Zementieren auf. Weiters wurde das Konzept des Bewertungstool problematische Sektionen zu finden mithilfe des Vergleichs von realen und theoretischen Rückflussmengen belegt. Das erlangte Wissen über die Leistung und Qualität des Bohrlochs hilft die Qualität zu verbessern und Verluste der Bohrlochintegrität zukünftig zu verhindern.

Wie schon erwähnt deckt das Bewertungstool nur das ab, was während der Konstruktion des Bohrloches passiert. Um die Integrität während des gesamten Lebenszyklus einer Bohrung zu erforschen und zu verstehen ist ein ganzheitlicherer Ansatz notwendig. Deswegen wird ein Spannungsmodell vorgestellt, um den Einfluss der geänderten Spannungen auf den Zementmantel während des Bohrungsbetrieb zu verstehen. Die Herstellung einer Testzelle nach dem entsprechenden Design soll helfen das Spannungsmodell zu verifizieren.

Diese Arbeit liefert einen wesentlichen Beitrag den ganzheitlichen Prozess der Bohrungsintegrität besser zu verstehen um letztendlich Kohlenwasserstoffbohrungen umweltfreundlicher, sicherer und kostengünstiger zu betreiben.

Acknowledgements

I am deeply grateful to Univ.-Prof. Kris Ravi, MBA, Ph.D. for his great guidance and supervision throughout the last months. Numerous personal meetings, skype calls, and messages have been incredibly illuminating and insightful. Without his experience and persistent help, this thesis would not have materialized.

I would particularly like to thank OMV for giving me the opportunity and financial support to write this thesis. Special thanks to DI Stefan Knehs and DI Markus Doschek for their support. I am also particularly grateful for the assistance given by DI Georg Ripperger.

Special thanks also to the academic and organizational staff of the Chair of Drilling & Completion Engineering, who gave insightful comments and suggestions.

My deep appreciation also goes to Christian Kosinowski from Halliburton, who has been very supportive in providing data.

Contents

Chapter 1 Introduction 1

1.1 Problem Statement & Motivation 1

1.2 Aim & Scope of the Work 2

Chapter 2 Well Integrity-Fundamentals & Risks 5

2.1 Threats to Well Integrity during Well Construction 7
  2.1.1 Fluid settling and sag 8
  2.1.2 Drilling fluid removal and cement slurry placement 9
  2.1.3 Annular gas migration 12

2.2 Threats to Well Integrity during Well Operation 14

Chapter 3 Pressure Testing-Best Practice & Existing Approaches 17

3.1 Pressure Testing Fundamentals 17
  3.1.1 Mechanical Barrier and Formation Strength Verification 18
    3.1.1.1 Shoe track 18
    3.1.1.2 Cementing 20
    3.1.1.3 Positive Pressure Test 21
    3.1.1.4 Negative Pressure Test 23
    3.1.1.5 Formation Integrity Test (FIT) 24
    3.1.1.6 Leak-Off Test (LOT) 25
    3.1.1.7 Extended Leak-Off Test (xLOT) 25

3.2 OMV-Current Best Practice 26

3.3 Industry-Best Practice 27

3.4 Influencing Factors on Pressure Testing 29
    3.4.1.1 Stresses and Deformations in Casing and Cement 30
    3.4.1.2 Fluid Compressibility & Thermal Effects 33
    3.4.1.3 Air entrapment 40

Chapter 4 Well Construction Scorecard Tool 41

4.1 Background-Wellbore Quality 41

4.2 Scorecard-Methodology 43
  4.2.1 Drilling Response 44
  4.2.2 Final Bottom Hole Assembly Pull-out of Hole Response 45
  4.2.3 Casing running response 47
  4.2.4 Cementing/Fluid Relevant Parameters 48
    4.2.4.1 Mechanical/Operational Well Design Factors 49
    4.2.4.2 Cementing Slurry Parameters 50

4.2.4.3 Hydraulic/Operational Parameters 52
4.2.4.4 Casing Pressure Test Parameters 54

4.3 Scorecard-Results & Interpretation 55
4.3.1 Backflow/Bleed-off volumes 58
4.3.2 Anomalies/Observations 60
4.3.3 Green Cement Test-Pressure Decline Rate 65

Chapter 5 Cement Stress Modelling 71

5.1 Analytical Model 73

5.2 Discussion of Results 75

Chapter 6 Test Cell Design 79

6.1 Sensors 81

Chapter 7 Summary, Conclusion, Discussion & Future Work 85

Appendix A Stresses and Deformations of cylinders 87

A.1 Thin-Walled Cylinders 88

A.2 Thick Walled Cylinders 89

Appendix B Approximate Solution of Compressibility Equation 95

Appendix C Green Cement Pressure Test Data 97

Chapter 1 **Introduction**

1.1 Problem Statement & Motivation

Designing and constructing a well, in a way that it will be of integrity through its whole life cycle, is one of the most important goals in well engineering. A lot of different parameters and responses during drilling, cementing, and pressure testing can indicate a well's integrity. However, changing conditions during production/injection or even in already plugged and abandoned wells might also be responsible for lack of well integrity. Well integrity is strongly dictated by the integrity of the cement sheath as well as the casing-cement and cement-formation bond. Therefore, it especially depends on the execution of a proper cementing job with a subsequent passing casing pressure test. Even if everything in the well construction process goes as per design, it does not mean that this well will be of integrity through its lifetime. During the transition time of liquid cement into solid cement, gas can migrate into the cement, failing to provide zonal isolation.

Experience has shown that after well operations like pressure testing, and other well interventions or fluid production/injection, the cement sheath may lose its ability to provide well integrity and zonal isolation. The yielding of the cement is most often caused by temperature- and pressure-induced stresses intrinsic in well operations (K. Ravi, Bosma, and Gastebled 2007). During a positive pressure test, the inside of the casing gets pressurized, resulting in radial expansion of the casing known as "ballooning." Through this process, the cement is exposed to significant hoop stresses, if set. This possible failure can create a potential pathway for formation fluids to enter the annulus, which can result in sustained casing pressure and make the well unsafe to operate or limit the economic life of a well due to premature water production. Therefore, if the cement bond fails at any time during the life of the well, its objective of providing zonal isolation may not be met. The pressure testing procedure should be designed in a way, so it does not harm the cement sheath and can withstand the stresses from the operation. Optimally, the pressure test should be performed before the cement has set quiescently, and sufficient gel strength has been developed. However, this is often not possible due to various operational constraints. In case of operation in a high pressure-high temperature environment, where cement integrity problems like casing eccentricity, cement voids, and cement channels are already a big problem, the limitations mentioned in normal operations above will only turn out to be more problematic.

Before conducting such a pressure test, many parameters must be defined. The desired casing test pressure criteria has to be established, including a procedure in case the "flatline"[1] could not be reached. If the pressure test is performed in the well-flowing direction through a leak rate, the leak criteria must be established. The question is, how much pressure drop and leakage is permitted before the test can be stamped as "failed" and remedial actions must be applied.

---

[1] Flatline indicated a successful casing pressure test with no pressure increase or decrease

In reality, it is challenging and time-consuming to achieve stabilized pressure, especially if temperature-, volumetric, and compressibility effects are not fully understood. Once the pressure test is conclusive, and a leak has been identified, it might be troublesome to determine which well barrier element is causing the leak. A failing pressure test only indicates that some barrier is failing. It might be the shoe track, the casing itself or the formation. Essential things like zonal isolation cannot be confirmed with a pressure test. Therefore, more criteria have to be established for a more precise evaluation of well integrity.

The motivation for this thesis is to develop a wellbore scorecard, that is scoring the well based on well construction responses and parameters from drilling, final BHA-pull out of hole, casing running and cementing. With the help of this scorecard low performing well sections, in terms of well construction, can be easily identified. It is aimed to spot shortcomings in the well construction process that are responsible for well integrity failure. Next step should help to link bad performing wellbore sections to shortcomings in the well construction process or any other reason resulting from production or injection. Wells that are already facing some well integrity or zonal isolation problems are especially interesting because the analysis should help determine the reason for their failure and proof the tool's effectiveness. As the scorecard tool is capturing everything going on while the cement is still in the liquid face, a basic analytical stress model helps to capture everything that is happening in the solid cement. The results of the analytical stress model should help to indicate if the hoop stresses in the casing might have damaged the cement integrity and cement bond in any way. This should help to explain wells, that are having a high score but regardless show some well integrity problems. It is recommended that in a future work the stress analysis technique proposed here be expanded for robustness and calculations validated. A testing apparatus (test cell design) is proposed in this work which could be used as the basis.

1.2 Aim & Scope of the Work

The main goals of this thesis are:

- Develop a well construction scoring tool using field data during drilling, cementing, and well performance data to capture and detect well integrity shortcomings in the well construction process
- Evaluate the feasibility of a relationship between the KPI score and well integrity performance
- Review the current OMV Pressure Testing Operation Policy
- Review casing pressure test industry best-practices and procedures for pressure testing during well construction
- Develop an analytical relation (analytical stress model) between the pressure applied inside the casing and the effect on cement sheath integrity.

- Take steps to validate the analytical stress model in the lab by proposing a test cell design, that helps to better understand cement-casing interaction during pressure testing

Chapter 2 **Well Integrity-Fundamentals & Risks**

Norwegian recognized standard NORSOK D-010 for well integrity and drilling operations, which is among the most accepted and proved standards in well engineering, defines well integrity as "application of technical, operational and organizational solutions to reduce the risk of uncontrolled release of formation fluids throughout the life cycle of a well." The challenge aligned with this is the fact that well integrity is critical in all stages of a well's life. From well construction, completion, production, or injection to plug and abandonment, as shown in Figure 1. It is also crucial to assure that a well has the lowest possible downtimes and impairments due to well integrity failure and required workovers, to keep the production losses as small as possible. Differentiation between well integrity failure and well barrier failure is essential when talking about well integrity. Well integrity failure means that the leakage of a produced or injected fluid is not contained by one of the multiple barriers installed in the well. In this case, they all failed, and the fluid will leak into the subsurface formation or surface well surroundings. A well barrier failure occurs when one of the well barriers is failing, but containment within the well is given by other barriers that are still intact. A total loss of well integrity will not occur when other barriers can withstand leakage loads in case one barrier fails. Nonetheless, it will be a contributing factor that might lead to a well integrity failure (Prohaska 2017).

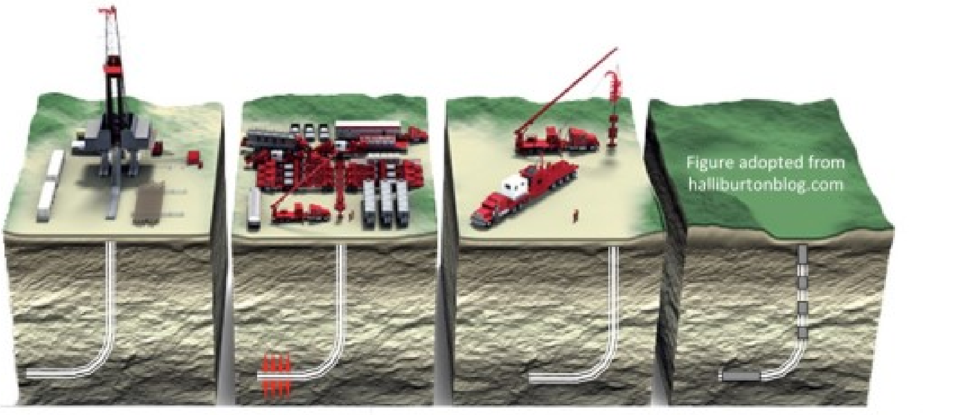

Figure adopted from halliburtonblog.com

Well Construction: Well control barriers by mud, cement, safety valves, wellhead, blow-out preventer. Primary cement job evaluated, remedial cementing sometimes required.

Completion: Cement barriers may fail under hydraulic stress during perforation and fracturing.

Production: Cement barriers subjected to long-term degradation and fatigue failures due to dynamic stresses in the wellbore. Tubing may corrode. Sustained casing pressure requires costly work-over.

Plug and Abandonment: Perfect barriers required by regulations. Long term integrity monitoring beyond abandonment desirable.

Figure 1: Well Integrity must be implemented through the life cycle of a well; Source: (Prohaska 2017)

The risk of well barrier failure can result in a negative impact on the net present value (NPV) of wells or developments, as the risk of well integrity failure can lead to the following:

- Unexpected water production
- Aquifer contamination
- Interzonal communication
- Reduced hydrocarbon production
- Surface spill and risk to health safety and environment

In extreme cases, well integrity failure could lead to a catastrophic event such as what happened with the Deepwater Horizon platform (British Petroleum 2010).

Even if well integrity is not at risk due to other barrier's ability to withstand the additional leaking loads, the failure of a well barrier element could still threaten the economic viability of a well or an asset. Figure 2 and Figure 3 show all the possible leakage pathways in a well that is abandoned with a cement plug.

a) Between the cement and outside of the casing (e.g., micro annulus)
b) Between the cement and inside of the casing (e.g., micro annulus)
c) Through the cement (e.g., due to gas migration through hydrating cement)
d) Through the casing (e.g., due to corrosion or leaking connections)
e) Through fractures in the cement
f) Between the formation and the cement

Additionally, to the possible leakage pathways shown in Figure 2, completion equipment like packers, mechanical plugs, safety valves, and tubing-, casing- and liner hanger can also be possible leakage pathways in a well.

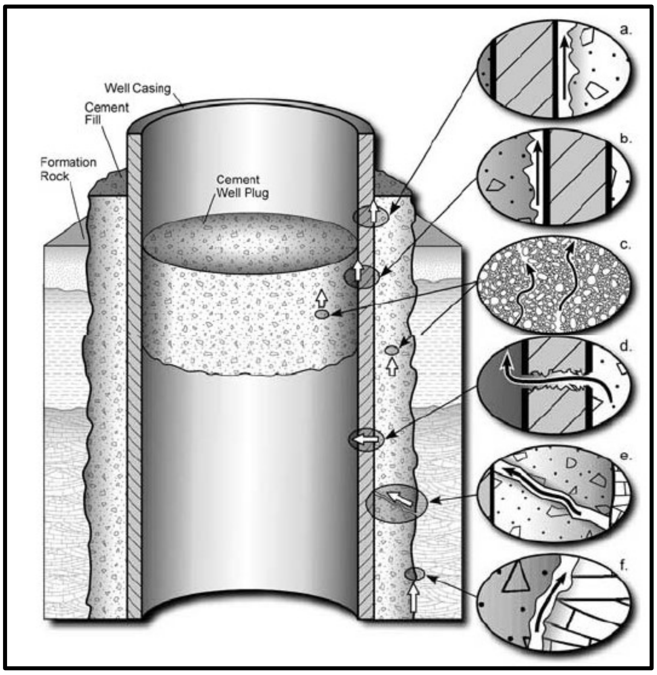

Figure 2: Different fluid migration pathways in an abandoned well; Source: (Global CCS Institute 2019)

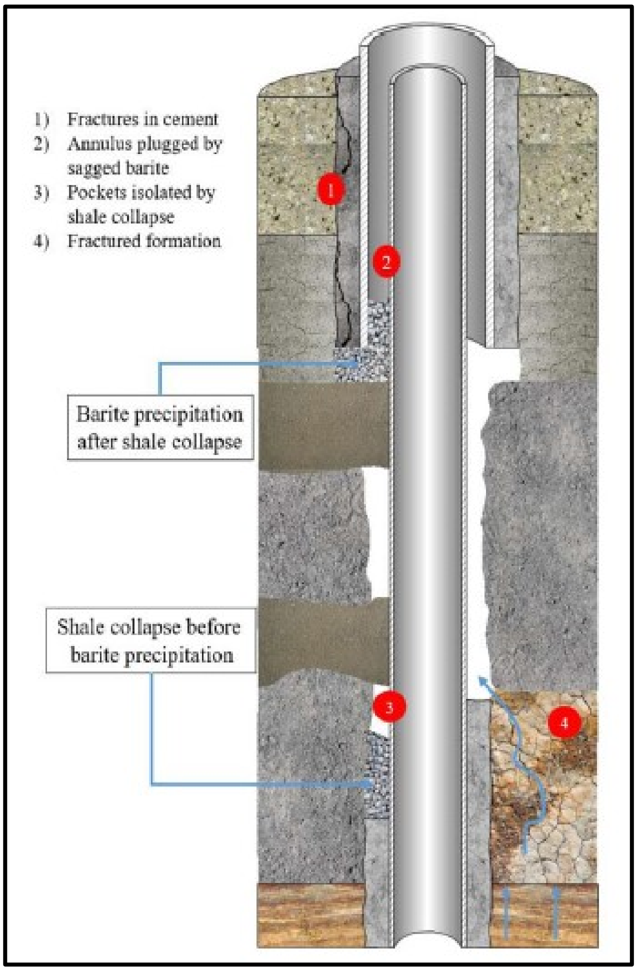
1) Fractures in cement
2) Annulus plugged by sagged barite
3) Pockets isolated by shale collapse
4) Fractured formation
Barite precipitation after shale collapse
Shale collapse before barite precipitation
1
2
3
4

Figure 3: Multiple fluid migration paths leading to potential well integrity failure; Source: (Brechan et al. 2018)

2.1 Threats to Well Integrity during Well Construction

Well integrity is jeopardized by numerous threats that can either happen during well construction or well operation. In this section, some of those threats that can happen during well construction, are discussed in detail. The methodology of the wellbore scorecard presented in Chapter 4 is based on responses and parameters, that are aimed to identify those threats described below as roots cause for a low score. Drilling fluid removal and cement slurry placement are imperative to assure a proper cement job providing zonal isolation.

Furthermore, subsequent casing pressure testing serves the purpose to know about the integrity of the freshly constructed section. Those well integrity test, positive and negative casing pressure tests, respectively, are designed to test the integrity of the casing, wellhead, and seal assembly. However, gas migration during cement hydration and zonal isolation is rather strenuous to detect, before severe problems occur. Those processes occur behind the casing in the cemented annulus. Even perfectly “textbook”-passing positive and negative pressure tests can not indicate gas migration during cement hydration and lack of zonal isolation. A passing positive pressure test only indicated the integrity of the casing, wellhead, seal assembly, and top cementing plug, whereas a negative pressure test analyses the float valves and shoe tracks ability to hold back any gas influx. This makes it very difficult to detect any well integrity issue behind the casing during well construction.

2.1.1 Fluid settling and sag

Fluid settling occurs when the weighting material or any other material in the fluid, separate, breakdown or deteriorate from the liquid phase and settle down. Fluid settling, also referred to as sag leads to different density values in the lower and upper part of the wellbore. It occurs more frequently in low gel strength, low viscosity, and low shear rate fluids. Whereas sag in vertical wells can only happen when circulation is stopped, in deviated wells, it can also occur during circulation. Notably, at deviations from 30° to 65° where the boycott effect increases the settling rate of the particles in the fluid due to shorter sedimentation paths. Heavier particles settle on the low side and lighter fluid remains on the high side of the well.

A primary indicator for barite sag is the variation in mud density during circulation after logging and casing running. MI-Swaco has determined the main issues that lead to sag in drilling fluids:

- Annular velocity and pipe rotation/reciprocation are a vital consideration
- Inclination-sag occurs at 30°-65°, most severely at 45°-65°
- Mud type/weight-in OBM and SBM at a density greater than 12 ppg becomes problematic
- Rheology-elevated shear rate and viscosity reduces sag
- Weight material-sag depends on the specific gravity and particle size
- Rotary vs. Sliding-sliding makes it worse because the pipe is not rotating
- Time-sag increases with time

Fluid settling and barite sag are increasingly essential when talking about drilling fluid removal to achieve optimal slurry placement. As the high density and immobile part of the fluid column sags and forms a sediment bed as depicted in Figure 4. Mud displacement by spacer and cement placement might be poor leaving mud pockets and channels in the cement, that later threaten zonal isolation and well integrity.

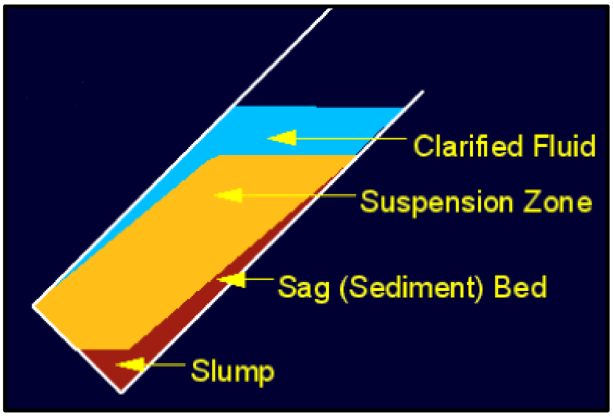

Figure 4: "Boycott" settling of barite and cuttings in an inclined well; Source: (MI-Swaco 2017)

2.1.2 Drilling fluid removal and cement slurry placement

Proper drilling fluid removal and displacement are crucial for well integrity purposes. In case the well is static after or during casing running and open-hole logging, the fluid might gel up and removal will become challenging. Low mobility mud will form around the filter cake leading to the formation of drilling fluid channels or mud pockets, as shown in Figure 5. Therefore, the displacing fluid has to be designed in a way that it can displace the entirety of the annulus and does not flow past the displaced fluid. Also, removal of the partially dehydrated gelled mud is crucial to achieving zonal isolation, through 360° annular cement placement. In order to achieve proper removal of partially dehydrated mud, it is crucial that the shear stress at the fluid interface is higher than what is required to erode them. Therefore, increasing the shear stress in the annular gap is key to the right displacement (Moroni et al. 2009).

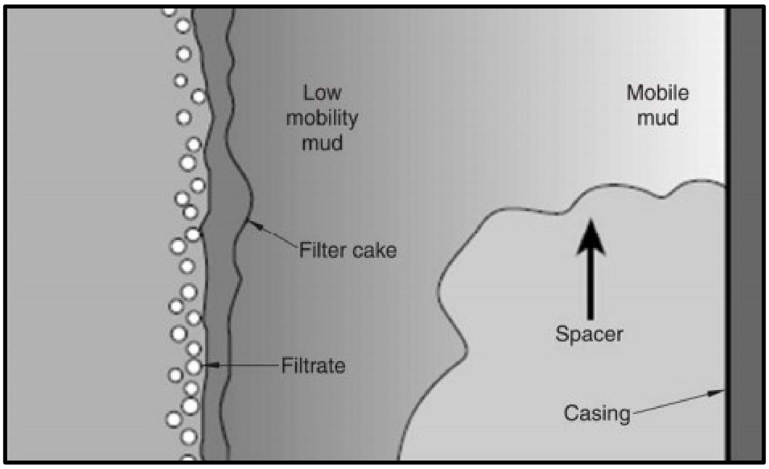

Figure 5: Proper drilling fluid removal and mud displacement might be jeopardized by gelled-up, low mobility mud around the filter cake; Source: (Moroni et al. 2009)

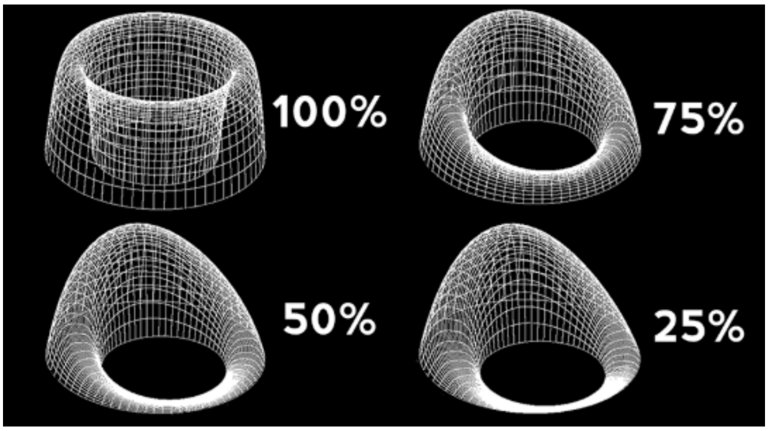

Figure 6: Velocity profile for different casing standoff values. Low standoff leads to a high velocity-wide side, and low velocity-narrow side; Source: (Pegasus Vertex 2015)

Casing standoff and hole eccentricity are essential to achieve the desired drilling fluid removal and cement slurry placement. A casing with 100 % standoff means a perfectly centered pipe, while 0 % standoff means the casing is in contact with the wellbore. An uncentered casing will result in a narrow side and a wide side in the annulus. Figure 6 shows the velocity profile for different casing standoff values. As the fluid always takes the path of least resistance, it tends to flow through the wide side. As the flowrate on the wide side of the annulus is high, the flowrate on the narrow side is reduced, according to the velocity profile in Figure 6. This means that the slurry on the low side could fail to reach velocity, turbulence, and shear stress levels needed to remove the mud, and also cement levels (TOC) on the low side might be too low to seal off the reservoir section or other gas-bearing horizons (Figure 4 and Figure 7). In this case, the cement failed its objective to be a primary barrier element, and formation fluids could leak into the exposed annulus, leading to annular pressure build-up (APB) or other issues during the life cycle of the well.

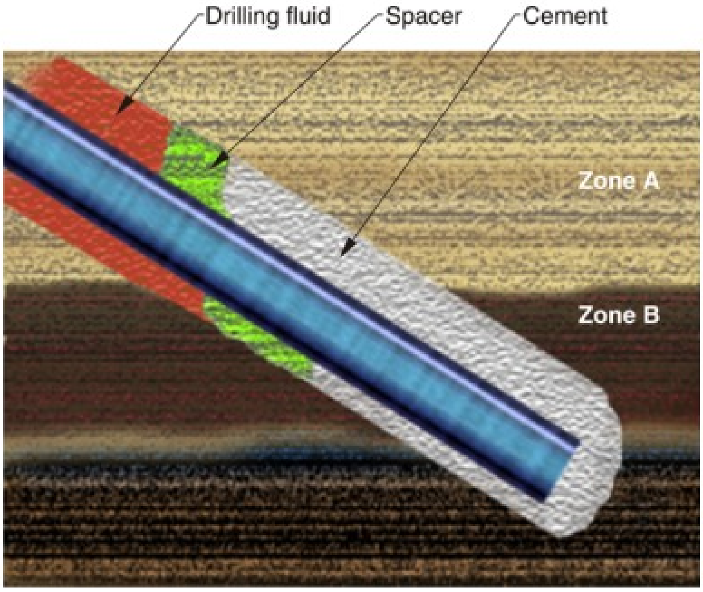

Figure 7: Low casing standoff is increasingly appearing in horizontal wellbores and might lead to missing zonal isolation between zone A and zone B; Source: (Moroni et al. 2009)

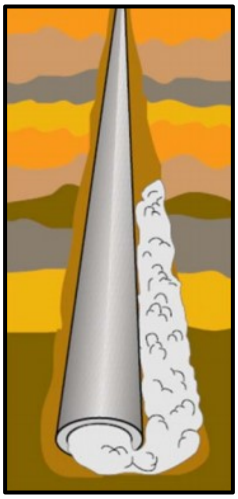

Figure 8: In case of low standoff value and highly gelled up mud, the narrow side of the annulus might remain uncemented, leading to various well integrity issues; Source: (Moroni et al. 2009)

In some extreme cases, where the standoff is very low, and gelled fluid is immobile, there might not be any flow at all on the narrow side of the annulus, as indicated in Figure 8. With one side of the annulus left uncemented, casing corrosion, sustained casing pressure, and zonal connection between multiple zones, leading to water flow and potential well abandonment, is prone to happen more frequently. With the hole already drilled and ready to be cased and cemented, the following parameters can influence the drilling fluid removal and cement slurry placement (Moroni et al. 2009).

- Casing standoff (100 %-casing is perfectly centered)
- Pipe rotation
- Flushes and spacers as displacement aids
- Flowrate and rheology of drilling fluid, flush, spacer and cement slurry

Rheology and flowrate of drilling fluid and spacer optimization are very practical to enhance mud removal and slurry placement. The desired drilling fluid to achieve this in most cases is a non-Newtonian, shear-thinning fluid with pseudoplastic behavior. Both Power-Law and Herschel-Bulkley models show this behavior. What makes them so attractive for a drilling operation is their behavior, in which the slope, specifically the viscosity, of the shear stress versus shear rate curve decreases with increasing shear rate. Also, the viscosity increases with lower shear rates. This unique behavior benefits improved cuttings lifting in the annulus, where a reduced shear rate increases the effective viscosity but also reduces parasitic friction pressure losses inside the drill pipe, where increased shear rates reduce the effective viscosity.

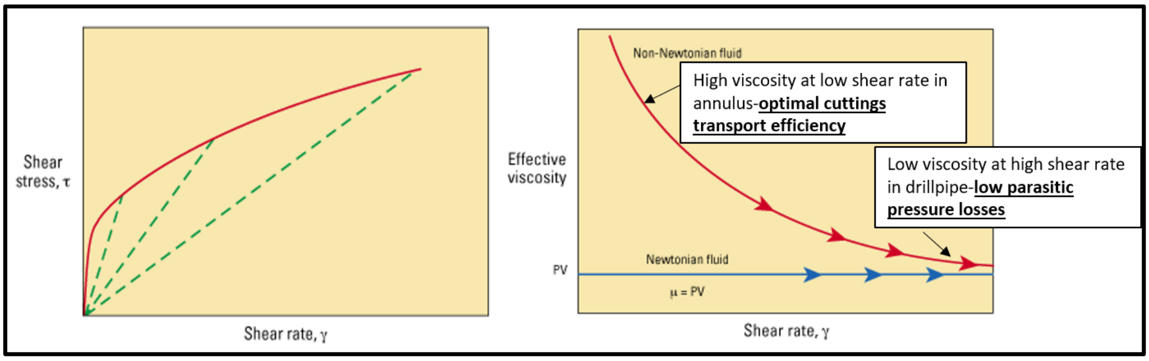

Figure 9: For non-Newtonian fluids the viscosity decreases with increasing shear rate, resulting in the desired shear thinning behavior; Source: edited after (Schlumberger Oilfield Glossary 2019a)

In a drilling environment, where the drilling mud is much heavier than water, it will become inefficient to use flushes. However, usually, spacers and flushes are intended to displace the drilling mud from the annulus, leaving the formation and casing water wet and also isolate the drilling fluid from the cement slurry. The limiting factor for high casing standoff values is the number of casing centralizers, that can be run in the casing structure. Sometimes the desired standoff cannot be reached across the entire string, especially in holes that are under-reamed. The last operational measure to achieve proper cement placement across the whole annulus, including the narrow side, is casing rotation during cementing. This will help to achieve the turbulence needed (Moroni et al. 2009).

2.1.3 Annular gas migration

Gas migration in the annulus is the most common source for zonal isolation failure. Two failure mechanisms can occur, gas migration during cement hydration through unset cement, or due to mechanical failure of the set cement or cement bond at an interface (Economides 1998). However, gas migration through cement is very common during its transition from liquid to solid. As long as the cement is still unset, it is the hydrostatic pressure that is preventing the gas from migrating through the cement. As long as this pressure is higher than the formation pressure, gas migration will not occur. The cement's ability to transmit the hydrostatic pressure is also dependent on gel strength development. The lower the gel strength, the better the transmissibility of the hydrostatic pressure against the formation. As the cement starts to hydrate, it transitions from a liquid, pumpable slurry to a gelled-up material, that is somewhat self-supporting. The cement will form a cohesive matrix, that no longer transmits the hydrostatic pressure. The hydrostatic pressure of the slurry is trapped in the cement pores. Therefore, this pressure determines the ability of the annular cement to prevent gas migration. If it is greater than the formation pressure, it will not occur. This hydrostatic pressure in the pores is dictated and controlled by the amount of water in the cement slurry, meaning, that any decrease would lead to a hydrostatic pressure reduction, potentially allowing the gas to migrate through the cement (Al-buraik et al. 1998).

Unfortunately, during cement hydration, two factors are contributing to a reduction of the water volume in the cement. The hydration process itself consumes water, but also fluid loss into the formation inevitably uses a part of the water. Fluid loss is much easier to control and influence to serve our needs than the hydration process. Maintaining API-fluid loss values below 50 ml/30 min is one of the most essential and widely accepted measures to effectively prevent gas migration. Fluid loss is dictated by the amount of fluid the cement can contain across a pressure differential, which means that a lower API fluid loss also means a lower reduction of pore pressure.

Furthermore, the loss of fluid additionally weakens the cement structure and leads to an increase in cement permeability. Cement static gel strength, which is the shear stress brought about by force required to set a fluid in motion together with transition time, is an essential parameter, that has much influence on gas migration (Prabhakar et al. 2019). Transition time is characterized by the minutes needed to change the static gel development, shear stress respectively, from 100 lbf/100 ft^2 (48 bar) to 500 lbf/100 ft^2 (240 bar). The shorter this transition time takes, the lower the chance for annular gas migration. At shear stresses greater than 500 lbf/100 ft^2 the cement is said to be set, and no gas migration will occur.

An ideal solution to combat gas migration during cement hydration has involved the use of quick-setting cement slurries, also referred to as right angle set cement. These cement systems are well dispersed and show a very rapid and abrupt setting reaction due to high hydration reaction kinetics, compared to conventional cement systems, that exhibit a more progressive gelation tendency. The system has a rather low initial consistency value, enabling the slurry to maintain full hydrostatic pressure until cement setting kicks in with high speed to avoid significant gas influx. Usually, the consistency in burden units of consistency (B_c) shoots up to 100 units within a few minutes and could be one indication of a right angle when plotted on a graph. In addition to testing this in a lab, it is highly recommended that the slurry characteristic is confirmed using other test methods. However, most labs test only until the slurry reaches 70 B_c units because this is the threshold value where the slurry is not pumpable anymore.

Figure 10 and Figure 11 show the difference between a conventional setting cement, that shows rather progressive gelation, where the slurry takes almost an hour between 30 B_c and 70 B_c, and a typical right-angle setting cement, that requires only 16 minutes to go from 30 B_c to 70 B_c.

One limitation in the application of quick-setting cement systems is temperature, as below 100-120 °C the hydration reaction kinetics are too low for the cement to make use of his full "right-angle setting potential." Also, the shear transmitted during the API thickening lab test is significantly different from conditions during a real cementing operation. Therefore, the test results only serve as a qualitative measure.

In order to achieve this right-angle setting cement property, many gas migration additives are commercially available. By the help of delaying gel strength development and shortening transition time, they allow the cement slurry column to pass on the hydrostatic pressure to gas-bearing formations entirely.

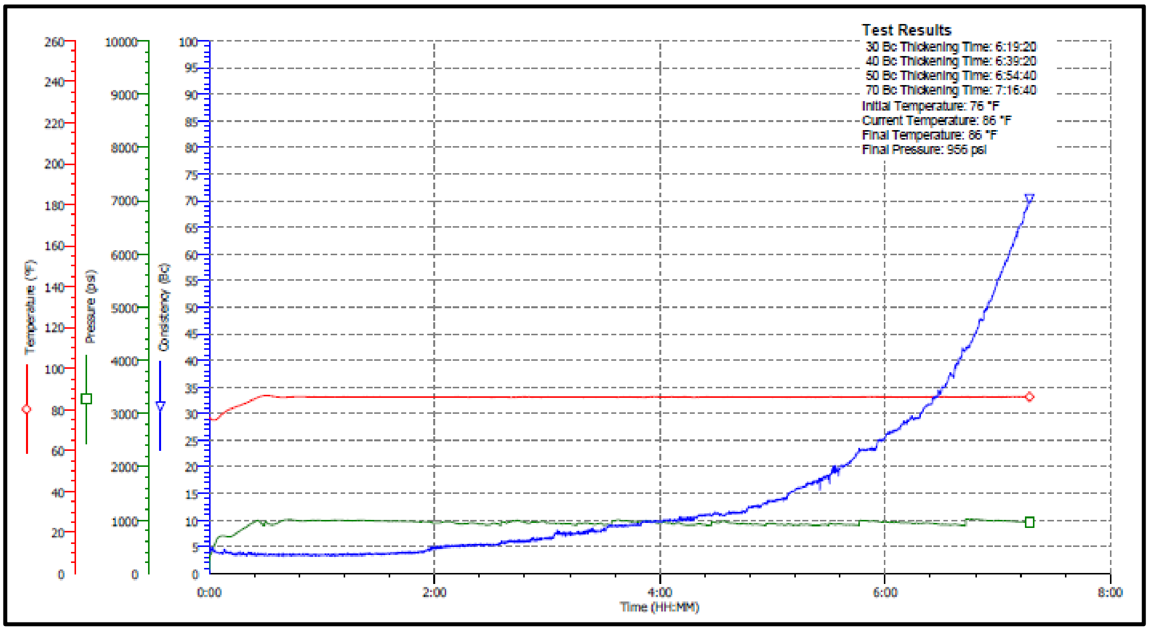

Figure 10: Conventional cement slurry with progressive gelation tendency, tested by Halliburton's Celle, Germany-lab, for OMV Austria's Bockfließ-204 13 3/8" lead section cement slurry

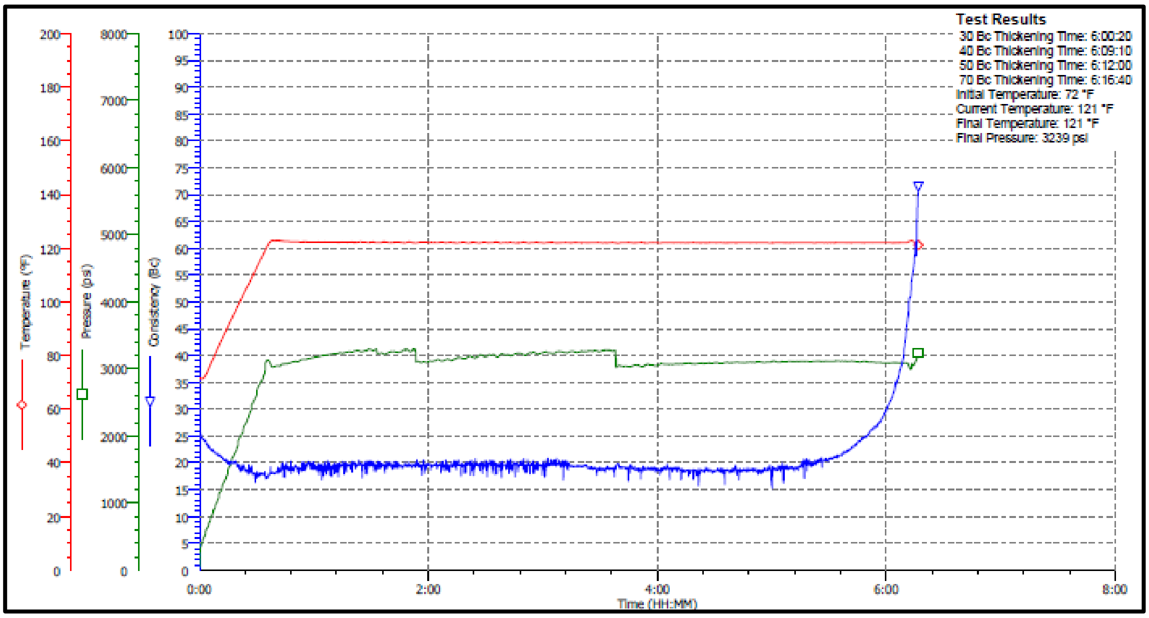

Figure 11: Quick-setting cement, tested by Halliburton's Celle, Germany-lab, for OMV Austria's Bockfließ-204 9 5/8" lead section cement slurry

2.2 Threats to Well Integrity during Well Operation

Once the well construction is finished, and production is about to start, the risks mentioned above hopefully have been successfully handled. However, this does not mean that the integrity of every single well barrier is safe until the end of the well's life cycle. As the well is producing or injected, downhole conditions leave their influence on the constructed wellbore. Changing pressure and temperature conditions and wear on the tubing and numerous seal assemblies like packer elastomers and wellhead seal assemblies are not necessarily contributing to well integrity. Quite the contrary, it might accelerate the failure of one or more well barrier, eventually leading to well integrity failure.

This thesis concentrates mostly on the well construction process and pressure testing and its effect on well integrity. Nevertheless, the following points show the different risks that could lead to well barrier or well integrity failure (Kris Ravi 2019).

1. Casing integrity
    - Collapse-annular pressure build up-increasing temperature in a high-temperature environment causes fluid expansion that can potentially over-stress the casing and tubing if not mitigated.
    - Corrosion-H2S, CO2, formation fluid
    - Burst
2. Equipment failure
    - Threads, casing collar, wellhead, tubing hanger, safety valve
3. Cement sheath chemical integrity
    - Strength retrogression-high temperatures (>110 °C) might decline cement's strength-silica additives might help
    - Exposure of cement to CO_2, H_2S, brines, aggressive salt or other chemicals might do their part to the cement sheath's damage

4. Cement sheath mechanical integrity
    - Changing pressure and temperature might induce stresses on the cement
    - Formation subsidence
    - Halite and aggressive creeping salt zones
    - Cement sheath expansion/shrinkage
5. Cement sheath porosity and permeability
6. Cement sheath mechanical properties

Chapter 3 **Pressure Testing-Best Practice & Existing Approaches**

As already mentioned, pressure testing is a vital part to ensure well integrity. However, the definition of a conclusive pressure test is still not clearly defined in the literature. This chapter gives a basic introduction to pressure testing. It consists of basic pressure testing fundamentals and describes the possible types of equipment, that can be pressure tested. Technological advancements in the field will be presented and discussed in detail. The concept of pressure testing will be discussed in detail, and OMV-internal best practice pressure testing procedures as well is industry-wide best practices will be reviewed.

3.1 Pressure Testing Fundamentals

Since well construction and intervention operations require the handling of fluids under a substantial amount of pressure, all necessary precautions must be made to make sure these fluids stay within their designated containment during all time of the well life cycle. The reason for this is not only due to environmental consideration but also due to crew health and safety considerations. One popular way to verify the seal of a vessel containing fluids under pressure is through a “pressure test.” The term “pressure test” is generally used in the industry, but the real meaning behind it is leak detection by pressurization, containment, and analysis. The steps to do this analysis are seemingly simple (Franklin et al. 2011):

- Establishing the criteria for a valid test.
- Evaluating the data to determine whether the criteria have been met.
- Providing notification of the test result; i.e., passed (no leak) or failed (leak detected).

On a typical oil rig, many different types of equipment are pressure tested. Figure 12 shows all the possible ways on an onshore drilling operation. On the surface, testing of all the equipment that is used to pump and carry fluid under pressure, most crucially the BOP, is necessary. In the wellbore, casing, and the wellhead seal assembly are pressure tested through a positive pressure test. A negative pressure test assesses the integrity of the casing shoe track, the casing, and the wellhead sea assembly to hold back formation pressure. This is a vital part of the verification of the mechanical barriers, that should provide well integrity and zonal isolation for the entire life cycle of the well.

As the industry moved into operating in deep offshore environments using synthetic-based fluids, the challenges associated with obtaining useful pressure tests continued to grow as thermal influences on the pressure test are complicating the interpretation. After the Macondo blow-out and subsequent explosion of Transocean’s *Deepwater Horizon*, many lessons in the interpretation of positive and negative pressure tests were drawn from this accident. As the investigation team concluded that the misinterpretation of the negative pressure test was one key finding that is supposed to have contributed heavily to the blowout and explosion of the drilling platform. Figure 12 gives an overview of all the possible equipment that can be pressure tested on a floating offshore rig. For the extent of this thesis, the focus is put on the pressure testing, that is performed in the subsurface. However, the principle of pressure testing is practically the same; no matter which part is tested.

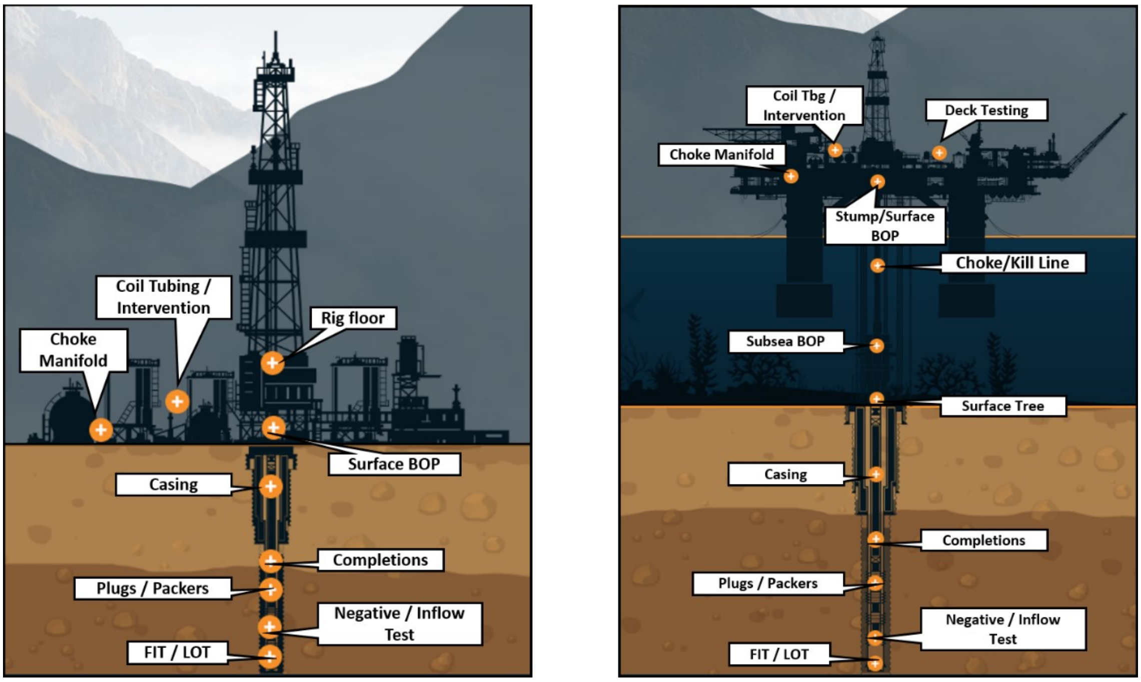
Coil Tubing / Intervention
Choke Manifold
Rig floor
Surface BOP
Casing
Completions
Plugs / Packers
Negative / Inflow Test
FIT / LOT
Coil Tbg / Intervention
Deck Testing
Choke Manifold
Stump/Surface BOP
Choke/Kill Line
Subsea BOP
Surface Tree
Casing
Completions
Plugs / Packers
Negative / Inflow Test
FIT / LOT

Figure 12a & 12b: Potential equipment in an onshore (a) and offshore (b) well construction operation, that can be pressure tested; Source: edited from (IPT Global 2019)

3.1.1 Mechanical Barrier and Formation Strength Verification

Casing pressure testing is mainly performed to test the integrity of the mechanical well barriers (shoe track, production casing, and casing hanger seal assembly) and is not designed to test the integrity of the cement sheath. However, before this can be done, it is essential to understand the principle of these barriers and how they are brought in place.

3.1.1.1 Shoe track

The shoe track is the first part that is run in the hole as part of the casing string. It is a mechanical well barrier that serves as an aid during cementing placement and to prevent hydrocarbons from entering through the bottom of the casing and is tested through a negative pressure test. There are many different configurations, but it usually consists of the reamer shoe on the bottom, the cement inside the casing and a single or double-valve float collar (Refer to Figure 13). The shoe track cement (tail cement), usually 2-3 casing strings, ensures that good cement remains on the outside of the bottom of the casing. It reduces the risk of over-displacing the cement due to improper casing volume calculations and leaves the well designer a safety margin to guarantee that the high-quality cement is right where it is needed, in the bottom of the well.

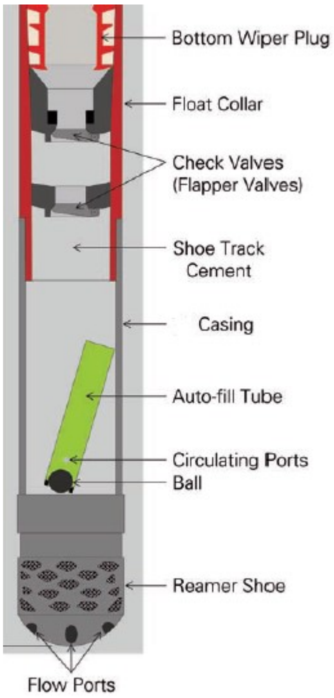

Figure 13: Typical Shoe Track; Source: (British Petroleum 2010)

The float collar is comprised of a single- or double-check valve, that once closed, it only allows fluid passage in one direction. It is designed to prevent hydrocarbon backflow or ingress from the formation into the well. Initially, during casing running, these check valves are held open by an auto-fill tube, allowing mud to pass through, minimizing surge pressures on the formation to prevent lost circulation. Before the casing is cemented in place (see below) and a positive pressure test (see below) can be conducted, the float collar must be converted (Refer to Figure 14). This is done during mud circulation when the mud is diverted through two small ports in the auto-fill tube due to a ball sealing in the auto-fill tube. Circulation through these ports creates a differential pressure over the float collar, resulting in the release of the auto-fill tube and the closing of the check valves. When this float collar conversion is completed, the check valves can move into a closed position, restricting any hydrocarbon fluid flow into the casing. However, problems or even inability of the conversion might occur, if the float collar itself or the reamer shoe is plugged. After the conversion, the cementing operation can be resumed.

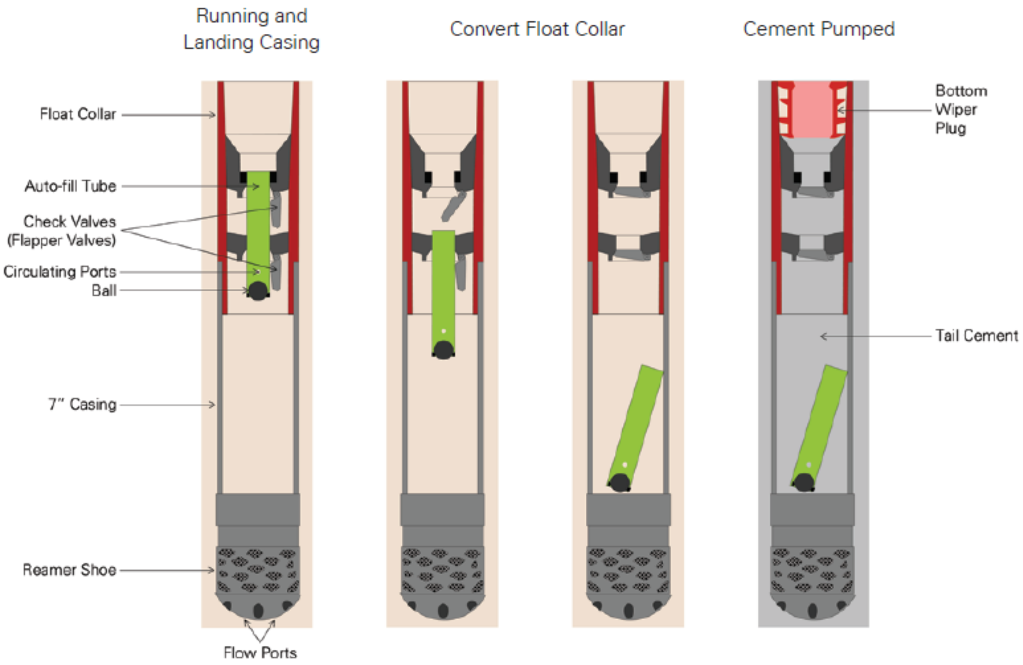
Running and Landing Casing
Convert Float Collar
Cement Pumped
Float Collar
Auto-fill Tube
Check Valves (Flapper Valves)
Circulating Ports
Ball
7" Casing
Reamer Shoe
Flow Ports
Bottom Wiper Plug
Tail Cement

Figure 14: Float Collar Conversion; Source: (British Petroleum 2010)

3.1.1.2 Cementing

Understanding, how a classical cementing job is performed is crucial to understand why a pressure test is so important. In this case, the casing with all required cementing equipment such as float collars and centralizers are run in the hole until the shoe track is just a few meters off bottom. Two cement plugs are used to perform the job (Refer to Figure 15), which need to be correctly placed in the cement head. After circulating mud to clean the casing, the first cement plug (wiper plug) is pumped down ahead of the cement to wipe the casing clean and enhance the displacement process. Then the spacer and cement slurry are pumped followed by the second cement plug (top plug). As soon as the wiper plug reaches the float collar its rubber diaphragm ruptures and allows the displacement of the cement through the shoe track into the annulus. When all cement is displaced, the top plug lands on the wiper plug and stops the displacement process. Usually, the pumping rate should be lowered before the top plug reaches the float collar, resulting in a gentle bump. As long as the cement has not yet developed gel strength, this is the perfect time to conduct a positive pressure test, which is also referred to as "green cement test," because the cement is still in a liquid state.

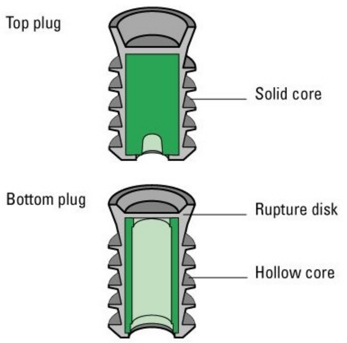
Top plug
Solid core
Bottom plug
Rupture disk
Hollow core

Figure 15: Cementing plugs crucial for the Placement of the uncontaminated Slurry; Source: (Schlumberger Oilfield Glossary 2019b)

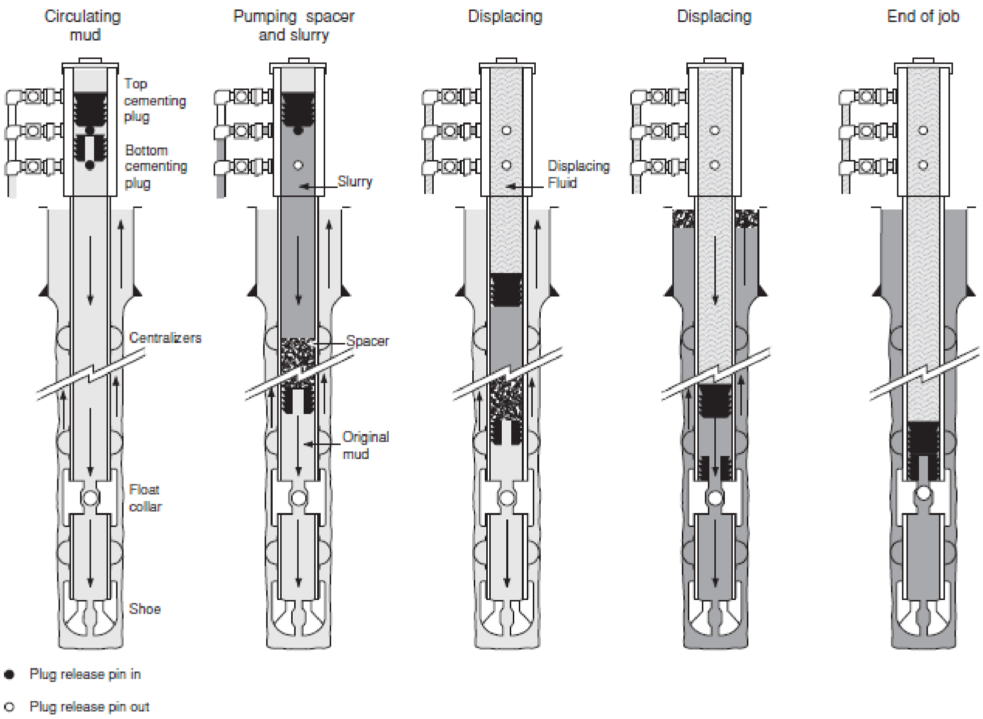
Circulating mud
Pumping spacer and slurry
Displacing
Displacing
End of job
Top cementing plug
Bottom cementing plug
Slurry
Displacing Fluid
Centralizers
Spacer
Original mud
Float collar
Shoe
● Plug release pin in
○ Plug release pin out

Figure 16: Single-Stage Cementing Job Sequences; Source: (Drillingcourse.com 2015)

3.1.1.3 Positive Pressure Test

A positive pressure test confirms the mechanical integrity of the casing itself, as well as if the casing seal assembly can contain pressure inside the casing. Note that the fluid used to pressure up the casing is usually the displacement fluid used to drill the next section, and the pumping power comes from the cementing unit. The positive pressure test is conducted against the rubber cement displacement plug on top of the float collar and is not testing the integrity of the cement or the check valve in the shoe track. Therefore, the plugs must be able to separate the fluid inside the pipe, effectively wiping the inside diameter of the pipe, to provide the desired positive pressure indication at the surface. If the plug is not able to contain the fluid, intermixing and contamination will occur, and if the plug is not effectively wiping the casing, this will cause a myriad of problems for the positive pressure test.

People also use the term "Green cement test" to describe a positive pressure test, meaning that the cement is still liquid or "green" and that the pressure test is conducted right after the top plug bumped the wiper plug. However, during some cementing operations, the top plug does not bump the wiper plug after pumping the theoretical amount of displacement volume. In that case, to avoid leaving a wet shoe (shoe surrounded by poor cement quality), it is recommended to pump an additional volume of half the shoe track volume before stopping the operation. This over-displacement should help to achieve the goal that the shoe track is left with cement and ready to be pressure tested. However, in many cases, a significant amount of cement is found above the float collar. The leading cause of not bumping the plug is an inexact casing inside diameter used as the basis for the calculation of the displacement volume. Another reason for displacement volume errors is failing to account for the displacement's fluid compressibility, especially when highly compressible oil-based muds are in use. In case the top plug does not bump the wiper plug, a green cement test, with the cement still in a liquid state is not recommended. In this instance, it is recommended to wait for the cement to develop sufficient hardness before the positive pressure test is conducted. In this case, a testing packer could be used to isolated and save the cement integrity of the upper part of the hardened cement(Nelson, Erik; Guillot 2006).

Note that the casing, surface lines, wiper plug, and float collar arrangement need to be rated for the planned test-differential pressure. Usually, a positive pressure test is conducted in two stages:

1. Low-pressure test
2. High-pressure test

For the low-pressure test, the pressure is slightly increased to a predetermined value and held for some minutes (Refer to Figure 17; ~250 psi for 7 minutes), to assure that no significant leak is occurring. Also, some leaks, that might close during high testing pressures can only be detected at lower pressure values. In the next step, the pressure is increased to a predetermined value roughly ten times higher than that of the low-pressure test and observed for a more extended period (Refer to Figure 17; ~2700 psi for 35 minutes). Note that maximum test pressure is limited by the burst pressure of the casing or the pressure rating of the surface equipment. A leak in the casing or the rubber cement displacement plug would be indicated by a pressure decrease. In case no leak is identified, and the deterministic "Flat Line" (see Figure 17) is stabilized through the course of the test, the crew can proceed with a negative pressure test to confirm the integrity of the casing shoe as a mechanical well barrier. Ironically, the data depicted below in Figure 17 shows the "passed" positive pressure test of the Macondo Well in the Gulf of Mexico. Only later the investigation team found out, that it was probably the misinterpreted/ignored outcome of the negative-pressure test, that led to the hydrocarbon flow from the formation through the shoe track into the wellbore.

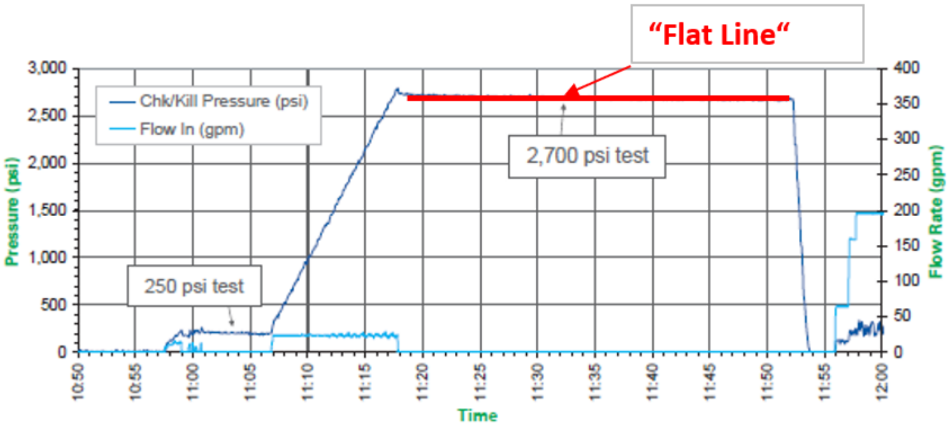

Figure 17: "Successful/Passed" Positive-Pressure Test of the 9 7/8 in. X 7 in. production casing of BP's Macondo Well conducted approximately 11 hours before the explosion of Transocean's Deepwater Horizon Platform; Source: edited from (British Petroleum 2010)

3.1.1.4 Negative Pressure Test

Negative pressure or inflow testing is intended to verify the integrity of the mechanical barriers, including the shoe track, production casing, and casing hanger seal assembly. During the test, the well is placed in an underbalanced condition, when the hydrostatic head is reduced to below the reservoir pressure. The objective is to "simulate" a condition and test the well's ability to withstand a pressure differential as it would occur during post-well construction situations. Negative pressure tests are particularly significant in an offshore environment. Commonly, deep water wells, are drilled with a floating platform and then temporarily abandoned and completed as production wells at a later stage. For temporary abandonment, drilling mud is usually displaced with lighter seawater to a certain depth, and a temporary cement plug is set in the production casing. This procedure is necessary for the rig and all the well control equipment to move off-site. Therefore, the negative pressure test is crucial in simulating this temporary abandonment phase, with the hydrostatic underbalanced condition of having lighter seawater instead of denser mud in the riser.

The test concept is straightforward, but no real standards and procedures for conducting and interpreting negative pressure tests do exist. Industry experience in BP's Macondo well has shown the potential for these tests to be misinterpreted with catastrophic results. The accident investigation team concluded that the misinterpretation of the negative pressure test on the production casing was one of their key findings, that caused the blowout and explosion of the Deepwater Horizon platform. Nevertheless, negative pressure tests are widely recognized as an industry standard to assess well integrity.

As described above for the offshore test setting, the concept is similar in an onshore setting. The hydrostatic head inside the well is decreased to below the reservoir pressure outside the well, by reducing the hydrostatic pressure at a targeted position in the well as in a drill stem test. Typically, a test string with a test valve is used to circulate the lighter fluid down the well until the hydrostatic is reduced by the intended amount. Then, a retrievable packer is set to isolate the denser fluid in the annulus above the packer from the test interval. Opening the test valve in the test string makes the well underbalanced and allows to identify a faulty mechanical barrier, in case a backflow is observed. Once the string is closed again, and a pressure build-up is identified, this is a strong indication of a leaking shoe track. Note, that for passing the negative pressure test, both the flow check and the pressure check must be satisfied, because a low-rate leak through the shoe track might not be detected with one of the checks but is commonly noticeable with the realization of both checks. One problem with the test is fluid compressibility. As the lighter fluid is circulated in the test string, it is compressed. As the test string is opened after circulation and the fluid is drained, the compressibility of the fluid might mask a leak or lead to a falsely interpreted leak. The volume of fluid expected to bleed during the flow check portion of the negative pressure test can be predicted with calculations. Also, Horner Plots can be a meaningful tool to provide trend analysis to negative pressure test data collected over a shorter period to allow identification of compressibility and temperature effects.

Negative pressure tests are also very commonly applied to test the effectiveness of a cement squeeze or a cement seal at the top of a liner. Figure 18 shows the pressure response of a typical negative pressure test after a successful cementing job, with no downhole pressure change during the opening of a downhole valve.

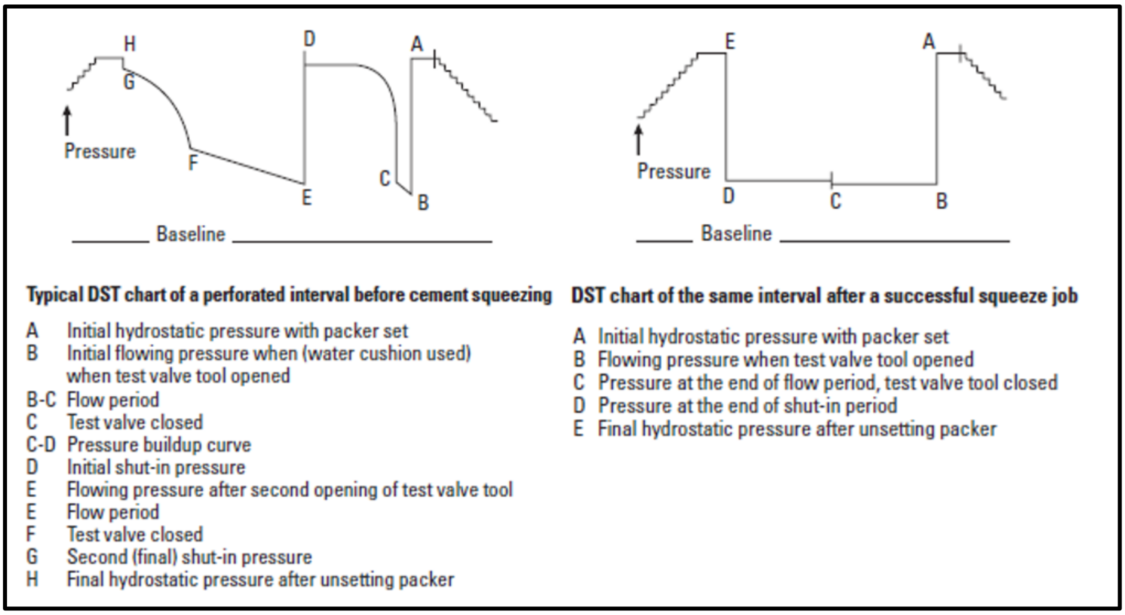

Figure 18: Typical negative-pressure test pressure chart; Source: (Nelson, Erik; Guillot 2006)

3.1.1.5 Formation Integrity Test (FIT)

Formation integrity testing is conducted after drilling out the casing shoe and is used to test and verify the integrity of the cement in the shoe track and the formation, up to a predetermined maximum pressure expected during drilling this section. The purpose is to investigate the strength of the cement bond around the casing shoe to ensure zonal isolation and to investigate the well’s capability to withstand pressure from below the shoe to validate the well plan regarding casing setting depths. The FIT result does not give much information about the strength of the formation, as the maximum pressure is in the linear region of the pressure vs. volume plot. It is a quick, cheap and fashionable test, and provides just enough information to drill ahead safely and is therefore preferred against the leak-off test. Another advantage of the FIT is the fact that the danger of formation damage due to the test is significantly reduced compared to the leak-off test. However, the downside is the absence of information about the actual strength of the formation and the limit during drilling in terms of fracturing.

3.1.1.6 Leak-Off Test (LOT)

During the LOT, the wellbore is shut-in and pressured up until the fluid will enter the formation or leak-off, either moving through permeable zones or through fracture creation in the rock. The leak-off pressure is the deviation point from the linear part in the pressure vs. volume plot. After this deviation is recognized, the pumps are stopped, and a pressure drop can be observed, which reflects the friction pressure losses in the well. It can be quite complex to determine the leak-off pressure because it takes a certain time and volume to be pumped beyond this point, which means that the maximum test pressure must be above the leak-off pressure. The purpose of this test is to determine the fracture gradient of the formation at the casing shoe, which dictates the maximum equivalent mud weight applied during the drilling operation. FIT and LOT are open hole tests, and factors like filtration and borehole expansion have to be considered. Whereas during negative and positive casing pressure tests, no open hole section influences the test curve behavior. After shut-in, the pressure is observed for some time before it is bled-off. This shut-in period can give valuable information on the formation's filtration properties.

3.1.1.7 Extended Leak-Off Test (xLOT)

An xLOT is an extended version of a leak-off test and is defined by pumping beyond the leak-off pressure point until a stable fracture propagation pressure is reached. Purpose of this test is to get information about the in-situ stresses unaffected by near-wellbore effects. Usually, these tests are performed in two or more cycles to witness fracture reopening to avoid counteracting with the formation tensile strength. Flow-back periods are crucial in the interpretation of an xLOT. Commonly, the xLOT is not part of the basic integrity tests frequently conducted during standard, conventional well construction. It is frequently performed in areas, where the in-situ stress magnitude is essential to know, such as before hydraulic fracturing.

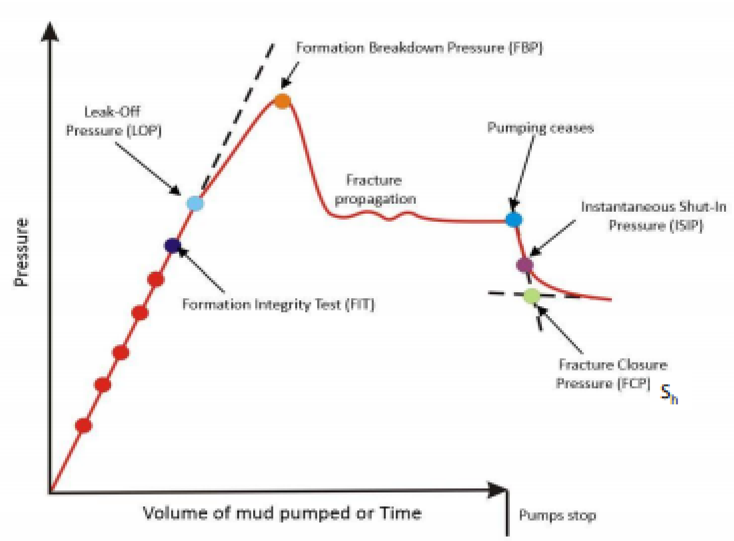

Figure 19: FIT and LOT pressure curves; Source: (Lahann, Rupp, and Medina 2016)

3.2 OMV-Current Best Practice

Positive Pressure Testing

OMV Well Engineering Technical Standards (WETS) include a chapter dedicated to positive-pressure testing. However, no real distinction in the procedure and passing criteria is made on the equipment that is tested. The test shall be preceded by a low-pressure integrity check for 5 minutes to detect severe leaks. Then pressure is increased in a stepwise manner to the anticipated testing pressure. The test is deemed to be successful if the recorded pressure has stabilized for at least 10 minutes. In terms of well integrity, all pressure containing casing, liner, completion, and production strings should be pressure tested. Also, all test data, including pumped and returned volumes, shall be recorded and stored correctly. Anticipated test pressure should not exceed the following: 90% of API burst rating, triaxial stress 80% of the nominal yield stress, connection pressure rating, or 75% of connection tensile rating. Surface and intermediate casing shall be tested to the burst design case (circulating out the calculated kick tolerance volume of influx using the Driller's Method) and the planned casing seat test (FIT, LOT) inclusive an upside margin. Casing and liners, where production or testing is anticipated shall be minimally tested to the shut-in tubing pressure. Also, liner laps shall be tested to assure integrity concerning the anticipated service pressure loads.

Negative Pressure Test/Inflow Test

OMV's operational well barrier integrity technical standard includes a short chapter about the inflow test. As already described, to conduct an inflow test, the hydrostatic pressure inside the well has to be reduced below the lowest pressure anticipated during the life cycle of the well in that configuration. Following test criteria must be defined as part of the approved test program:

1. Indications of success
2. Indications of failure
3. Plan to return the well in an overbalanced condition

Also, the fluid displacement shall be recorded in terms of pressures and volumes per a pre-defined schedule.

Formation integrity test (FIT) & Leak-off Test (LOT)

Usually, around 3-5 meters of new formations are drilled out, and then the drill string is pulled back into the last casing. Then the system is pressured up using a cementing unit by pumping small volumes of drilling fluid through the closed BOP. A rate of 0.25 bbl/min to 0.5 bbl/min is recommended (van Oort and Vargo 2007). As the final test pressure is surpassed, marked by a deviation from the straight line (for the LOT), pumps are stopped, and the well is shut-in. If a FIT is performed, pumps are stopped earlier at a pre-determined pressure. Instantaneous shut-in pressure is recorded at that point, reflecting the friction pressure losses during pumping. After the well is shut-in for a certain amount of time, the pressure is released from the shut-in valve, and if the test indicated sufficient formation strength to drill ahead safely, drilling is resumed. In case there is distrust about the validity, the test is repeated, preferably with the same test conditions.

Field experience has shown that using an RTTS^{R} Packer (for remedial-, treating-, testing- and squeezing operations) when performing a FIT/LOT helps to avoid excessive casing expansion in the upper part of the well. Excessive casing expansion can lead to damage of cement sheath, with eventual loss of well integrity, even if the cement has sealing properties after it had set. Based on experience, a rule of thumb has been established within OMV E&P Austria to use an RTTS packer, when the wellhead pressure is expected to exceed 50 bar (725 psi) during the testing operation.

3.3 Industry-Best Practice

United States Code of Federal Regulation-CFR 30 contains the first set of rules and regulations issued by federal agencies regarding national mineral resources. § 250.423 describes the requirements for pressure testing casing in federal U.S. waters. Following points are mandatory by law (Office of the Federal Register 2018):

- If pressure declines more than 10 percent in a 30 minutes test, the test has failed, and remedial action has to be done in the form of re-cementing or and additional casing string
- Minimum test pressure for the conductor casing is 200 psi and 70 % of minimum internal yield for surface, intermediate and production casing
- A positive and negative/inflow pressure test on the intermediate and production sections must be performed to ensure proper casing installation
- Test procedures and criteria for a successful test have to be submitted for approval together with the application for a permit to drill (APD) to the Bureau of Safety and Environmental Enforcement
- All test results have to be documented and recorded

A particular design for running and interpreting the test is not specified in the regulations.

Norwegian recognized standard NORSOK D-010 for well integrity and drilling operations is more detailed on the needed specifications to determine acceptable pressure testing criteria (NORSOK D-010 2004). The acceptable leak rates shall be zero, but for practical purposes, an acceptance criterion should be established to account for volume, temperature effects, air entrapment, and fluid compressibility. For situations where the leak rate cannot be monitored, the criteria for a maximum allowable pressure leak should be established. Pressure test direction should be in the direction of flow. This would be a negative pressure/inflow test in a producer and a positive pressure test in an injector well. However, if the well barrier element (casing shoe track) can seal the well in both directions, the test pressure can be applied against the direction of flow. NORSOK D-010 is also straightforward concerning pressure values and test duration. Pressure testing in drilling, completion and intervention activities should commence with a low-pressure test to 15-20 bar (217-290 psi) for a 5 minutes stable reading, followed by a 10 minutes high-pressure test at least equal to the maximum differential pressure that the well barrier equipment may become exposed to. In the production/injection phase, a 70-bar differential should be applied during the positive pressure test. The following applies to qualify a pressure test:

- Consideration of monitored volume when setting test acceptance criterion
- Establish a maximum deviation of the test pressure (e.g., 5 bar for a 345 bar pressure test)
- Establish a maximum allowable pressure deviation over the defined interval that makes the test a "pass" or a "fail" (e.g., 1% of the 345 bar pressure test or 3,45 bar)

Negative pressure/inflow tests should last for at least 30 minutes to reach stable readings or longer due to large volumes, highly compressible fluids, and temperature effects. According to NORSOK D-010, the execution of a negative pressure test shall be described by a detailed procedure containing the following:

- Identification of the tested well barrier elements and the consequences of a leak
- A diagram showing the configuration of lines and valve positions and an acceptance criterion for a "passed" test
- The risk of an inconclusive pressure test due to temperature effects, migration or large volumes and a plan of action in the event a leak occurs (remedial cementing) or the test is inconclusive (repetition)

During the execution of an inflow test, it shall be possible to displace the well back to the overbalanced fluid at the indication of flow or in case of inconclusive test results. Also, the displacement to an underbalanced state shall be performed with a closed BOP.

As already mentioned earlier, there is no industry-wide standard definition on how to conduct a negative pressure/inflow test, but after the Macondo incident, a lot of the major operating companies developed their own in-house detailed pressure testing procedures. Also, academia still was not able to develop a standard procedure. After extensive research (Mair 2015; DrillingForGas.com 2019; Baltes et al. 2017), it was found that many operators follow a similar procedure for a negative pressure test:

1. Calculate anticipated displacement volumes and pressures

2. Based on transmissivity[2], determine how much to underbalance the well
    - If $k_h > 1000\ mD$ - underbalance by 5% of the pore pressure
    - If $k_h < 1000\ mD$ - underbalance by 15% of the pore pressure
3. Calculate compressibility of drilling fluid in the hole
4. Pick up and run a retrievable inflow test packer with a circulating valve (RTTS)
5. Set the packer at the advised depth and test the annulus with ~1000 psi in order to check that the packer is appropriately sealing and that the tool assembly is functioning properly before running in hole further
6. Pick-up and circulate the calculated volume of lighter test fluid with an approved spacer ahead to underbalance the well
7. Utilize a cement unit for pumping
8. Ensure that the tool joint is not across the annular preventer or the blind shear rams
9. After displacement set the packer to perform the test
10. Bleed off drill-pipe pressure, bleed volumes should match compressibility calculations
11. Monitor the well up to 4 hours for deep wells, but at least 30 minutes
    - If the test valve is open, no returns should be seen
    - If the test valve is closed, pressure should remain at 0 psi
12. In the case of cement unit returns, or pressure increase → Failed Test
13. In case of trip tank losses → Failed packer bypass
14. Note: Monitoring for pressure is believed to be more controllable should the test fail
15. If successful, unset the packer and re-displace well to other fluid
16. If packer fails, re-set and re-test
17. If a negative test fails, displace to kill weight fluid and discuss way-forward
18. Otherwise, pull out of hole and lay down retrievable packer

3.4 Influencing Factors on Pressure Testing

In this section, the whole operational system, involved in pressure testing, will be investigated in great detail, and influencing factors on pressure tests are discussed. During a positive-pressure test, fluid is pumped into the wellbore through the kill line and a closed BOP, resulting in increasing pressure, controlled by the compressibility of the fluid. Increasing the pressure causes the stresses in the casing and cement to increase, which results in an expansion of casing until the system is balanced. The extreme case would result in damage to the casing or cement.

The examined effects are related to cased hole effects, as opposed to open effects during formation integrity testing. They include stresses and subsequent expansion/deformation of the casing, temperature effects, fluid compressibility, and air entrapment. These effects govern the behavior of a casing pressure test and can account for possible delusions in the interpretation. Understanding these effects determines the conclusiveness of a pressure test.

---

[2] Rate at which water passes through the rock horizontally, expressed in terms of horizontal permeability

3.4.1.1 Stresses and Deformations in Casing and Cement

All considerations about casing deformation or expansion during casing pressure testing are dependent on the outside and inside pressure, respectively the testing pressure plus the hydrostatic in the well, material properties of the casing and the cement and the geometry of the casing. Therefore, the cemented and uncemented parts have to be assessed separately. For the uncemented part, the outside pressure is represented by the hydrostatic pressure of the fluid in the previous casing annulus, whereas in the cemented part the casing is sustained due to the restriction of the hard cement. In the latter case, casing expansion due to positive pressure testing will be less significant, if not negligible. Also, the state of the cement hydration is essential to consider. In case the cement behind the casing subject to testing is still in a liquid state, no danger of cement bond destruction is likely to occur, whereas if the cement has already developed a bond, it will experience tensile loading from the casing and possibly break. It is therefore essential to know where the top of cement (TOC) is placed in the wellbore. However, this can be quite difficult to identify, as the cement and spacer form a transition zone during pumping. The uncemented part of the casing can expand quickly in the radial direction as it is not restricted by cement, opposed to the cemented part's inability to expand due to the strong cement bond right behind the casing. However, in case the cement job was poorly due to micro-annuli occurrence, the casing could allow for expansion leading to damage in the cement bond.

The bigger part of a production casing is not cemented up to the surface and has no cement in place. For cost and time reasons, only the lower part including the casing shoe is cemented. As mentioned, the uncemented part will be subject to deformation to a much greater extent than the cemented part.

The physical process of pressure testing, either in positive or in the negative direction, can be physically described with the help of machine elements and mechanics. Appendix A is dedicated to the derivation of the different types of stresses and deformations in a concentric cylinder, that is either internally pressurized as in a positive pressure test or externally pressurized as in a negative pressure test-not directly, but reducing the inside pressure leads to the same effect. Figure 20 shows a thick-walled cylinder, that is pressurized both internally and externally. Shear stresses in the circumferential and radial direction are not present due to the symmetry of the cylinder and the loading. Therefore, only normal stresses in the radial σ_r and circumferential direction σ_θ (hoop stress) are present. When talking about stresses and deformations in the casing, the casing is assumed to be an ideal thick-walled continuous concentric cylinder with an inside and outside pressure. During positive pressure testing, the pressure inside the casing is greater than outside, and during negative pressure testing, it is vice versa. As the pressure differential is increased, the pipe will begin to uniformly deform according to Hook's law and the strain and stress curve. First, the pipe will deform elastically until the yield point is reached, the onset of plastic deformation, eventually resulting in yield failure of the pipe. However, the aim of pressure testing is to keep the deformation elastic.

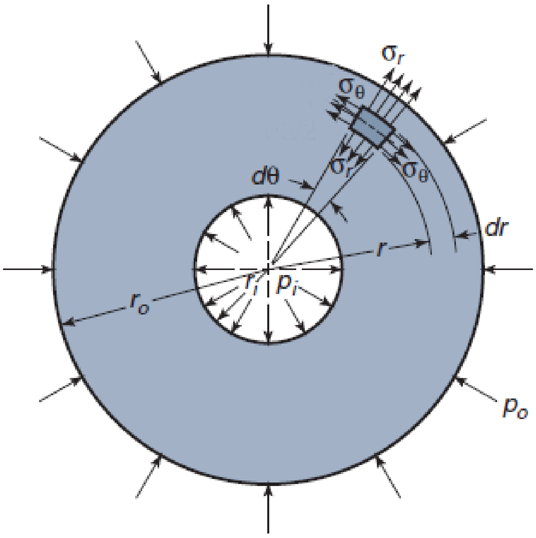

Figure 20: Pressures and stresses acting on a casing during expansion; Source: (Schmid, S.R.; Hamrock, B. J.; Jacobson 2014)

The radial displacement of a casing subject to internal and external pressure as depicted in Figure 21 can be described by Equation 1, derived in Appendix A

$$\delta_r = \frac{p_i r_i}{E}\left(\frac{r_o^2 + r_i^2 - 2\left(\frac{p_o}{p_i}\right) r_o^2}{r_o^2 - r_i^2} + \nu\right) \qquad 1.$$

Equation 2 gives the volumetric expansion of a casing subject to expansion. It is dependent on the pressure differential across the casing, the material properties, the geometry and length of the casing.

$$\Delta V = 2\pi L_{csg} r_i^2 \frac{p_i}{E}\left(\frac{r_o^2 + r_i^2 - 2\left(\frac{p_o}{p_i}\right) r_o^2}{r_o^2 - r_i^2} + \nu\right) \qquad 2.$$

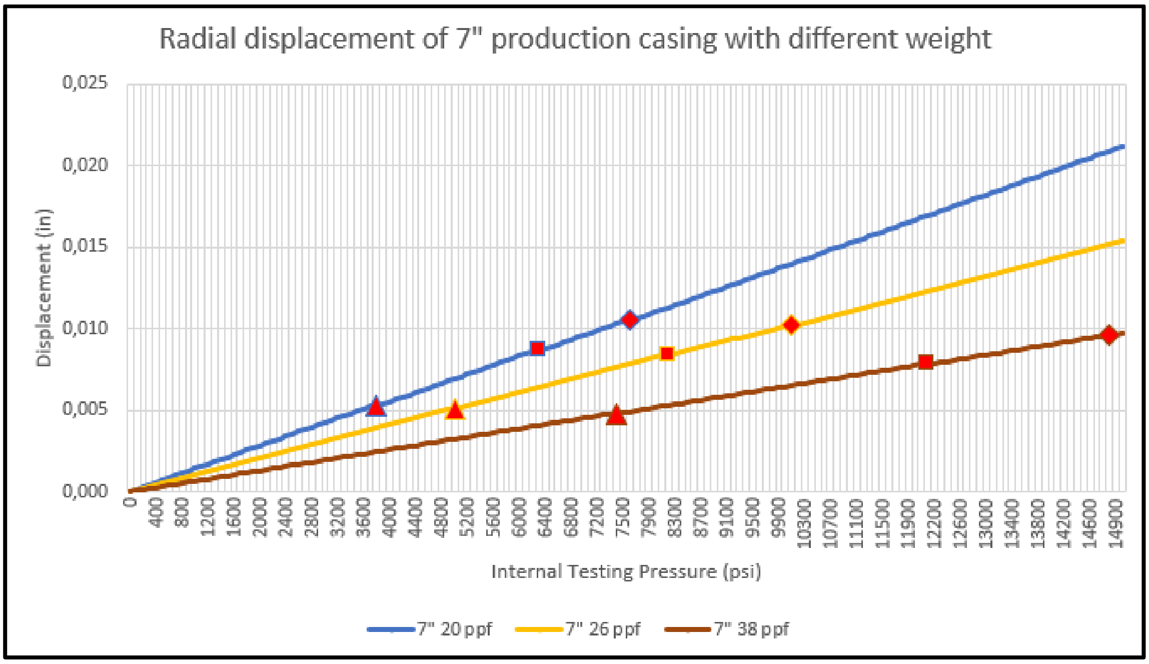

Figure 21: Radial displacement due to internal pressure marked by maximum internal yield pressure of K55, C90 and P110 casing grades with zero outside pressure

Figure 21 shows the radial displacement for 7-inch production casings with different weights based on Equation 1. With increasing internal testing pressure, the expansion in the radial direction is also increasing. Also, the expansion is less for a casing that has a higher nominal weight than for a casing with a lower nominal weight. The markers in the graph represent the maximum internal yield pressure for different casing grades. The triangles mark the yield pressure for a K55-casing, the squares mark the yield pressure for a C90-casing, and the twisted squares mark the yield for a P110-casing for the casings with the respective nominal weight. The markers can be associated with the limits of elastic deformation. Every testing pressure, exceeding these yield points, will result in permanent plastic deformation. Displacement values depicted in Figure 21 are based on the assumption that the outside pressure is zero. Material properties used to calculate the radial displacement have been assumed constant, even though different casing qualities would result in slightly different material properties. However, they are not very powerful in the calculation. Young's Modulus of 29 Mpsi and Poisson's ratio of 0.3 has been assumed.

Figure 22 shows the differential volumes in barrels due to the casing expansion for a 2000 feet long casing, with the same weights. In this example, an outside pressure of 1000 psi has been assumed. The outside pressure has a counteracting force to the casing expansion and is, therefore, reducing the radial displacement. During a green cement test, where the cement is still liquid, this pressure will be supplied by the cement slurry, spacer, and fluid. In the case presented in Figure 22, the casing expansion corresponds to differential volumes of below one barrel (159 liters) and is dependent on the length of the casing. Figure 23 shows the differential volume as a fraction of the original volume to make it independent of the casing length.

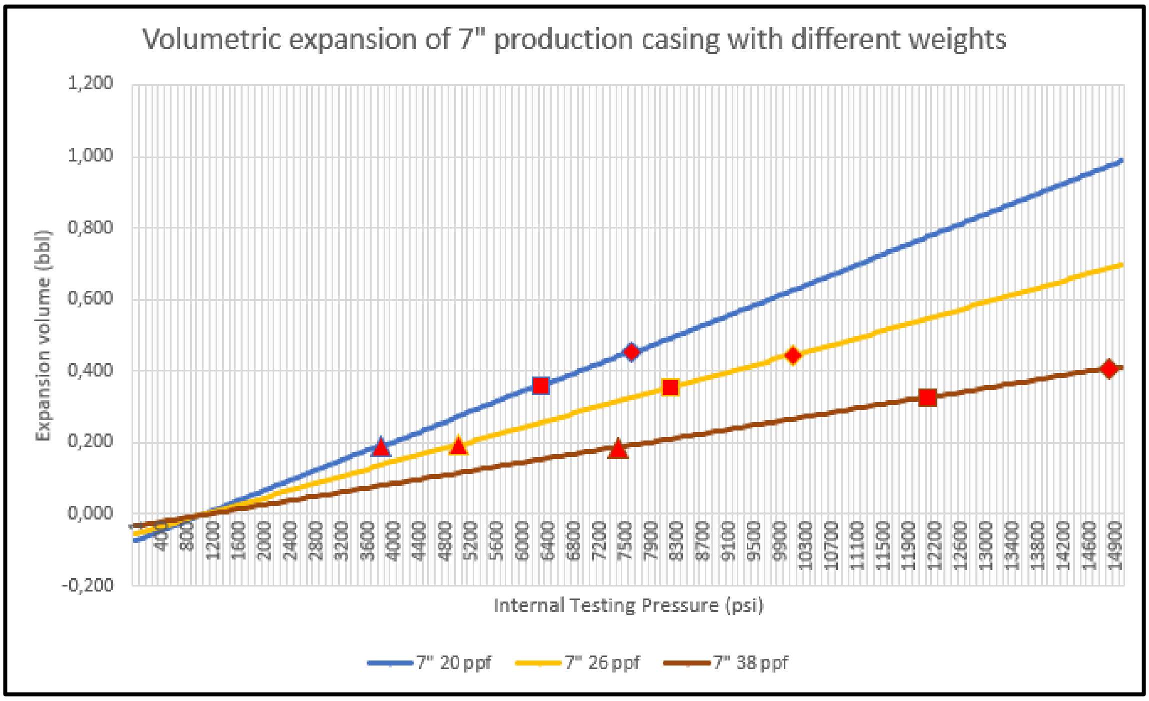

Figure 22: Volumetric expansion due to internal pressure, marked by yield pressure limits of K55, C90 and P110 casing grades with constant 1000 psi outside pressure

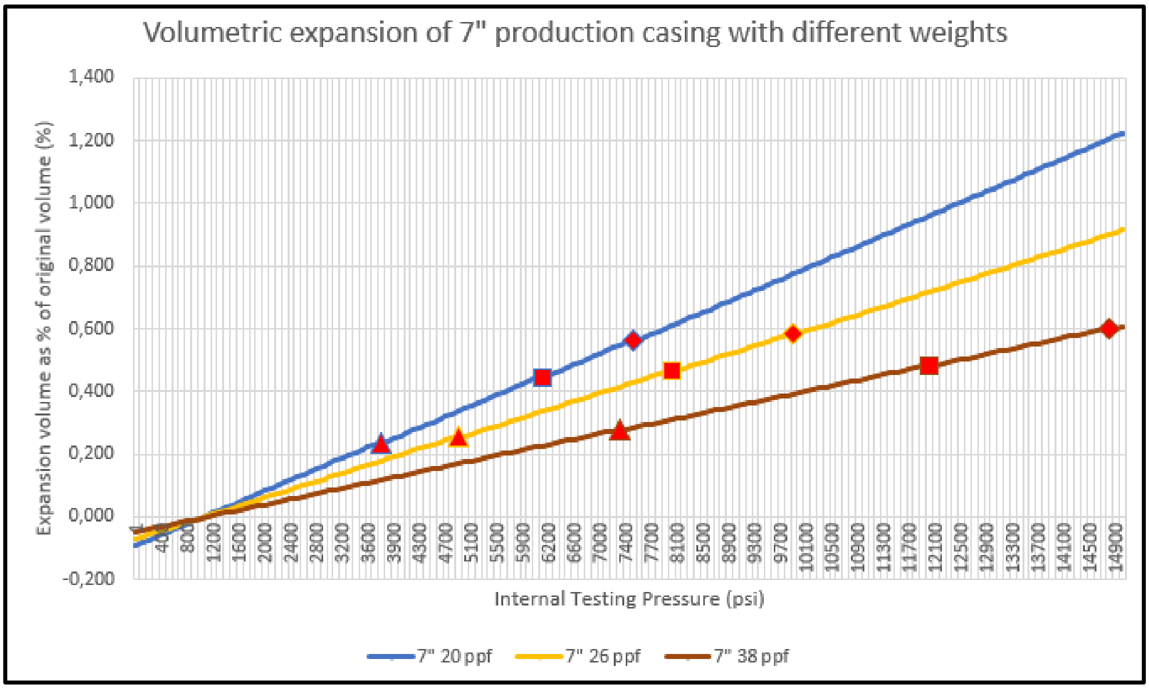

Figure 23: Volumetric expansion as a percentage of the original volume, marked by yield pressure limits of K55, C90 and P110 casing grades with constant 1000 psi outside pressure

3.4.1.2 Fluid Compressibility & Thermal Effects

The drilling fluid is the responsible transmitter of the desired testing pressure in the wellbore. The pressure acting inside the wellbore is dependent on the surface pressure and the hydrostatic pressure, with the latter being dependent on the density of the fluid and the height of the fluid column, referring to Equation 3

$$p_{hyd} = 0.052 * \rho * h \qquad 3.$$

Regarding Equation 3, the depth h of the well is fixed, but the density of the mud is subject to changes due to the compressibility of the fluid and thermal expansion and, or contraction. These effects are particularly prominent in oil-based muds and synthetic-based muds since they are significantly more compressible than water-based muds. Therefore, they must be adequately predicted with calculations to achieve a conclusive test outcome. During pressure testing, these effects are responsible for misleading, early data, falsely indicating a leaking barrier in the wellbore. Compressibility and thermal effects especially, significantly increase the duration of the negative pressure test and complicate the flow-check portion of the test. A plausible positive test result can only be identified, when the decreasing flow eventually diminishes to zero, and the fluid reaches steady-state conditions. This becomes even more challenging in deep wells, where large volumes and drawdowns may show effects related to expansion and contraction of steel or fluids. During negative pressure testing in deep wells of large volumes with a large density and temperature difference between the original fluid and the new underbalanced fluid, early measurements may be extensive and particularly misleading towards a failed test.

In deeper offshore wells, with their relatively cold downhole temperatures, compressibility is the predominant effect and leads to an increasing downhole fluid density, meaning that the downhole density is much higher than the surface density. Contrary, high-pressure, high-temperature wells are more prone to thermal effects, because the significant increase in temperature, leads to mud volume expansion, and the downhole density will be less than the surface density. However, the degree of density change is rather tricky to predict, as both the fluid compressibility and the thermal expansion coefficient are dependent on pressure and temperature changes along with the depth of the wellbore (refer to Equations 4 and 5). Therefore, the density function in the wellbore is non-linear (van Oort and Vargo 2007).

$$c_{mud} = \left(-\frac{1}{V}\frac{\Delta V}{\Delta P}\right)_{P,T} \qquad 4.$$

$$\alpha_{mud} = \left(\frac{1}{V}\frac{\Delta V}{\Delta \mathrm{T}}\right)_{P,T} \qquad 5.$$

Pressure surveillance during pressure testing in most of the cases still relies on the surface standpipe pressure. Downhole pressure gauges would help to avoid the misleading effects of compression and thermal effects on the interpretation of test results.

The negative sign in Equation 4 is vital in order to keep the value of mud compressibility positive since an increase in pressure would lead to a decrease in volume. However, in the case of a positive pressure test, the minus sign can be omitted, since the decrease in volume is compensated by pumping fluid. Appendix B shows a detailed derivation of the approximate solutions of the compressibility equations, relating the differential volume, mud compressibility and expansivity, original volumes, and pressure and temperature changes.

$$\Delta V = c_{mud} V_0 \Delta P \tag{6.}$$

$$\Delta V = \alpha_{mud} V_0 \Delta \mathrm{T} \tag{7.}$$

The compressibility c_{mud} is representative of the effective compressibility of the whole system, accounting for water and other synthetic or diesel base fluid components and solids. It can become quite complicated to calculate the exact system compressibility, as the fluid is comprised of multiple components in multiple phases. Therefore, for quick fluid compressibility calculations, usually performed by the mud engineer on-site, a simplified, effective fluid compressibility c_{eff} (refer to Equation 8) is established to calculate the volume of fluid, that will compress during the pressure test. The mud engineer provides the volume, usually in numbers of barrels, that is expected to flow back during the pressure test. In case the real backflow is significantly more than the calculated, inflow through the casing shoe is very likely to be present.

$$c_{eff} = c_{water} \cdot F_{water} + c_{synth} \cdot F_{synth} + c_{soldis} \cdot F_{solids} \tag{8.}$$

Equation 8 represents the effective compressibility of the fluid system by merely multiplying the compressibility of the single components with their fraction in the fluid system.

The following example shows the fluid compressibility for a specific negative pressure test. As already mentioned in Chapter 3, during the negative test, the hydrostatic head inside the well is decreased, by reducing the hydrostatic pressure at a targeted position in the well. Typically, a test string with a test valve is used to circulate the light fluid, water in this case, down the well until the hydrostatic is reduced by the intended amount. After this fluid displacement, there is a fluid column comprised of the lighter fluid and the heavier fluid in the wellbore. Due to their different components, the compressibility of these fluid columns each has to be calculated separately.

Fluid Compressibility Calculation for Light Fluid (effect of temperature not accounted for)			
Inputs: Fluid compressibility for a negative pressure test			
Percent Water (%)	100	Production Csg Volume (bbl)	
Percent Synthetic (%)	0	Drill String Volume (bbl)	
Percent Solids (%)	0	Open Hole Volume (bbl)	
Drill pipe pressure before the test (psi)	1200	Kill Line Volume (bbl)	
Average wellbore pressure (psi)	1416,6		
Base Oil Type (1 for Diesel, 2 for synthetic)	2	Total Volume (bbl)	500
Results:			
Number of Barrels compressed during the pressure test (bbl)			2,12
Rule of Thumb for Compressibility (0.000003*psi*bbl)			2,12
Calculation:			
$c_{eff} = c_w \cdot F_w + c_{syn} \cdot F_{syn} + c_s \cdot F_s$ (1/psi)			3,0*10^-6
Where,	fluid ρ (ppg)	8,33	
c_{eff}=effective compressibility (1/psi)	Depth (ft)	1000	
c_w=water compressibility = (3,0*10^-6)			
c_{bo1}=synthetic compressibility = (5,06*10^-6)			
c_{bo2}=diesel compressibility = (4,56*10^-6)			
c_s= solids compressibility = (0,2*10^-6)			

Table 1: Fluid compressibility calculation for the lighter fluid part (water in this case) of a negative pressure test

Fluid Compressibility Calculation for Heavy Fluid (effect of temperature not accounted for)			
Inputs: Fluid compressibility for a negative pressure test			
Percent Water (%)	30	Production Csg Volume (bbl)	
Percent Synthetic (%)	55	Drill String Volume (bbl)	
Percent Solids (%)	15	Open Hole Volume (bbl)	
Drill pipe pressure before the test (psi)	1200	Kill Line Volume (bbl)	
Average wellbore pressure (psi)	1486		
Base Oil Type (1 for Diesel, 2 for synthetic)	2	Total Volume (bbl)	500
Results:			
Number of Barrels compressed during the pressure test (bbl)			2,76
Rule of Thumb for Compressibility (0.000003*psi*bbl)			2,23
Calculation:			
$c_{eff} = c_w \cdot F_w + c_{syn} \cdot F_{syn} + c_s \cdot F_s$ (1/psi)	3,713*10^-6		
Where,	fluid ρ (ppg)	11	
c_{eff}=effective compressibility (1/psi)	Depth (ft)	1000	
c_w=water compressibility = (3,0*10^-6)			
c_{bo1}=synthetic compressibility = (5,06*10^-6)			
c_{bo2}=diesel compressibility = (4,56*10^-6)			
c_s= solids compressibility = (0,2*10^-6)			

Table 2: Fluid compressibility calculation for the heavier fluid part (Synthetic-oil based mud in this case) of a negative pressure test

Heavier fluid part compressed (bbl)	2,76
Lighter fluid part compressed (bbl)	2,12
Total fluid compressed (bbl)	4,88

Table 3: Total fluid compressibility of a negative pressure test

Table 1 shows the fluid compressibility calculation for the water-filled part of the hole during a negative pressure test. As already mentioned earlier, during a negative pressure test, fluid compressibility is essential to know. Table 2 shows the fluid compressibility calculation for the heavier part, filled with the mud. In the example above, the pressure on the drill pipe before the test valve is opened is 1200 psi. As soon as the test is started and the test valve is opened, 4,88 barrels of fluid should be recovered from the wellbore, for the negative pressure test to be deemed successful. In case more barrels would be recovered, this might indicate a well integrity problem at the shoe or another mechanical barrier. As in wellsite drilling operations often the case to simplify things, a rule of thumb exists, that can be used during “quick and dirty” calculation.

Through the multiplication of 3,0*10^-6 (compressibility of water) with the drill pipe pressure and the hole volume in barrels, a rough estimate can be calculated.

The following example shows the fluid compressibility calculation of a positive casing pressure test or green cement test. Input parameters have been taken from an actual cementing operation with a subsequent casing pressure test, performed on April 23rd, 2019 on a 9 5/8 casing (1650 m MD) on OMV's Bernhardsthal Süd 10 well, a producer targeting the Eggenburg Sandstone in Mistelbach County, Lower Austria. After bumping the plug, the casing has been tested to 250 bar (~3620 psi) for 10 minutes. The provided fail/pass criteria was a pressure drop of more than 5% within the 10 percent observation time. Cementing service has been provided by Halliburton. The fluid used for green cement test was a water-based potassium carbonate mud, which was also used to drill the next section (8 ½" hole with a 7" production casing).

Fluid Compressibility Calculation (effect of temperature not accounted for)			
Inputs: Fluid compressibility for a positive-casing pressure test (green cement test)			
Percent Water (%)	80	Production Csg Volume (bbl)	400
Percent Synthetic (%)	5	Drill String Volume (bbl)	
Percent Solids (%)	15	Open Hole Volume (bbl)	
Surface test pressure (psi)	3625	Kill Line Volume (bbl)	
Average wellbore pressure (psi)	3625		
Base Oil Type (1 for Diesel, 2 for synthetic)	2	Total Volume (bbl)	400
Results:			
Number of Barrels compressed during the pressure test (bbl)			3,9
Rule of Thumb for Compressibility (0.000003*psi*bbl)			4,4
Calculation:			
$c_{eff} = c_w \cdot F_w + c_{syn} \cdot F_{syn} + c_s \cdot F_s$ (1/psi)	2,658*10^-6		
Where,	fluid ρ (ppg)	9	
c_{eff}=effective compressibility (1/psi)	Depth (ft)	5000	
c_w=water compressibility = (3,0*10^-6)			
c_{bo1}=synthetic compressibility = (5,06*10^-6)			
c_{bo2}=diesel compressibility = (4,56*10^-6)			
c_s= solids compressibility = (0,2*10^-6)			

Table 4: Fluid compressibility calculation for a green cement test on OMV's Bernhardsthal Süd 10 well

While fluid compressibility due to pumping is only one cause for the backflow after a green cement test, expansion of the drilling fluid due to geothermal heating also plays a role. Green cement pressure tests and positive pressure tests, in general, are usually very short in duration and range from 10-30 minutes. Geothermal heating of the mud leading to fluid expansion is minimal during a 10 minutes green cement pressure test. However, it has to be considered to predict the backflow/return as accurate as possible. Equation 71, derived in Appendix C, gives the volume gain due to geothermal heating and subsequent expansion of the drilling fluid. The biggest challenge and uncertainties in that equation are dictated by the fluid expansion coefficient α and the actual temperature in the wellbore. It is tough to predict the average temperature in the wellbore after 10 minutes. However, the example provided below should give an approximation to make a sound conclusion on the backflow/return after the green cement pressure test, which is dictated by the fluid compressibility due to pumping and the thermal expansivity of the fluid due to geothermal heating.

Thermal Expansivity Calculation			
Inputs: Thermal Expansivity for a positive-casing pressure test (green cement test)			
Surface Mud Temperature (°C)	36	Production Csg Volume (bbl)	400
BHCT (°C)	45	Drill String Volume (bbl)	
BHST (°C)	60	Open Hole Volume (bbl)	
Avg. mud temperature in the wellbore (°C)	40,5	Kill Line Volume (bbl)	
Avg. temperature difference before & after test (°C)	4,5	Total Volume (bbl)	400
Results:			
Number of Barrels expanding due to thermal heating (bbl)			1,1
Thermal expansion coefficient of mud (1/°C)	6,00*10^-04		

Table 5: Thermal expansivity calculation for the Bernhardsthal Süd 10 well

Calculated returns due to fluid compressibility (bbl)	3,9
Calculated returns due to thermal expansivity (bbl)	1,1
Total expected returns (bbl)	5
Actual returns (bbl)	4,25

Table 6: Calculated versus actual returns

Table 4 shows the fluid compressibility calculation of a green cement pressure test. With an anticipated testing pressure of 3625 psi (~250 bar), some 3,9 barrels due to fluid compressibility and 1,1 barrels due to thermal expansivity should flow back after bleed-off. Given the uncertainties in this calculation, dictated by compressibility, thermal expansion coefficient of the mud, average pressures, and temperatures before and during the test and the fraction of the single mud components, the total expected calculated returns of 5 barrels are a somewhat acceptable solution compared to the actual returns of 4,25 barrels.

3.4.1.3 Air entrapment

It is imperative to condition the mud used during a casing pressure test, to confirm a mud of even density, which is free of gas and solids. At least one complete hole volume (“bottoms up”) should be circulated to achieve that. In case any gas or air is entrapped in the system during pressure testing, this will influence the test in the early pumping phase but also provide an extended tail at the end when bleeding-off the pressure. Air entrapment is also a significant factor to account for when doing formation integrity tests like LOT or xLOT. The equipment should be prepared and rigged up in a way to avoid air entrapment. Also, enough homogeneous drilling fluid should be available to do the test. Use defoamers in case the fluid is exhibiting a foaming behavior to avoid air entrapment.

Chapter 4 **Well Construction Scorecard Tool**

One primary motivation for this thesis is to develop a wellbore scorecard, that is scoring the well based on well construction responses and parameters from drilling the section of interest, final BHA pulls, casing running and various cementing and green cement test parameters. With the help of this scorecard low-performing well sections, in terms of well construction, can be easily identified. Next step should help to link bad performing wellbore sections to shortcomings in the well construction process. The scorecard tool is capturing everything going on while the cement is still in the liquid phase. Wells facing some well integrity or zonal isolation problems are especially interesting because the analysis should help determine the reason for their failure.

Another goal of this scorecard was to potentially replace the execution of often inconclusive and unsatisfactory negative pressure tests with something less expensive and time-consuming. Therefore, the aim of the score is also to determine whether a section is prone to problems, and a negative pressure test for well integrity assurance is indispensable. With the help of field data, the quality of the scoring tool should be tested on its ability to prescribe or avoid the execution of a lengthy and expensive negative pressure test based on the score for the section of interest. However, as OMV Austria is conducting these negative pressure tests only on liner laps, bridge plugs and cement plugs and only limited tests were conducted in the last years, the tools ability to prescribe the negative pressure test is still unsure and needs further testing.

Measuring the wellbore quality, targeted to make future decisions in a meaningful way is potentially a highly complex process. Literature shows that scoring the well based on different operational KPIs, responses, and parameters have been used successfully in the industry. Mason et al. used scoring as a new initiative which has the aim of reducing subjectivity around the quantification of wellbore quality. The resulting scheme is a process which includes enhanced drilling performance, ease of running casing, improved logging tool responses, and excellent cement jobs to give the term "wellbore quality" a meaning. Ravi et al. introduced cementing best practices scorecard to asses well reliability and zonal isolation in Indonesian geothermal wells. The most recent approach using scoring has been made by Heu et al.. In a deepwater development campaign, offshore Malaysia, cement isolation between the 9 5/8" production casing is a critical parameter for zonal isolation and well integrity reliability throughout the life of the well. Their approach to achieving this was to deploy a structured approach focused on designing and optimizing KPIs.

4.1 Background-Wellbore Quality

Knowledge of the quality of the drilled, cased and cemented wellbore sections is crucial to determine the necessity of further testing to assess the integrity of the well. Therefore, it is vital to inspect the possible reasons for wellbore quality damage. Many of these damages and impairments happen during the drilling process, final bottom-hole-assembly (BHA) pull, casing running, and cementing. Choosing the optimal BHA has a significant influence on the wellbore's shape and will determine if the wellbore will be spiralled and look like a corkscrew. This will result in a negative influence on subsequent BHA pull, casing running, and proper cement displacement. Selection of the mud type and weight will influence wellbore breakouts, possible overbalanced conditions resulting in fracturing and fluid loss. The rate at which the rock is crushed at the bit and the properties and flowrate of the mud control the efficiency of cleaning the wellbore from cuttings. Vibration tendencies of the BHA string will also be a result of inappropriate drilling practices. Tripping in and out of the wellbore will determine swab and surge pressure cycles in the wellbore, which might even lead to rock fatigue failure. Casing and completion running might lead to extreme surge pressure cycles, if not handled properly.

It is also evident that the maximum wellbore quality that can be achieved is limited by subsurface conditions. If the drilling environment is favorable, high wellbore qualities can be achieved. However, if weak and younger formations are drilled, lower levels of wellbore quality are achieved. Also, the trajectory of the well and how it intersects with these formations have an influence.

There are many interconnected parameters dictating the quality of the wellbore. The nature of these interactions is somewhat complicated, and it would be highly impracticable to measure them directly to assess the wellbore quality. Therefore, the best approach to do it is to capture the output responses of drilling, BHA pull, casing running, and cementing. In the following paragraph, planning and well delivery criteria, as well as subsurface conditions, that influence wellbore quality are listed. As already mentioned, the complex interactions between these variables attempt to rank them in any way very hard. However, understanding the sensitivity of the wellbore quality to the various controls is crucial during the planning and execution phase of the well (Mason et al. 2006).

1. Well planning
    - Drilling fluid: type, weight, rheological properties
    - Drilling assembly: weight, diameter, connections, bit and BHA design
    - Well profile/trajectory: depth, azimuth, inclination, dogleg severity, tortuosity
    - Drilling practice/parameter: flow rate, weight-on-bit (WOB), revolutions per minute (RPM), rate of penetration (ROP)
    - Hole size: low or high annular clearance
    - Casing design: geometry, weight, depth, and length of the shoe
    - Ideal casing running (surge) and centralization practices
    - Ideal tripping and connection practices (surge and swab)

2. Well Delivery
    - Drilling assembly vibrations: different modes leading to equipment failure
    - Hole cleaning efficiency: residual cuttings accumulation
    - Ledges and key seatings: formation transitions (hard-soft), might lead to stuck pipe

  - Wellbore instability: wellbore breakouts-hole roundness/ovality
  - Wellbore profile: spiralling, micro-tortuosity, amplitude and pitch
  - Torque and drag responses
  - Real casing running and centralization practices
  - Real tripping and connection practices

3. Subsurface Conditions
   - Pore pressure and fracture gradient: mud overbalance, sensibility to circulation losses
   - Geothermal gradient: thermal effects influence cementing and pressure testing
   - Lithology: rock types, strengths, tectonics (fault)
   - Gas readings: cement might get channels during curing

4.2 Scorecard-Methodology

Reviewing the context and usage of the term wellbore quality in a meaningful way can be rather complicated. For the operator, a wellbore of high quality means a well section, that is drilled safely, cost-effectively, meeting the reservoir and production objectives. For the drilling contractor, it could mean that no equipment failures and unplanned maintenance have occurred during well construction. For the cementing contractor, it could mean a well that is ideally in gauge with 100 percent casing stand-off and the planned slurry characteristics and volumes and displacement process match with the proposed job design. Whereas, for the driller, it might mean that all the anticipated drilling parameters were kept in their range. Comprehensively, the meaning of wellbore quality as a generic term involves all these considerations.

Consequently, to make predictions about possible well integrity events, especially the cementing part of the wellbore delivery process becomes essential. If specific cementing parameters are not meeting industry standards, well integrity of casing shoes and liner laps might potentially be jeopardized at a later stage of the well life cycle. Therefore, the pressure test scoring tool was proposed to capture 57 parameters and responses that are assessing the performance of the well construction process, to find root causes of well integrity events.

Each response and parameter is weighted to represent its contribution to a proper well construction process. The tool emphasizes on a set of the following four different parameters and responses. Meeting the design goal or recommended value for these parameters is crucial to achieving a reliable well construction process assessment.

1. Drilling response
2. Final BHA pull-out-of hole response
3. Casing running response
4. Cementing and fluid relevant parameters

The tool was created to meet the following design criteria

- Simplicity: if the tool is too complicated to use and it takes time to understand its usage and handling, no one will use it

- Objectiveness: it is essential that the user understands the tool's functions but also its constraints
- Robustness/Consistency: it is essential that the tool is used steadily, no matter the geographic or geologic change
- Applicability: The scorecard is a new approach to find root causes for possible well integrity events not carved in stone. Further evaluation of more data should be made, and the user is encouraged to modify the tool and add any operations or parameter she/she finds indispensable to make a sound and reliable statement

The tool has been designed to reach a maximum score of 100. A score of 0 means that the wellbore section was not able to reach total depth due to a stuck pipe and the maximum score of 100 represents the "perfect wellbore." A score in the range of 0-65 strongly indicates very low wellbore quality, while a score of 65-80 suggests a somewhat mediocre wellbore quality. A score range of 80-100 indicates impeccable wellbore quality as indicated by Table 7.

100-80	Perfect/impeccable wellbore quality
80-65	Moderate wellbore quality
<65	Poor wellbore quality

Table 7: Scoring ranges define the wellbore quality

4.2.1 Drilling Response

The influence of the drilling response on the pressure test scoring tool is limited. During drilling, a lot of interconnected parameters are actively influencing wellbore quality, making a quality analysis of the wellbore very complicated.

Furthermore, the well construction process can usually recover from minor incidents like inadequate hole cleaning due to cuttings bed accumulation of minor mud losses. Therefore, only a moderate impact on the overall achievable score is made. The maximum score that can be achieved in the drilling section is 10, which accounts for only 10 percent of the total score. The drilling responses are ranked from the most severe response to the most favorable one. For drilling, the primary indicator of a low score is stuck pipe or near stuck pipe events, as seen in Table 8. Events like stuck pipe incidents, near stuck pipe incidents or severe mud losses, might represent a challenging drilling environment and can lead to various problems during BHA pull, casing running and cementing operation, deteriorating the integrity of the well.

Usually, during drilling, hook load and torque, and drag parameters are continuously monitored. The torque and drag readings, often provided by the directional drilling contractor and indications in the daily drilling report are the primary source of information to assess the drilling response. If the torque and drag data follows a smooth and expected trend instead of an erratic, noisy and elevated one, this is indicating a somewhat acceptable drilling quality. In case the torque and drag parameters are even lower than what the simulation or findings from offset wells suggest, wellbore quality in the drilling response is considered to be at the highest level. Elevated gas readings might influence the integrity of the cement, indicating possible micro-channel formation during the transition time and are therefore also included in the scoring tool.

The response corresponding to the most severe event occurring should be entered into the scoring tool and also represents the total drilling score.

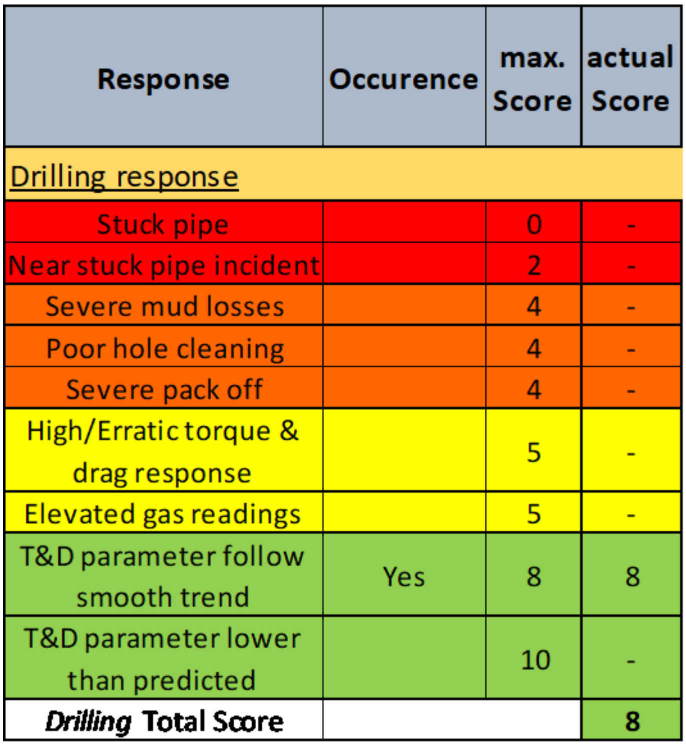

Response	Occurence	max. Score	actual Score
Drilling response			
Stuck pipe		0	-
Near stuck pipe incident		2	-
Severe mud losses		4	-
Poor hole cleaning		4	-
Severe pack off		4	-
High/Erratic torque & drag response		5	-
Elevated gas readings		5	-
T&D parameter follow smooth trend	Yes	8	8
T&D parameter lower than predicted		10	-
***Drilling* Total Score**			**8**

Table 8: The drilling responses are ranked from most severe to most favorable. The most severe response is determining the total drilling score for the section, high/erratic torque and drag in this case

4.2.2 Final Bottom Hole Assembly Pull-out of Hole Response

The last BHA pull before casing running gives important indications on the condition of the wellbore and determines if it is ready for completion. The last pull might be tripped out of hole with the assistance of the mud pumps, or it might be back reamed. Wiper trips, cleaning trips, or test trips are also frequently run to assure optimal conditions for further operations.

As in the previous section, a stuck pipe event results in the lowest possible score during the final BHA pull. A less severe incident would be sections with persistent and continuous overpulls. This phenomenon might indicate a potential differential sticking environment, triggered by the presence of a residual cuttings bed. The next less severe response might be indicated by isolated overpulls due to ledges and key-seatings. They frequently occur while drilling in sequential formations, consisting of alternating soft and hard layers, as shown in Figure 24. BHA and tool joints quickly wear the soft and naturally fractured formations, while the harder and more abrasive formations are still in gauge.

Ledges occur in the harder-in gauge formation and key seatings in the softer out-of-gauge hole part. Both lead to mechanical stuck pipe event. Some ledges might not be detected when pulling out of hole, but only when running back into the hole and also the other way round, some might be detected when pulling out of hole but not when running back in. Therefore, it is essential to run the BHA across possible ledges multiple times to assure the subsequent passage of the casing and proper cement distribution in the annular space.

Table 9 shows the BHA pulling response scorecard. The maximum score that can be achieved in this section is 9, which is characterized by lower than expected drag values. So, it is considered to provide a somewhat similar contribution to the complete scorecard, as the drilling response, around 10 percent.

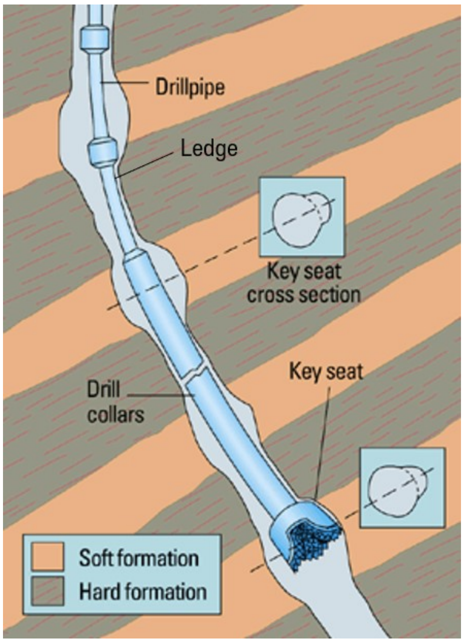
Drillpipe
Ledge
Key seat cross section
Drill collars
Key seat
Soft formation
Hard formation

Figure 24: Key seats and ledges occur when drilling in sequential formations; Source: (Schlumberger Oilfield Glossary 2018)

Responses	Occurence	max. Score	actual Score
Stuck pipe		0	-
Section lengths with overpulls >100 klbs due to residual cuttings		1	-
Section lengths with overpulls >25 tons due to residual cuttings		2	-
Isolated overpulls >50 tons due to ledges		3	-
Isolated overpulls >15 tons due to ledges		4	-
Tight spots	Yes	5	5
Loss circulation		6	-
Unplannned circulation		6	-
Unplanned reaming & backreaming		6	-
Drag follows smooth trend		8	-
Drag lower than predicted		9	-
Final BHA pull-out of hole Total Score			5

Table 9: The final BHA POOH responses are ranked from severe to favourable. The most severe response is determining the total final BHA POOH-score for the section, tight spots in this case

4.2.3 Casing running response

The casing running process is the last well construction process before cementing. According to experience, it is assumed, that casing running response already provides a more significant measure to detect wellbore quality and future well integrity problems. That is why a maximum score of 15, out of 100 can be reached, based on the fact that the casing running process is hypersensitive to remaining wellbore construction shortcomings. Any defects like ledges and keyseats or tight spots are not so quickly dealt with anymore, once the casing is in the hole. Also, the casings have relatively large diameter, leading to lower annular clearance compared to the drill pipe, high weight, and stiffness, and elevated surge pressures are making casing running very delicate. Usually, given a proper drag analysis, the casing string can be run to total depth. In case there are any residual wellbore effects, it will impact casing running negatively. As in the two responses described earlier, a stuck pipe is again the most severe response and therefore serves as the lowest benchmark score.

The next less severe response is static friction, usually happens, when the casing travels through a zone that is prone to differential sticking, the most frequently occurring stuck pipe event, and is easily detectable from a static drag on connections. This can happen due to a thick filter cake in the wellbore. Given these circumstances, casing centralization is of great importance to avoid a stuck pipe event.

Further, less severe responses include tight holes, minor ledges, or residual cuttings. The first planned course of action for these problems are wiped joints to reduce elevated drag levels, unplanned rotation or reaming, circulation to lubricate the casing and clean residuals in the wellbore, as shown in Table 10.

Responses	**Occurence**	**max. Score**	**actual Score**
Casing running response			
Stuck casing		0	-
casing pulled due to inability to run it		0	-
static friction>50 tons on connection		2	-
static friction > 25 tons on connection		4	-
unplanned rotation to assist casing running		6	-
circulation used to assist casing run		8	-
joints wiped to reduce elevated drag levels		10	-
elevated but smooth drag levels		12	-
expected drag levels measured	Yes	14	14
better than expected drag levels		15	-
Casing running Total Score			14

Table 10: The casing running responses are ranked from severe to favourable. The most severe response is determining the total casing running score for the section. In this case, the drag level measured was as expected

The inability of running the casing to total depth might be owed to different factors, such as too low clearance between hole diameter and casing connector's outside diameter, tight spots, and ledges, sloughing shales, poor centralization practices, and poor operational practices.

4.2.4 Cementing/Fluid Relevant Parameters

Conventional textbook cementing practices describe a successful cementing job when the top plug bumps the bottom plug, execution of a successful casing pressure test, and no losses during cementing operation. Without any doubt, these parameters are undoubtedly crucial for a successful cementing operation, but there are numerous other KPIs that actively contribute to the indication of proper zonal isolation through the whole life cycle of the well. The proposed drilling fluid and cementing scorecard proposes a set of 27 parameters that are not only essential for a successful cementing job but also zonal isolation and well integrity. Every parameter is weighted according to its contribution to a cement job. The parameters in this section are not ranked from most severe to most favourable. They are somewhat independent of each other and are compartmentalized in categories.

Indeed, there are many more parameters that are not included in the scorecard. For some it might even be easier to determine their design goal, and limit values might be self-evident for the crews involved. The complete scorecard is aimed to achieve greater well integrity through sparking awareness on all the influencing factors on well integrity. The cementing part of the scorecard is divided into four sections.

1. Mechanical/Operational Well Design Factors
2. Cement Slurry Parameters
3. Hydraulic/Operational Parameters
4. Casing Pressure Test Parameters

4.2.4.1 Mechanical/Operational Well Design Factors

Casing/Liner Centralization: Pipe Standoff should be above 70 percent in the critical zone of the well. High standoff values are critical for proper cement slurry placement in the annulus, as indicated in Chapter 2.

Drilled Hole Diameter: The minimum hole diameter should be higher than the casing outside diameter + 1,5 inches contingency, and the maximum hole diameter should be smaller than the casing outside diameter + 4 inches contingency. Calliper logs help to determine the exact geometry of the hole. Annular clearance and centralization are essential in very small annuli as pipe movement and displacement are restricted. In case of very large annuli, extreme high displacement rates are needed to achieve critical flow for proper mud and debris removal.

Mechanical Separation: Primary cementing success depends heavily on the mechanical wiper plugs. It is imperative to run a wiper plug ahead of the lead cement, behind the spacer and also a wiper plug tight behind the tail cement and ahead of the displacement fluid. This separation of fluids should avoid cement contamination, which is a significant contributor to cementing failure. Never run the bottom plug ahead of the spacer.

Clearance: The casing clearance between the casing connector thread and the previous casing inside diameter is exceptionally narrow and could pack-off with cuttings. Therefore, a minimum clearance of 25 millimeters should be present.

Shoe track length: Shoe track is one of the most critical components when talking about well integrity because it is usually left with high-quality tail cement to ensure proper cement is placed around the shoe track casing joints. In case no cement would be left inside the shoe track, the risk of over-displacement due to volume miscalculation would be much higher. Therefore, it is recommended to use two joints for casing sizes greater than 9 5/8″ and three joints for casing size less or equal to 9 5/8″.

Casing outer surface: Sandblasting the outer surface of the casing might help to improve the casing-cement bond. The increased roughness on the casing's outside surface might prevent casing-cement debonding, potentially avoiding a well integrity incident.

Parameter	**Design Goal/Recommended Value**	**Design & Actual Match**	**max. Score**	**actual Score**
Mechanical/Well Design Parameters				
Casing/Liner Centralization	≥ 70% standoff & 500 ft above critical zone	Yes	6	6
Drilled hole diameter	Min. Hole Diameter ≥ Csg OD + 1.5 in Max. Hole Diameter ≤ Csg OD + 4.0 in	Yes	2	2
Mechanical Separation	Wiper plug immediately ahead cement & top plug immediately after cement	Yes	2	2
Clearance	Cased Hole ID ≥ 25 mm than casing connector OD	Yes	2	2
Shoe track length	2 joints for csg > 9 5/8 in; 3 joints for csg ≤ 9 5/8 in	No	4	0
Casing outer surface	Sand scratch/blast to remove mill varnish & improve casing cement bond	No	1	0
Mechanical/Well Design Total Score				12

Table 11: Parameters representing the mechanical/well design factors

4.2.4.2 Cementing Slurry Parameters

Thickening time: It is characterized by the time the cement slurry is pumpable. Therefore, the end of the thickening time is considered to be 70 Bc. Limitation for the thickening time is that the pumping time, including mixing and pumping cement, cement displacement, static periods, the time needed to release the plugs plus a safety factor of 2 hours, should be less or equal to the thickening time. However, excessive thickening time could lead to increasing free water, weak compressive strength of the cement, and solids settling. The extended gel strength development could lead to potential gas migration during cement hydration. Cement retarders like Halliburton's SCR™ help to adjust cement setting times.

Temperature: Temperature conditions have a strong influence on cement hydration. It is vital to provide the cementing contractor with the right temperature conditions so that they can design and test the slurry in conformity with the real downhole temperature conditions.

Spacer: The spacer is a valuable displacement aid for proper mud removal. The higher the density difference between the mud and the spacer, the better the mud is removed from the annulus.

Flush: They are used to thin and disperse solid parts in the mud. They are usually pumped ahead of the spacer and achieve high turbulence levels at low pumping rates. They were also referred to as washes.

Expansion/Bond-improving additives: Those additives usually work with the help of crystalline growth. They force the cement to expand slightly after it has set. This expansion should help to increase the quality of casing-cement bond and zonal isolation through control of gas migration, casing protection from the corrosive environment, avoiding unwanted water and gas production and eliminate communication between fracture/stimulation treatments.

Gas flow potential factor: As already described in Chapter 2, gas migration creates channels in the cement sheath reduces the compressive strength of the cement and is contributing to well integrity failure. This gas flow potential factor is representing the amount of gas that can be expected from a formation. The cement slurry's ability to transmit hydrostatic pressure is directly proportional to its static gel strength (SGS) development. Length and thickness of the cement column also influence the hydrostatic pressure loss. The loss of hydrostatic pressure due to the gel strength development is also referred to as maximum pressure restriction (MPR) (Crook and Heathman 1998).

$$MPR = \frac{SGS}{300} * \frac{L}{D} \tag{9.}$$

$$GFP = \frac{MPR}{hydrost. pressure - formation\ pressure} \tag{10.}$$

$MPR = theoretical\ max. pressure\ reduction, psi$

$SGS = static\ gel\ strength\ development, \frac{lb}{100} ft^2$

$300 = conversion\ factor\ to\ obtain\ MPR\ in\ psi$

$L = length\ of\ the\ cement\ slurry, ft$

$D = eff. diameter\ of\ the\ cement\ slurry\ (hole\ diameter - pipe\ diameter)$

$GFP = gas\ flow\ potential\ factor, dimensionless$

The scale for the severity of the gas flow potential factor is indicated by Figure 25 below. As a criterion for the scorecard, always try to keep the gas flow potential factor below 4.

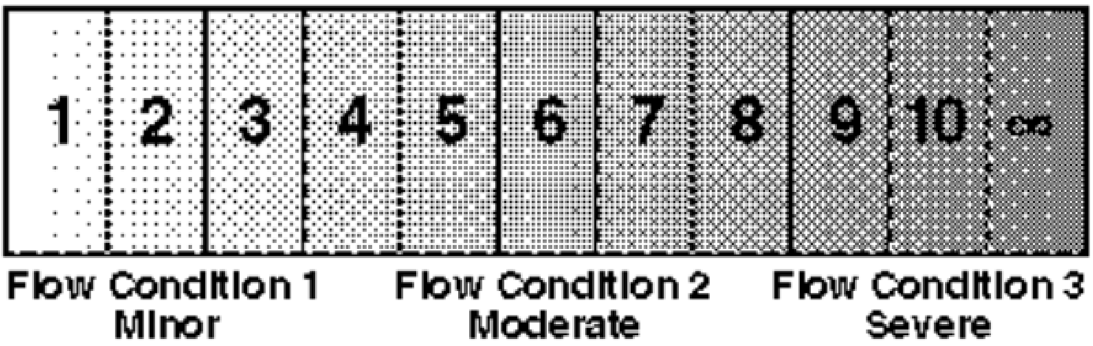

Figure 25: The gas flow potential factor represents the severity of gas flow that can be expected from a formation; Source: (Crook and Heathman 1998)

Fluid loss: Elevated API fluid loss values in the cement leads to a reduction of the hydrostatic pressure in the cement column. Fluid loss is dictated by the amount of fluid the cement can contain across a pressure differential. It can lead to increased gas migration during hydration. In order to avoid this, the goal is to keep the API fluid loss value below 50 ml/ 30 min.

Solid suspension in highly deviated wellbores: Due to the boycott effect, solid particles in the cement slurry have shorter sedimentation paths in the wellbore with deviations from 30°-65°. Heavier particles settle on the low side of the wellbore leading to an inhomogeneous cement sheath. A suspending agent (e.g., Halliburton's SA-1015™) is designed to prevent the solids from settling and keep them in suspension in the slurry. Often, suspension agents also help to control free water in the slurry, and to increase overall fluid stability.

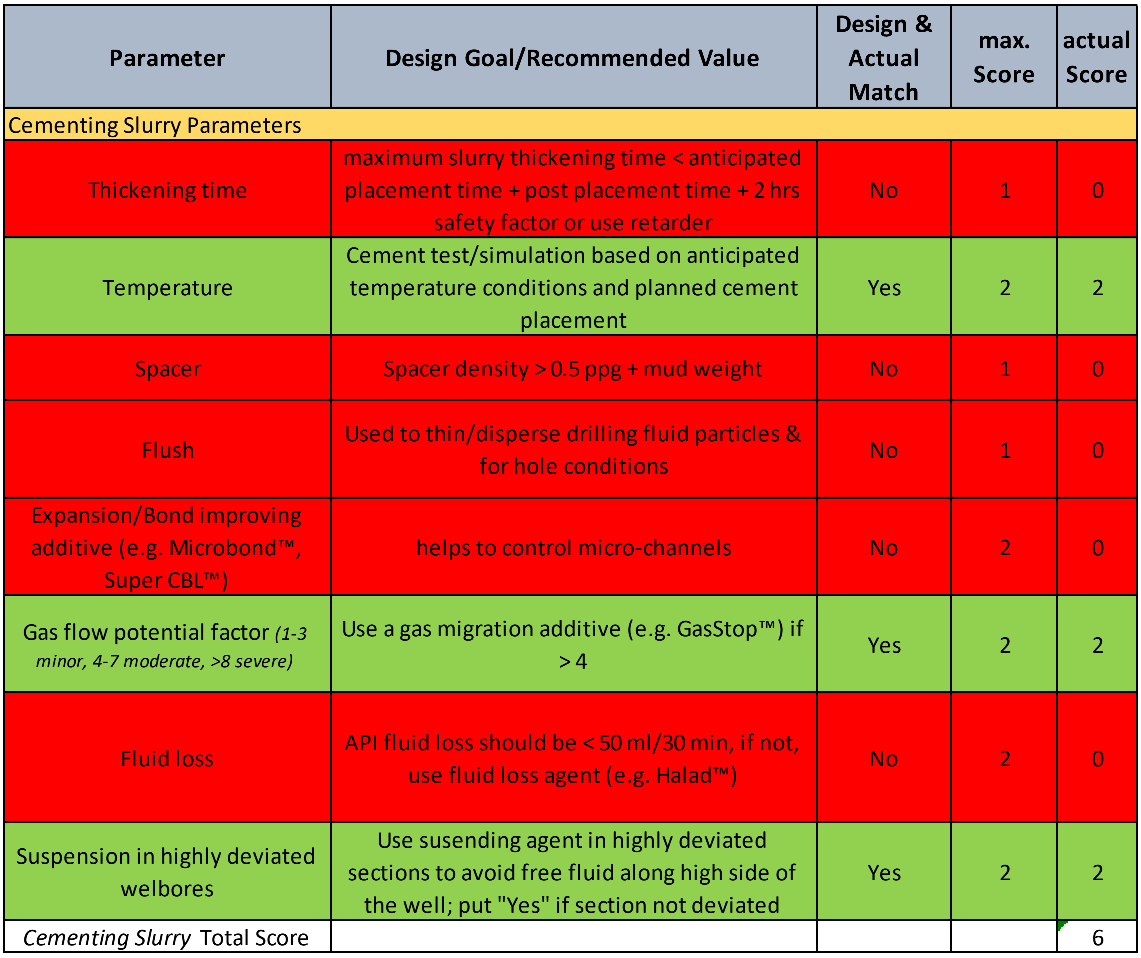

Parameter	Design Goal/Recommended Value	Design & Actual Match	max. Score	actual Score
Cementing Slurry Parameters				
Thickening time	maximum slurry thickening time < anticipated placement time + post placement time + 2 hrs safety factor or use retarder	No	1	0
Temperature	Cement test/simulation based on anticipated temperature conditions and planned cement placement	Yes	2	2
Spacer	Spacer density > 0.5 ppg + mud weight	No	1	0
Flush	Used to thin/disperse drilling fluid particles & for hole conditions	No	1	0
Expansion/Bond improving additive (e.g. Microbond™, Super CBL™)	helps to control micro-channels	No	2	0
Gas flow potential factor *(1-3 minor, 4-7 moderate, >8 severe)*	Use a gas migration additive (e.g. GasStop™) if > 4	Yes	2	2
Fluid loss	API fluid loss should be < 50 ml/30 min, if not, use fluid loss agent (e.g. Halad™)	No	2	0
Suspension in highly deviated welbores	Use susending agent in highly deviated sections to avoid free fluid along high side of the well; put "Yes" if section not deviated	Yes	2	2
Cementing Slurry Total Score				6

Table 12: Parameters representing the cement slurry aspects

4.2.4.3 Hydraulic/Operational Parameters

Circulation volume: Sufficient circulation, usually once the hole volume ("bottoms up") is essential to condition the mud and make sure, no low-mobile mud and cuttings pockets threaten the homogeneity of the subsequent cement slurry placement.

Circulation rate: Rule of thumb recommends keeping the annular fluid velocity above 200 ft/min to achieve proper hole cleaning before starting the cementing job. However, often, this number cannot be achieved if the fracture pressure of the formation is too low, and the annular clearance is too big.

Cementing losses: In case of observed losses during cementing, top of cement is supposed to be lower than anticipated in the design. In extreme cases, the top of cement could be so low, that zonal isolation between two formations is not provided. Therefore, this parameter is such an essential indicator of a successful cementing job.

Static time: As soon as circulation or movement of a fluid, either drilling mud or cement slurry stops, solid particles will start to settle. Solids settling is neither good for proper mud removal nor suitable for proper cement slurry placement. Therefore, static time from the start of mud circulation to condition the wellbore until completion of cementing operation should be below 5 minutes.

Density hierarchy: The density of the displacing fluid should always be higher than the density of the displaced fluid plus 0,5 ppg (0,06 kg/l) to ensure proper displacement efficiency.

Contact time: Spacer flush and cement contact time should be more than 10 minutes across the shallowest critical isolation depth, to provide proper removal of the drilling fluid. It is critical to have mostly pure cement across the whole critical zone.

Fracture Gradient: Equivalent circulating density should be below the fracture initiation pressure at all time during the cementing operation, especially in the open-hole, below the top of the critical isolation zone. In case losses are occurring there, it might prevent cement circulation above the zone, making zonal isolation physically impossible.

Pore pressure: The hydrostatic pressure should be above the formation pressure at all time during the operation. The cement job design should include an acceptable pore pressure and fracture pressure window, provided by the operator to the cementing contractor.

Minimum flowrate: To ensure fluid distribution in the annulus, the fluids shear stress at the narrow side of the wall must be above the fluids yield stress. It can be translated to a minimum flowrate needed to establish 360° flow distribution in the annulus. Usually, the cement contractor provides this.

Parameter	Design Goal/Recommended Value	Design & Actual Match	max. Score	actual Score
Hydraulic/Operational Parameters				
Circulation volume	>1 complete hole volume	Yes	1	1
Circulation rate	>200ft/min annular velocity	No	2	0
Cementing losses	No losses observed	No	2	0
Static time	<5 min of non-flowing time from start of mud circulation to condition wellbore until completion of cementing operation	No	2	0
Density hierarchy	For all fluid interfaces displacing fluid density > displaced fluid density	No	2	0
Contact time	Spacer, Flush & cement contact time > 10 min across shallowest critical isolation depth, to provide removal of drilling fluid	Yes	2	2
Fracture Gradient	ECD must be below-no dynamic losses	Yes	4	4
Pore Pressure	hydraulic pressure must be above at all times	Yes	4	4
Min. flow rate	Min. flow rate to achieve 360° flowrate	Yes	4	4
Hydraulic/Operational Total Score				15

Table 13: Parameters representing the hydraulic/operational aspects

4.2.4.4 Casing Pressure Test Parameters

Plug bump: Bumping the plug concludes the cementing operation. It ensures that the shoe track is left with cement and allows green cement/casing pressure testing of the casing.

Over-displacement: Usually, plugs are aimed to provide a barrier between fluids as they flow downhole. For an accurate displacement, detailed knowledge about the different volumes is essential. It is essential, because over-displacement of the cement slurry may lead to severe contamination. The plugs help to avoid this over-displacement and cement contamination. However, in case the top plug is not bumping the bottom plug, as planned, displacement volumes might have been miscalculated. For this reason, over-displacing the casing volume by a maximum of one half of the calculated shoe track volume should assure proper and pure cement in the shoe track annulus.

Test Pass/Fail Criteria: A criteria to determine when a green cement test is passing or failing must be set. The range for a passing green cement test is set to be a pressure reduction equal to or less than 5 percent within 10 minutes of observation time.

Bleed-off returns: During a green cement pressure test, the fluid that is used to displace the cement is exposed to compression and thermal expansivity, as described in Chapter 3. Due to the pumping, the pressure increases and the fluid gets compressed. Whereas, due to the thermal heating in the wellbore, the fluid is expanding. With the compression forces surpassing the thermal expansion, the total effect still accounts for a reduction in volume and leading to the volume that needs to be pumped to reach the anticipated test pressure. When the pressure test is concluded, and the valves are opened again, and the pressure is bled-off, the fluid will promptly expand, and backflow will be reported, usually in the designated container in the cementing unit. This actual backflow can then be compared with the calculated backflow.

Parameter	Design Goal/Recommended Value	Design & Actual Match	max. Score	actual Score
Casing Pressure Test Parameters				
Plug bump	Ensures that shoe track is left with cement; allows pressure testing of casing	Yes	4	4
Overdisplacement	In case plug is not bumped, overdisplace by max half shoe track volume		2	2
Test Pass/Fail Criteria	Pressure drop according to OMV pass/fail criteria < 5% within 10 min observation time	Yes	4	4
Bleed-off returns	Check returns according to fluid compressibility (Spreadsheet-FLUID COMPRESSIBILITY) and temperature (Spreadsheet-THERMAL EXPANSIVITY)	No	3	0
Casing Pressure Test Total Score				10

Table 14: Parameters representing the casing pressure testing aspects

4.3 Scorecard-Results & Interpretation

Data has been extracted from 11 wells in OMV’s Vienna Basin area leases. Out of those 11 wells, 29 sections have been interpreted. The results show that the sections score in a range of 51-83. With the most current score being 76, occurring four times. The two worst performing sections score 51 and 58. Well BO-205’s and PTS-3’s 13 3/8”-sections have both been drilled with the help of the “casing drilling”-technology. In this technology, the casing is used as a drill string and cemented in place after reaching total depth. However, what punctuates the tool’s ability to score the well construction processes very accurately is the fact that the two worst performing sections fail their respective pressure test, as seen in Figure 26. In case of the BO-205 13 3/8” section, the pressure was not stable, and no successful casing pressure test was conducted due to a leakage, most likely in the area of the float collar as indicated in Figure 27. In the case of the PTS-3 13 3/8” section, the pressure drop during the positive pressure test was more than 5 % within 10 minutes of observation time, as seen in Figure 28.

The third and fourth worst performing well sections, well EB-20’s 9 5/8” and 7” sections, respectively scoring 59 and 65 also show the scorecard’s functionality and ability to determine the quality of the constructed wellbore. These sections have a proven well integrity problem with lack of zonal isolation leading to water flow from higher pressured zones to the perforations resulting in water production.

Analysis of the scores, depicted in Figure 29, shows that the average score for the 7” production sections is higher than those for the intermediate and surface sections. One underlying reason for that is the fact, that especially surface sections, that were drilled with casing (DwC) instead of a regular bit and BHA configuration score particularly bad.

There are several key issues that explain the relatively bad score of DwC, that will be addressed later.

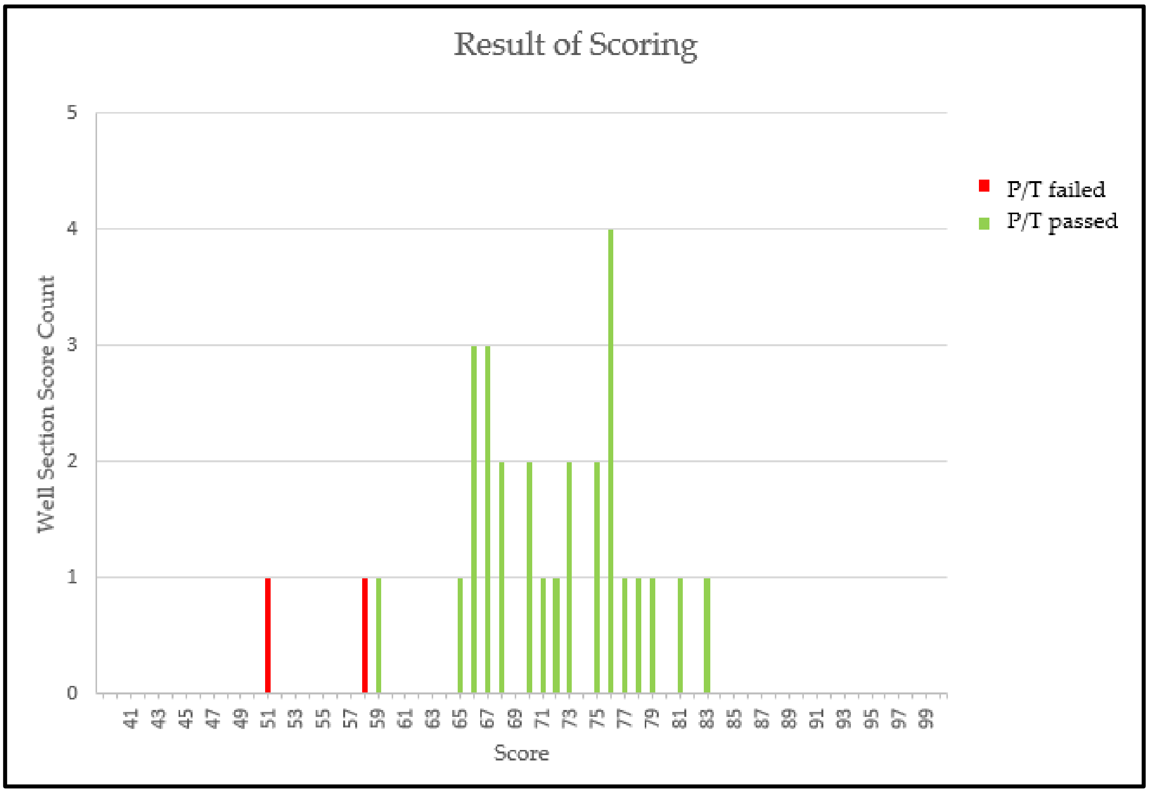

Figure 26: Scoring results show the tool's ability to score the well construction processes very accurately, as the worst-performing sections fail their green cement pressure test

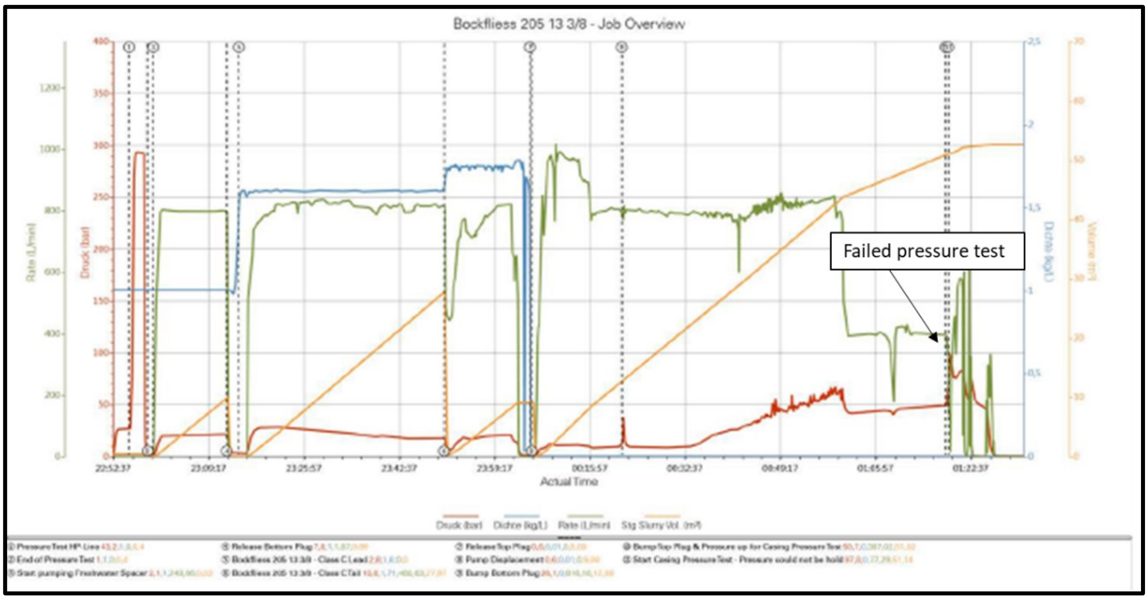

Figure 27: BO-205's 13 3/8" section green cement pressure test fails to deliver a stabilized pressure

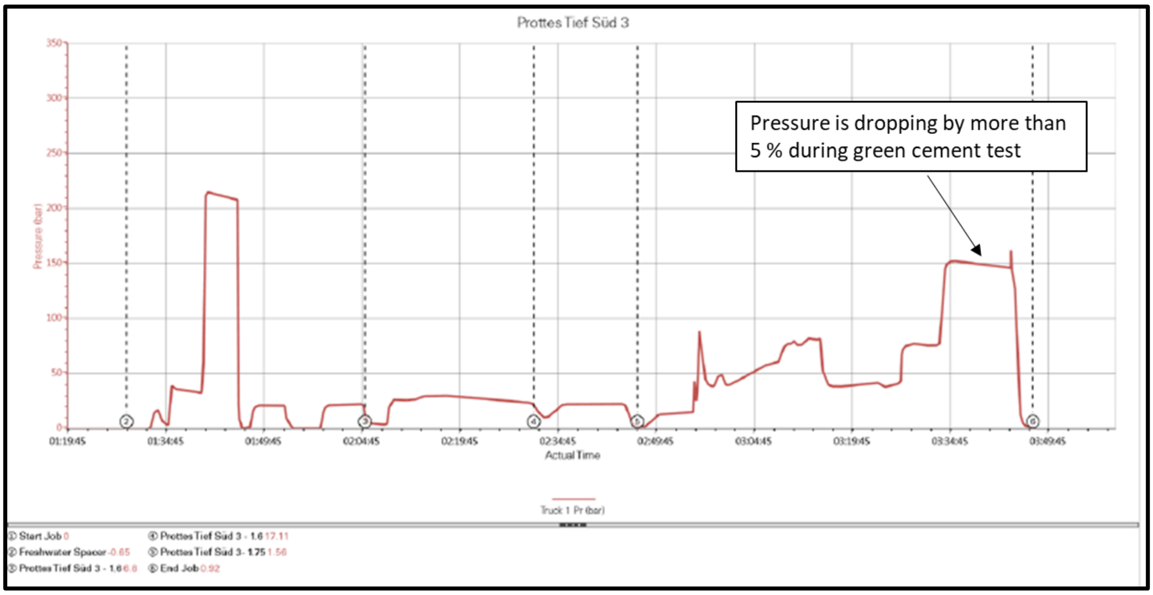

Pressure is dropping by more than 5 % during green cement test

Figure 28: During the green cement test of PTS 3's 13 3/8" section the pressure is dropping by 9 bar

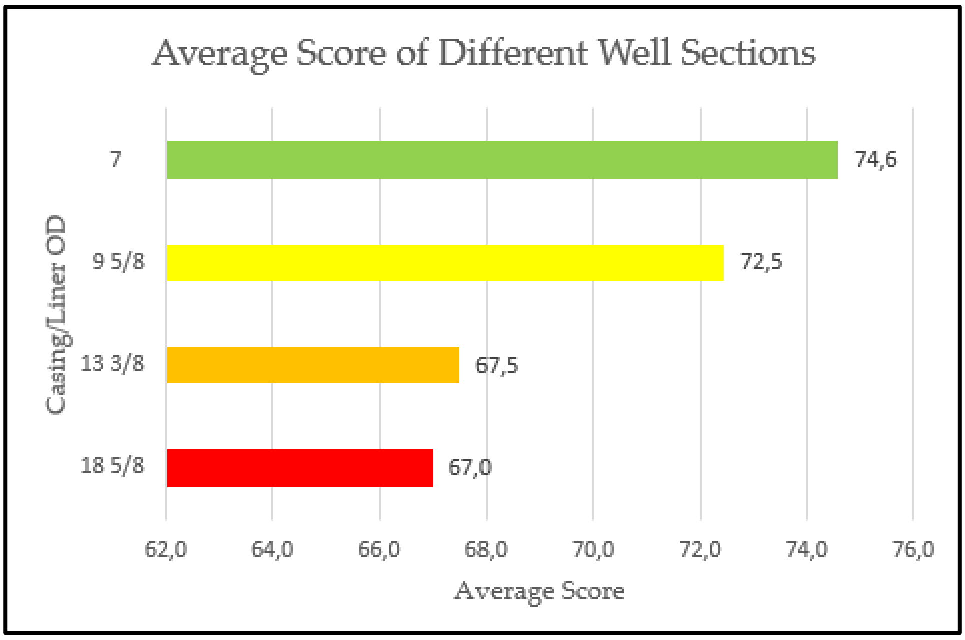

Figure 29: Average scores for production section (7") are higher than those of surface and intermediate sections

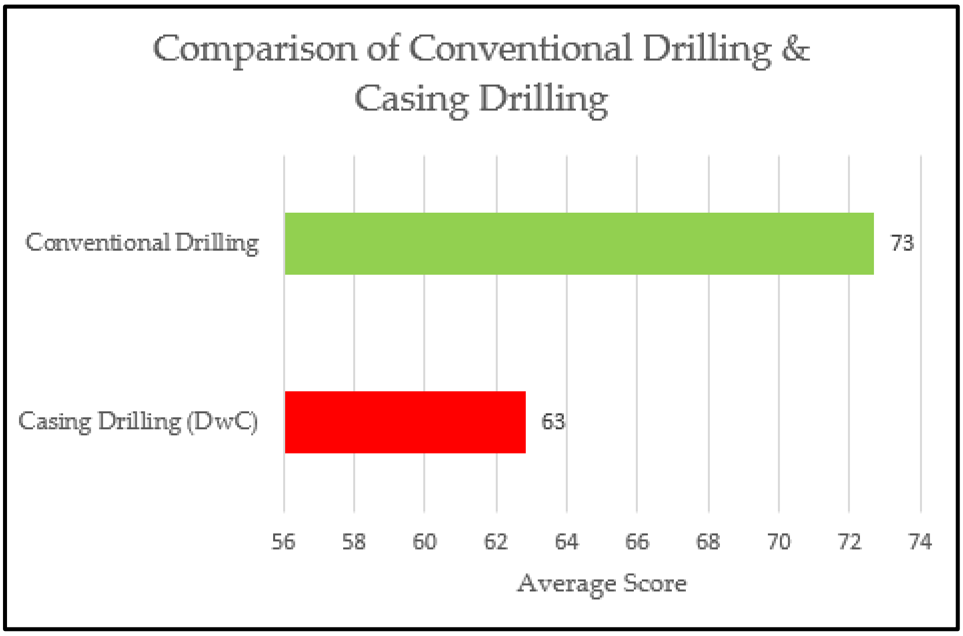

Figure 30: Casing drilling sections score particularly bad

4.3.1 Backflow/Bleed-off volumes

As indicated in the scorecard methodology part of the scorecard, pumping during pressure testing results in a fluid compression and thermal expansivity results in a fluid expansion as described in Chapter 3. With the compression forces surpassing the thermal expansion, the total effect still accounts for a reduction in volume and leading to the volume that needs to be pumped to reach the anticipated test pressure. Conclusion of the test, initiated by opening the valve, results in a backflow. Comparison of the calculated/expected and actual backflow gives essential information about the pressure test.

There are some uncertainties in this calculation that are somewhat difficult to include. Air entrapment somewhere in the system, which can be a result of improper handling or bacteria growth is the most significant uncertainty. In case the actual backflow is equal to or smaller than the expected one, this will emphasize a passing green cement test. However, in case the actual backflow is higher than the expected one, this might question the validity of a passing green cement test and expressly underline the validity of a failing green cement test. Table 16 shows a total expected backflow of 2,5 barrel (~400 liters). However, the actual backflow is only 300 liters, which is smaller than the calculated one. This result would expressly underline the validity of a passing green cement test.

Figure 31 shows the variation of the expected and the actual backflow of all the well sections, where backflow was reported. The red trendline strongly indicates a correlation between the score and the variation of the calculated and the expected backflow. A high backflow variation indicates a much higher actual backflow than an expected one, also indicating backflow from the well. This might question a positively-passed green cement test or underline the validity of a green cement test subject to pressure drop.

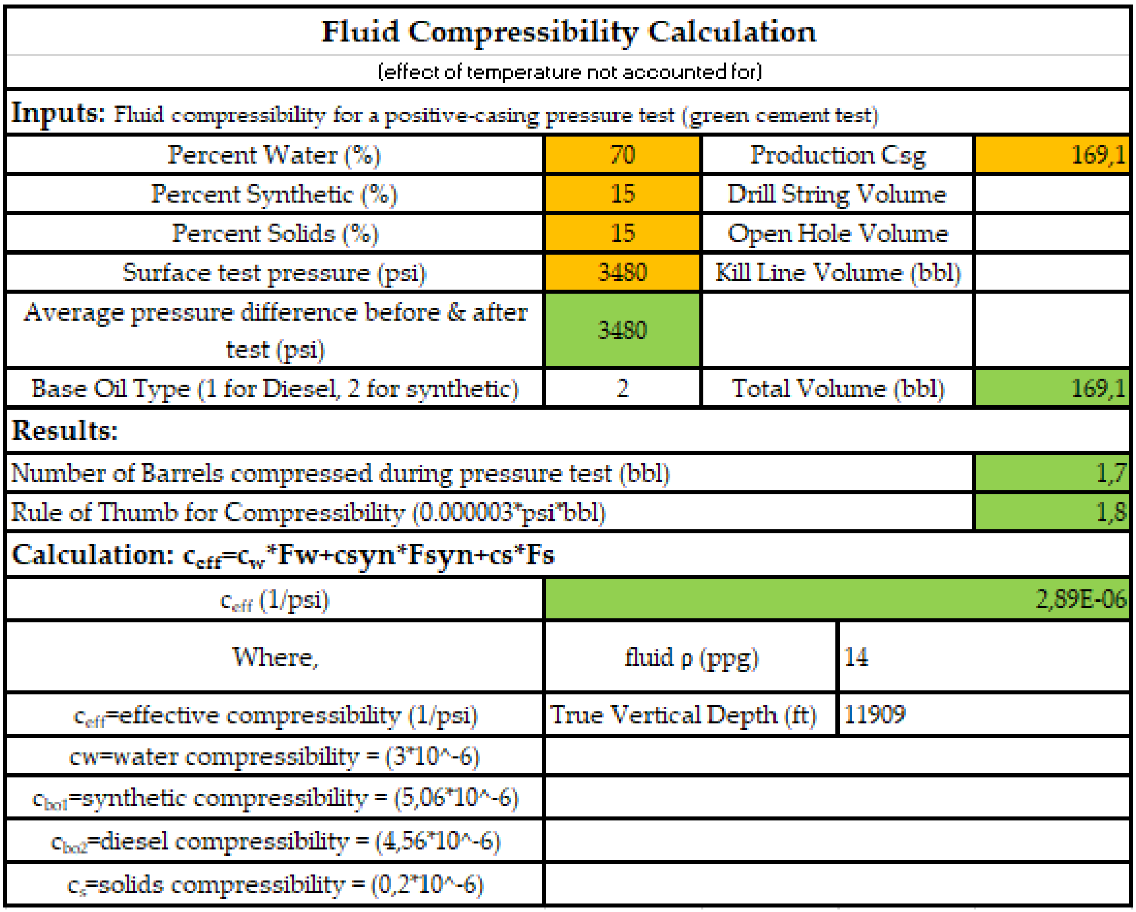

Fluid Compressibility Calculation			
(effect of temperature not accounted for)			
Inputs: Fluid compressibility for a positive-casing pressure test (green cement test)			
Percent Water (%)	70	Production Csg	169,1
Percent Synthetic (%)	15	Drill String Volume	
Percent Solids (%)	15	Open Hole Volume	
Surface test pressure (psi)	3480	Kill Line Volume (bbl)	
Average pressure difference before & after test (psi)	3480		
Base Oil Type (1 for Diesel, 2 for synthetic)	2	Total Volume (bbl)	169,1
Results:			
Number of Barrels compressed during pressure test (bbl)			1,7
Rule of Thumb for Compressibility (0.000003*psi*bbl)			1,8
Calculation: $c_{eff}=c_w$***Fw+csyn*Fsyn+cs*Fs**			
c_{eff} (1/psi)			2,89E-06
Where,	fluid ρ (ppg)	14	
c_{eff}=effective compressibility (1/psi)	True Vertical Depth (ft)	11909	
cw=water compressibility = (3*10^-6)			
c_{bo1}=synthetic compressibility = (5,06*10^-6)			
c_{bo2}=diesel compressibility = (4,56*10^-6)			
c_s=solids compressibility = (0,2*10^-6)			

Table 15: Fluid compressibility calculation; for this 3480 psi (240 bar) green cement test, the expected backflow due to the fluid's compression is 1,7 barrels

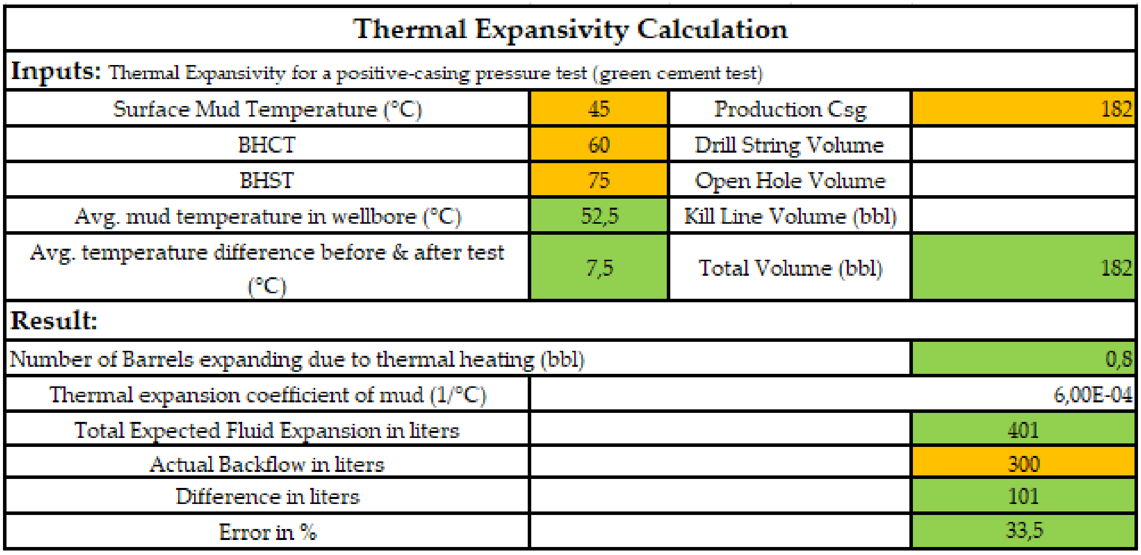

Thermal Expansivity Calculation				
Inputs: Thermal Expansivity for a positive-casing pressure test (green cement test)				
Surface Mud Temperature (°C)	45	Production Csg		182
BHCT	60	Drill String Volume		
BHST	75	Open Hole Volume		
Avg. mud temperature in wellbore (°C)	52,5	Kill Line Volume (bbl)		
Avg. temperature difference before & after test (°C)	7,5	Total Volume (bbl)		182
Result:				
Number of Barrels expanding due to thermal heating (bbl)				0,8
Thermal expansion coefficient of mud (1/°C)				6,00E-04
Total Expected Fluid Expansion in liters				401
Actual Backflow in liters				300
Difference in liters				101
Error in %				33,5

Table 16: The expected expansion due to the fluid's thermal expansion during the green cement test is 0,8 barrels.

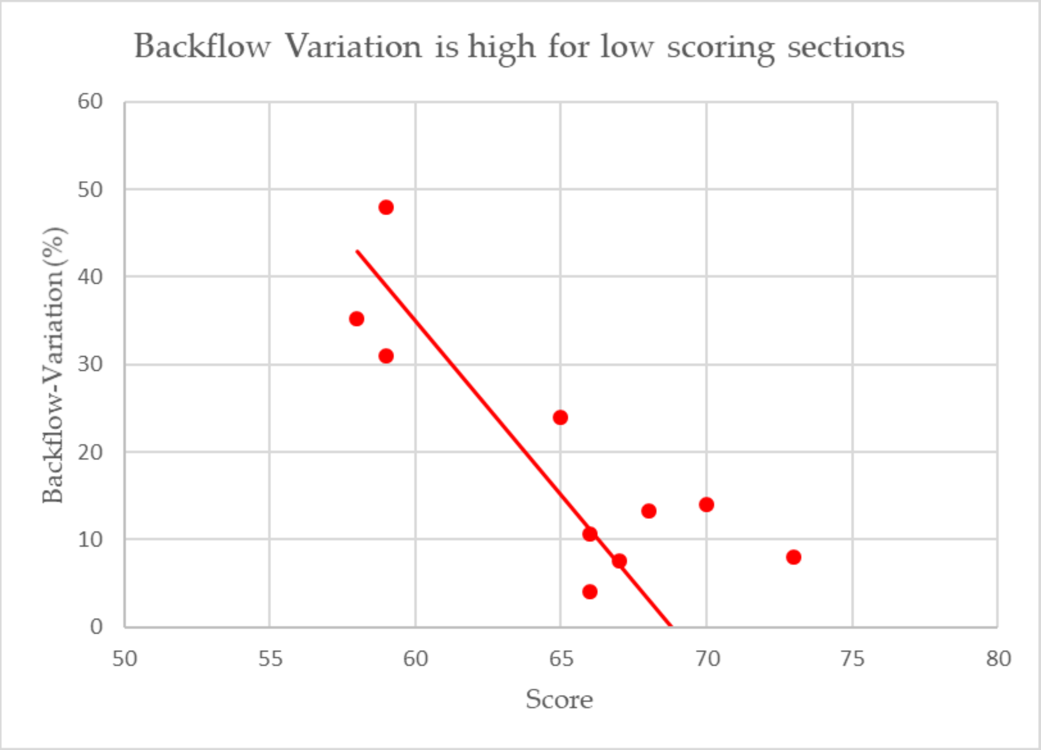

Figure 31: % Variation between expected and actual backflow shows a correlation between a low score and a high backflow variation

4.3.2 Anomalies/Observations

The analysis shows that well sections with a low score face various problems. Some of them depicted in the bar chart below are partly responsible for their low scoring, like failing pressure test, losses during cementing or overpulls and pack-offs during drilling and BHA-pulling. Other well sections face some real operational problems, indicating a low wellbore construction quality by a rather low score, like water production through failing zonal isolation. As already mentioned, and seen in Figure 30, many surface sections, that were drilled with casing (DwC) instead of a regular bit and BHA configuration, score particularly bad, which has several reasons:

- *Improper mud selection*: K_2CO_3-polymer-mud system appears not to have the desired impact on the calliper in the top-hole section. However, it was used for cost and operational reasons. The outcome of this were significant wash-outs in those well sections, leading to a suboptimal cement job.
- *Crew inexperience with DwC*: Drilling with Casing operation, is relatively new for all related personnel! Therefore, everybody should be made aware of the procedure. This inexperience increases the risks leading to a potential lousy job outcome.
- *Spacer*: For all the DwC sections, freshwater has been used as a spacer. Optimal spacers should have a higher density than the drilling mud they are displacing for better drilling fluid removal. Using freshwater as a spacer increases the risk of getting improper mud removal, leading to a lack of proper cement placement.

- *No lab data*: For most of the surface sections, no cement-lab tests have been performed. Therefore, nothing can be said about the cement's ability to keep its fluid (API-fluid loss), and its temperature behavior and thickening time.

Some of the following observations proof the tool's valuable ability to detect wellbore construction quality. As already mentioned, both Ebenthal 20 sections scored rather bad underlining poor well construction quality:

Ebenthal 20 (EB-20) 9 5/8" & 7" sections: The production well Ebenthal 20 (EB20) was drilled from August 17th, 2010 to September 7th, 2010 and reached a final depth of 2664.0m MD = 1828.39m TVD. The drilling path is strongly deviated, with a kick-off point at 1100m MD and a maximum deviation of 78°. The typical deviation at the target horizons is also roughly 78°. The well was cased with a 7′′ production casing from the surface to final depth, and its designed (calculated) top of cement is supposed to be at a depth of 668m MD behind a 9 5/8′′ intermediate casing. The well was perforated in 4 intervals in the 15.Z1 Tortonian Horizon and started production on January 19th. From the first day on it produced not even traces of oil, just water (42m^3/d) and gas (590m^3/d). For artificial lift support, a sucker rod pump was installed at a depth of 1450m MD and is producing at a drawdown of roughly 20bar. After 15 days, production was stopped because of the lack of oil. Two main findings did not meet OMV's expectations at that time:

- *No oil production*: In contrast to that, well logs from EB-20 for the perforated interval showed oil (on average 19% porosity and 40% S_w for the 15.Z TH), the neighbouring wells have similar logs and produce successfully.

- *Pressure mismatch:* The pressure measured at the well EB 20 (gauge and sonolog independently) was ~142 bar, at least 50 bar higher than the expected reservoir pressure of the 15.Z TH as indicated by all the neighbors and the reservoir simulation (80-90 bar).

Considering the above results, OMV's first explanation for the water production was communication behind casing. The 14 TH, a permeable, water bearing sand is situated only 120m MD above the top perforation. Since it has not been produced by nearby wells hydrostatic pressure can be assumed (or a pressure slightly below) and thus crossflow could explain all the observed phenomena including pressure mismatch and the complete lack of oil production. For an overview of the formation horizons, see Figure 32.

Assumption of a channel communication behind the zones as indicated in Figure 32, might indicate a tight hole or at least tight spots, that might be partly responsible for a poor cement placement, as shale layers, within the horizons are prone to swelling. However, this was not confirmed with calliper logs, the "as per design" cement job as well as Schlumberger's final cement evaluation (see Figure 33).

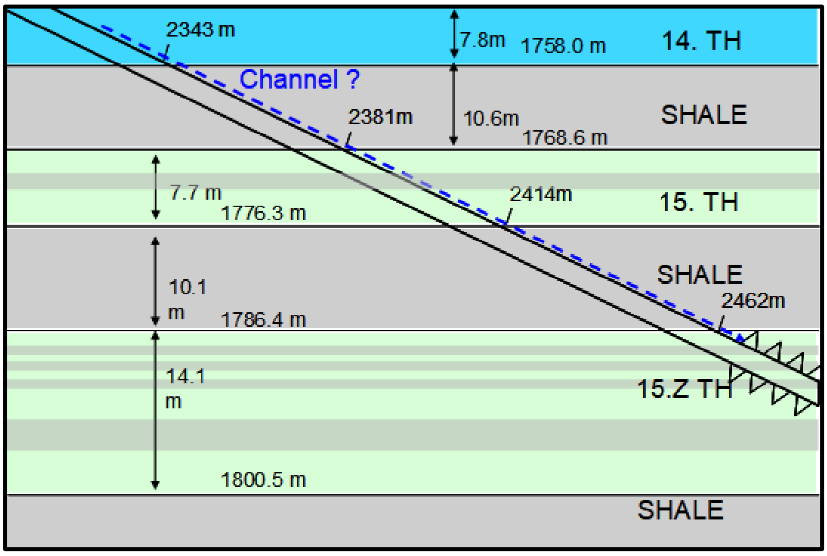
2343 m
7.8m
1758.0 m
14. TH
Channel ?
2381m
10.6m
1768.6 m
SHALE
7.7 m
1776.3 m
2414m
15. TH
10.1 m
1786.4 m
SHALE
2462m
14.1 m
15.Z TH
1800.5 m
SHALE

Figure 32: Assumption of channel communication; Source: OMV

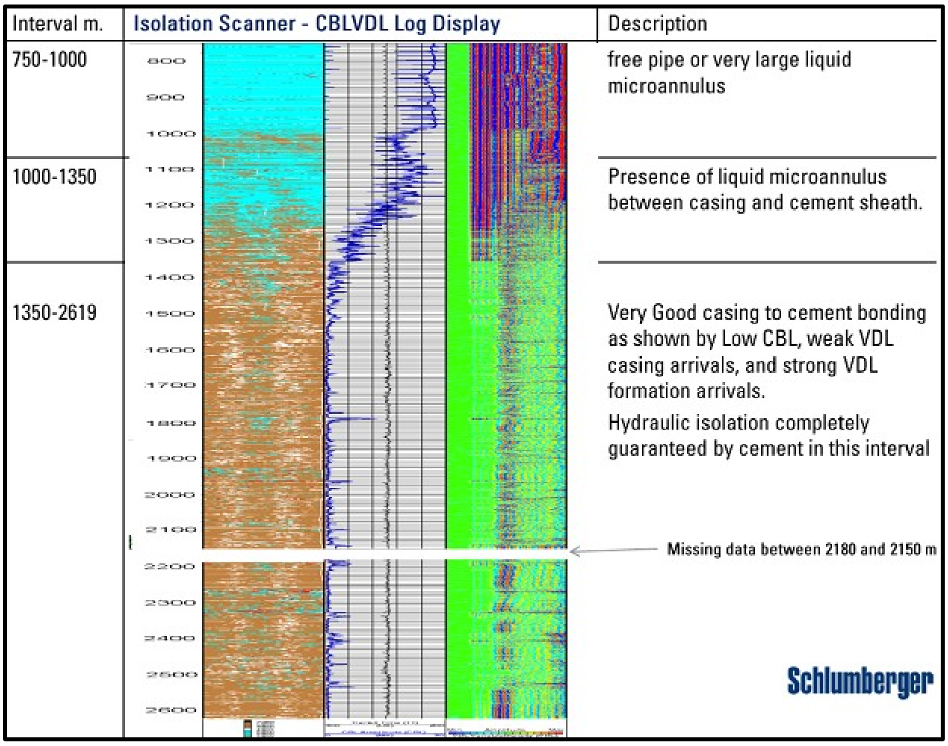

Interval m.	Isolation Scanner - CBLVDL Log Display	Description
750-1000		free pipe or very large liquid microannulus
1000-1350		Presence of liquid microannulus between casing and cement sheath.
1350-2619		Very Good casing to cement bonding as shown by Low CBL, weak VDL casing arrivals, and strong VDL formation arrivals. Hydraulic isolation completely guaranteed by cement in this interval

800
900
1000
1100
1200
1300
1400
1500
1600
1700
1800
1900
2000
2100
2200
2300
2400
2500
2600
Missing data between 2180 and 2150 m
Schlumberger

Figure 33: Schlumberger cement evaluation falsely indicates a completely guaranteed zonal isolation; Source: OMV

A communication test using Fluorescein as a tracer (yellow-green color) was successful in proving the above hypothesis. After pumping it through the annulus as depicted in Figure 34, it eventually returned to the surface, proving that there is a channel behind the casing. This example shows that cement evaluation through bond logs might often be questionable or non-conclusive. In this case, the cement evaluation (CBL) was not able to detect a channel behind the casing, however the scorecard tool was able to detect wellbore construction shortcomings leading to these well integrity events.

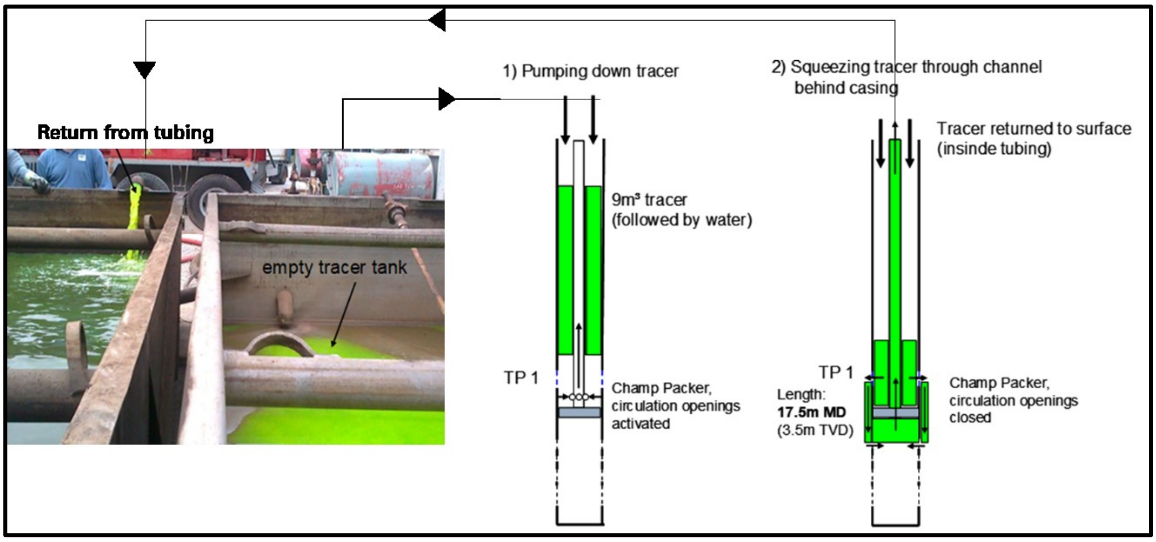
Return from tubing
empty tracer tank
1) Pumping down tracer
9m³ tracer
(followed by water)
TP 1
Champ Packer,
circulation openings
activated
2) Squeezing tracer through channel
behind casing
Tracer returned to surface
(insinde tubing)
TP 1
Length:
17.5m MD
(3.5m TVD)
Champ Packer,
circulation openings
closed

Figure 34: Tracer experiment proved that there is communication behind the casing; Source: edited from OMV

After the lack of zonal isolation was proved by the tracer experiment, remedial cementing through a squeeze job was performed. Soon after, the bottom hole pressure was much lower than before and closer to the values expected from neighbouring wells. Also, one month after the squeeze job, oil production started.

Bockfließ 207 (BO-207) 9 5/8" section: The calliper log for this well section shows tight spots. This is also reflected by the final BHA-pull-out of hole, where small overpulls and tight holes were detected. The drilling response shows that inadequate hole cleaning was detected, underlaid by the fact that a large number of cuttings and clay balls were observed over the shakers. Given the mediocre score of 70, the scorecard accurately represents the qualitative status quo of BO 207's 9 5/8" well construction process.

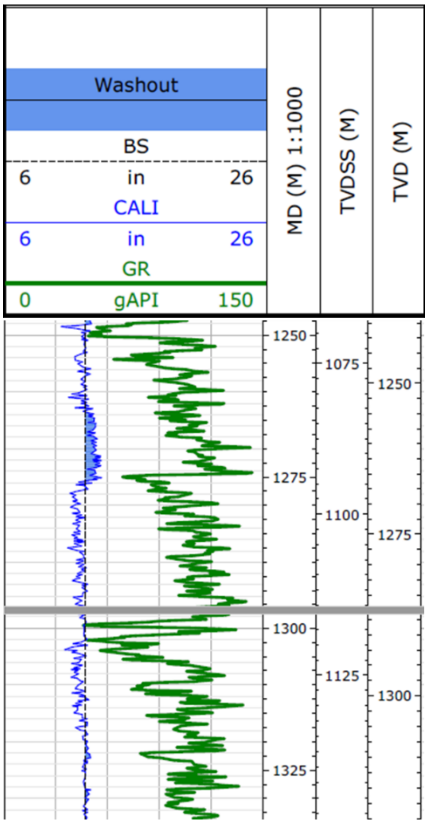

Figure 35: Calliper log shows tight spots; Source: OMV

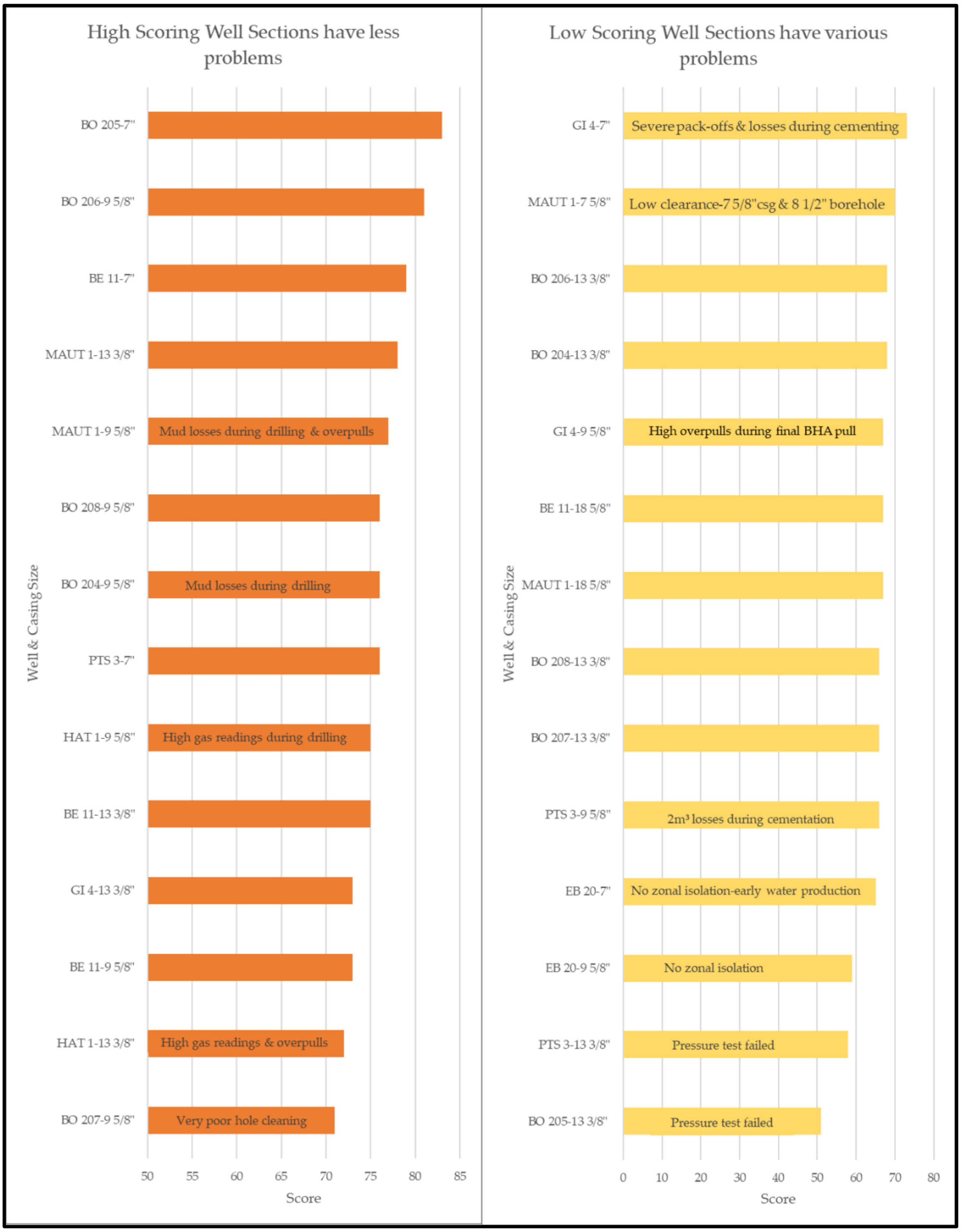

Figure 36: Summary of scores of every well section and the driving factor behind the low score

4.3.3 Green Cement Test-Pressure Decline Rate

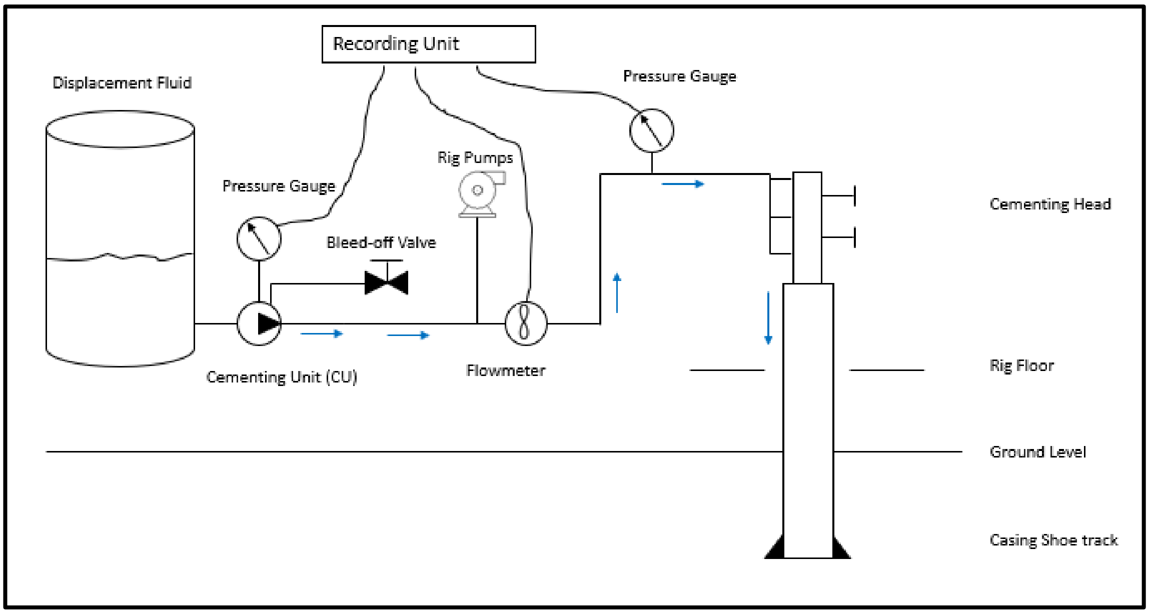
Recording Unit
Displacement Fluid
Pressure Gauge
Rig Pumps
Pressure Gauge
Cementing Head
Bleed-off Valve
Cementing Unit (CU)
Flowmeter
Rig Floor
Ground Level
Casing Shoe track

Figure 37: Equipment arrangement during a positive pressure test (green cement pressure test)

Figure 37 shows the recommendation of the equipment surface arrangement during a positive pressure test, a green cement test in particular. As already mentioned earlier, the test is resumed right after the cementing operation has concluded, assuming the plug has been bumped. The arrangement above shows that the pressure is measured at the surface by two pressure gauges.

The cementing unit is used to displace the cement and to conduct the test. This has two main reasons. Firstly, it is already assembled and connected to the wellbore as the cementing operation has just concluded, secondly, the pressure and flow-measurements are much more accurate than the rig pumps. The cementing unit also allows for more controlled pumping, fundamentally crucial for the low-pressure test. Figure 38 shows a *Halliburton* cementing unit arranged to conduct a green cement test as *OMV Austria* uses it.

Proper measurement of volumes pumped, and pressures are vital to achieving good testing results. Pressure sensors and flowmeters are used to digitally measure the parameters, which are transferred to the recording unit in the cementing truck via cables (see Figure 41)

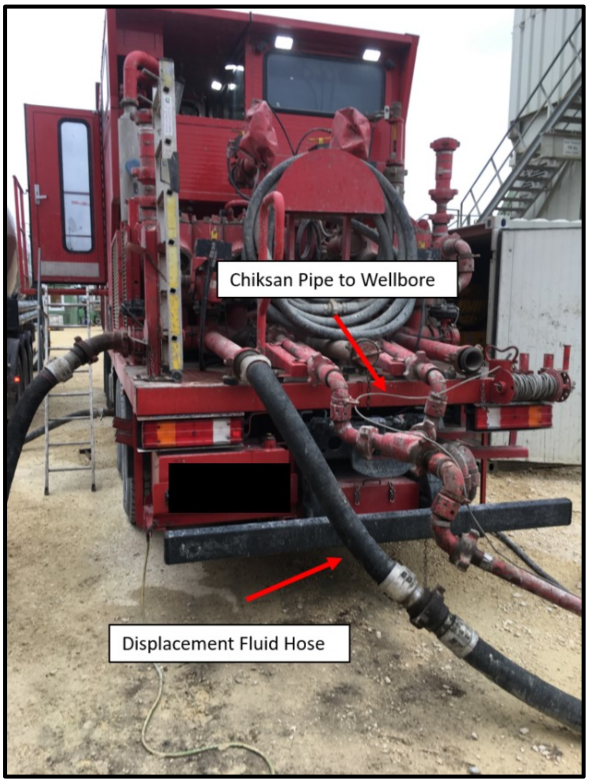

[redacted]

Figure 38: *Halliburton* Cementing unit used to displace cement and conduct a green cement test

Proper measurement of volumes pumped, and pressure is key to achieve good testing results. Pressure sensors and flowmeters are used to digitally measure the parameters, which are transferred to the recording unit in the cementing truck via cables.

An important green cement test parameter is the backflow from the wellbore after the test. This amount is dictated by the compressibility of the drilling fluid and the thermal expansivity of the mud due to geothermal heating in the wellbore. For a sound and conclusive test outcome, it is essential to calculate these factors and cross-check them with the actual backflow. Usually, the backflow is bled-off into a tank that is located on the cementing unit behind the control and recording unit (see Figure 43). The amount of backflow is measured with the help of a scale of 100-liter steps in the tank.

A very reliable and exact parameter to analyze a pressure test is the pressure decline rate. Delta pressure over delta time ($\Delta P/\Delta T$; (bar/min)) gives the pressure change rate. Pressure, and flow rate data from 20 cementing operations plus subsequent green cement tests (see Appendix C) out of the 30 scored well sections were analyzed. A high negative pressure decline rate means that the pressure is rapidly declining during the test, indicating a potential leak in the casing and casing shoe. Figure 39 shows a typical 10-minutes green cement test. Once the flow rate decreases to zero, dynamic effects are responsible for a further pressure increase. For that reason, a total of one-minute contingency was added once the flowrate decreased to zero to account for that dynamic pumping effects. The pressure values once the well was left quiescently for a minute were used to calculate the leakage rate.

The results show that sections that score lower are respectively experiencing a higher negative pressure decline during the green cement test (see Figure 40). Whereas higher scoring sections are seeing lower negative leakage rates or even positive leakage rates. These results, together with the fact that the two worst performing sections fail the test, badly scoring sections show high backflow discrepancy and also poorly scoring sections have well integrity problems (EB-20), strongly prove the scorecards ability to detect problems and shortcoming in the well construction process.

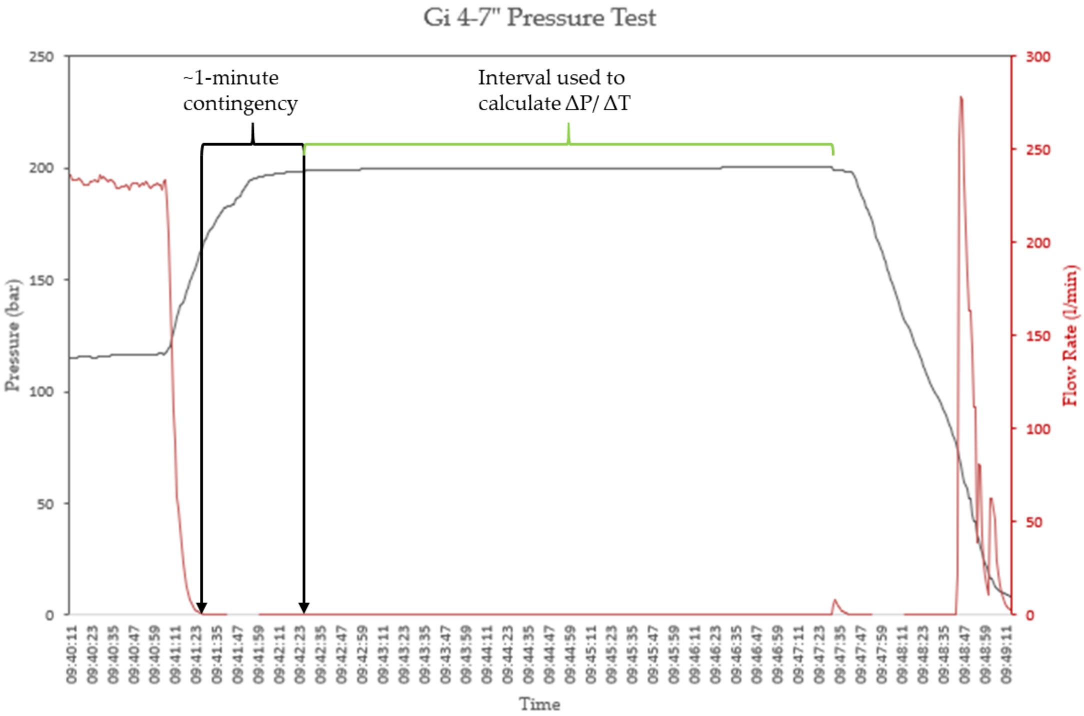

Figure 39: A 1-minute contingency after pumps were shut down was used to account for dynamic effects

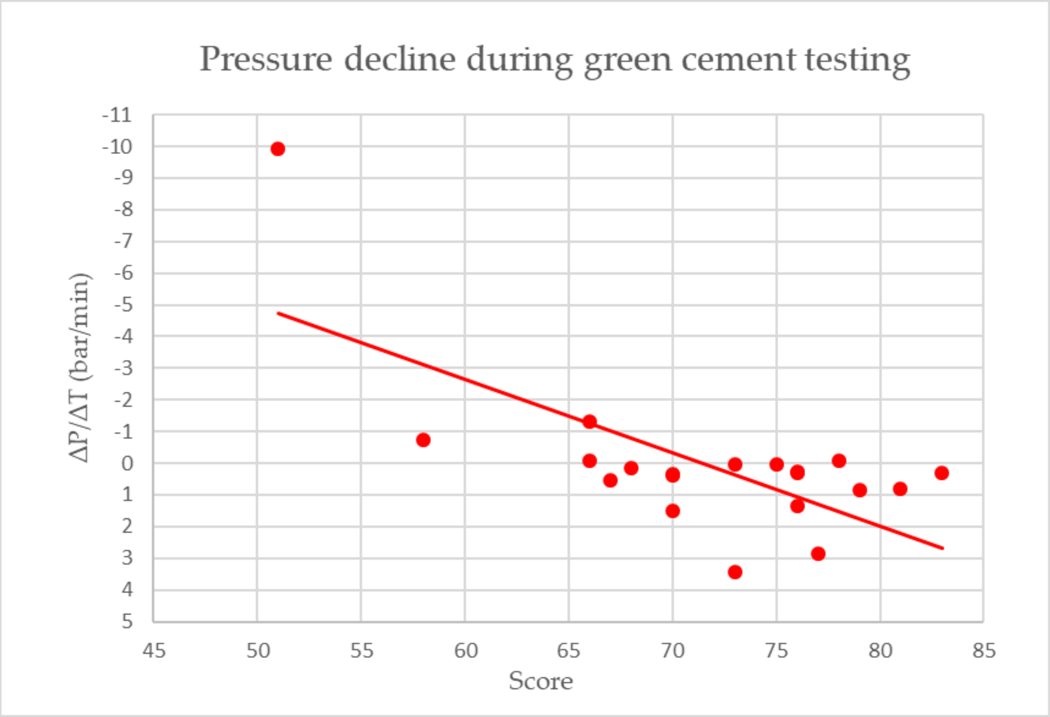

Figure 40: Results show that low scoring well sections have higher negative pressure decline rates, possibly indicating a leak

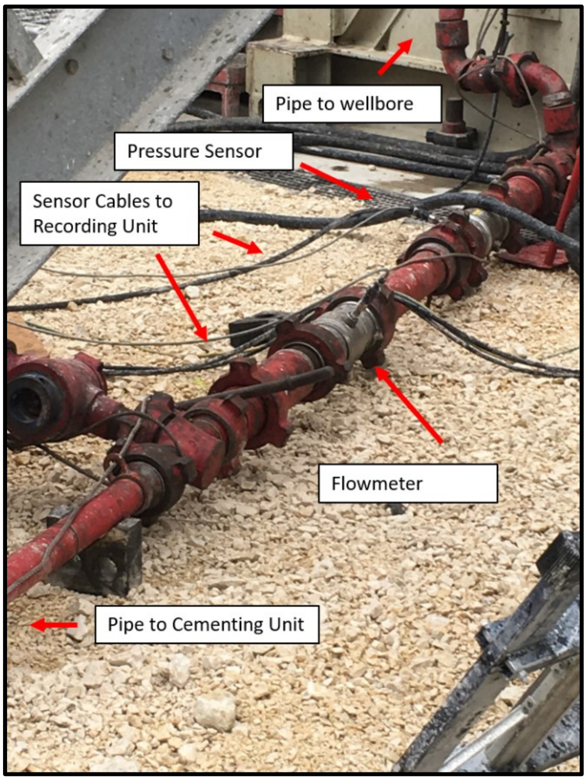
Pipe to wellbore
Pressure Sensor
Sensor Cables to Recording Unit
Flowmeter
Pipe to Cementing Unit

Figure 41: Sensor arrangement between the cementing unit and the wellbore

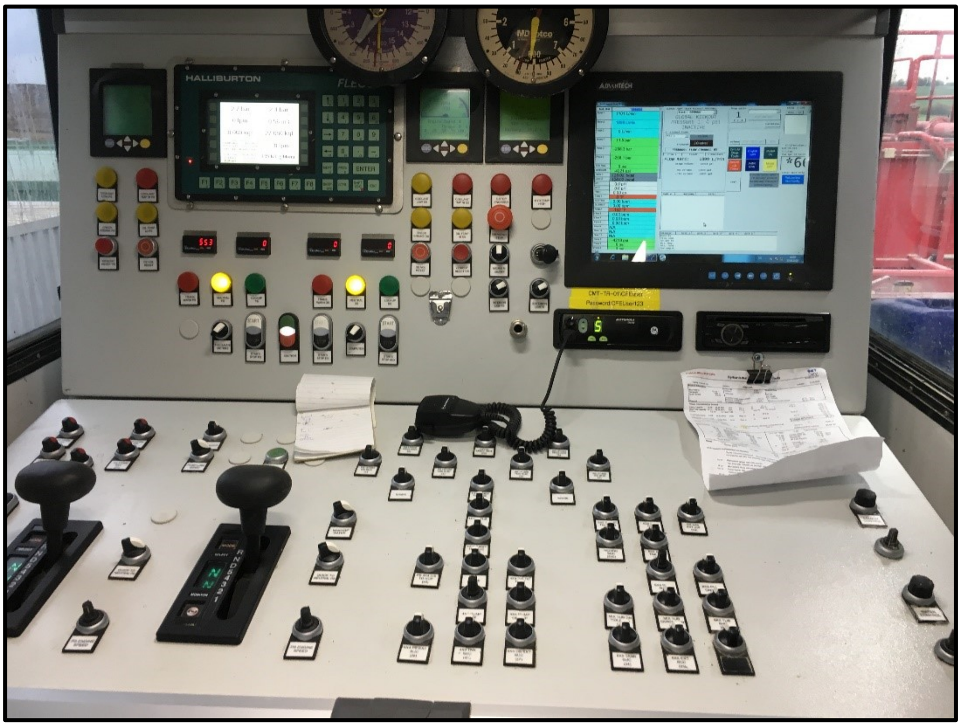

Figure 42: Recording unit of the cementing unit

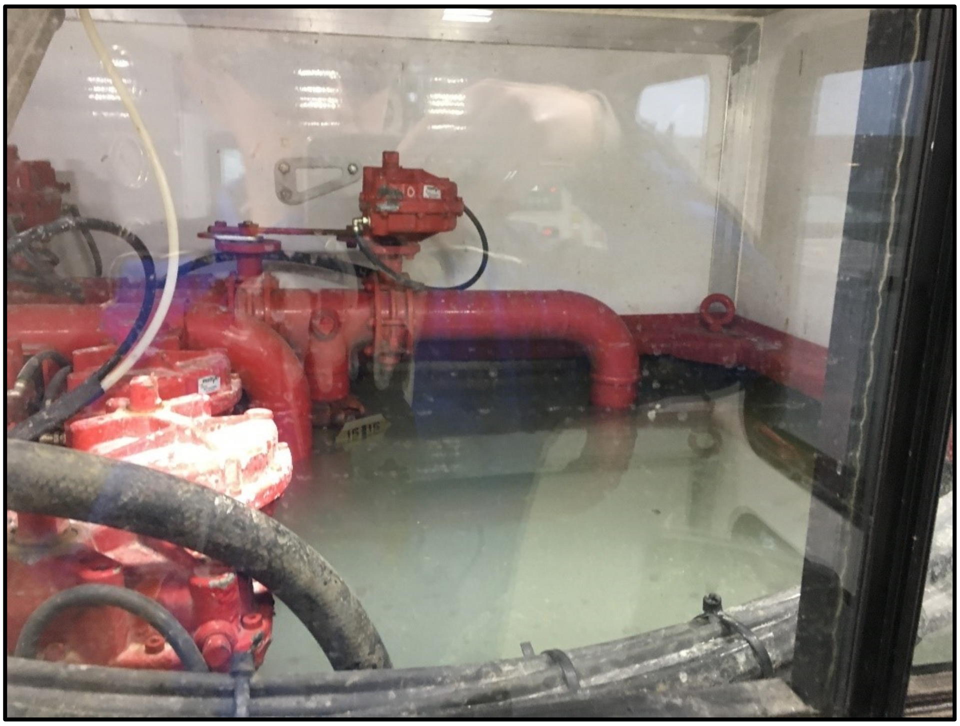

Figure 43: Tank/Container, where the backflow is bled-off and measured

Chapter 5 **Cement Stress Modelling**

The Well Construction Scoring tool presented in detail in the previous chapter is designed to find shortcomings in the well construction process, while the cement is still in its liquid state that might lead to well integrity issues. However, well construction shortcomings are the first out of numerous reasons, for well integrity issues to arise. Once the cement has set and the well section is constructed correctly, casing integrity testing (positive/negative pressure testing), formation integrity testing (FIT, LOT, xLOT) and production or injection starts, making the cemented casing subject to numerous stresses in the form of cyclic pressure and temperature changes. In this chapter, the stresses imposed on the cement during pressure testing, production, and injection are studied. A basic and simple analytical model that facilitates the stresses acting in the casing, hard-set cement, and formation is presented. Teodoriu et al. developed a similar analytical model, of wellbore stresses based on wellbore parameters. Appendix A shows already the general derivation of Lamè's Equations, describing the stresses in a steel cylinder, represented by the casing in our case. Extending this concept into the cement and formation aims to capture the stresses in the near wellbore area.

The casing-cement-formation unit can be described as a pressurized three concentric cylinder body. Pressure changes during operations mentioned above induce stress concentrations near the casing-cement and cement-formation boundaries. Figure 44 shows a profile of hoop stress and radial stress in a concentric cylinder under differing loading conditions. Casing expansion caused by an inner-casing pressure increase results in an expansion of the surrounding cement and formation. Consequently, the tangential hoop stress in the cement will become less compressive and more tensile, whereas the radial stress will become more compressive. Antithetical, when the pressure is decreased inside of the casing, the surrounding cement tends to move radially towards the well axis. Therefore, the hoop stress gets more compressive, and the radial stress less compressive. Inside pressure reduction often happens during hydrocarbon production due to natural pressure decline, in gas storage wells as part of the well operation cycle and during negative pressure tests.

Figure 45 shows an infinitesimal cement element and the stresses acting on it. The axial stress is perpendicular to both the radial and the hoop stress. The following assumptions have been made in the simple stress model.

- Casing-cement-formation interfaces are perfectly bonded. Therefore, radial displacement and stresses are continuous across the boundary without any discontinuities.
- Unlike as described in Chapter 3, in this case, the casing is regarded as a thin-walled pressure vessel for the sake of simplicity
- The cement and formation are regarded as thick-walled concentric cylinders with different material properties.
- The casing-cement-formation cylinder is under a triaxial-stress state

Failure criteria

The material strength in triaxial stress state is commonly described using one of the so-called failure criteria. It defines at which the material fails. The simplest ones are the maximum stress criterion and the Mohr-Coulomb failure criterion. Maximum normal stress criterion states that an isotropic material will fail once the most significant principal stress reaches a limiting value, corresponding to

$$\frac{\sigma_1}{\sigma_f} \geq 1 \qquad 11.$$

σ_1 is the maximum principal stress and σ_f is the tensile stress limit of the material. The smaller principal stresses play no role ($\sigma_1 > \sigma_2 > \sigma_3$).

The Mohr-Coulomb criterion does not account for a possible effect of the intermediate principal stress σ_2 on cement failure.

$$\frac{\sigma_1}{\sigma_{tensile}} - \frac{\sigma_3}{\sigma_{compressive}} \geq 1 \qquad 12.$$

$\sigma_{tensile}$ and $\sigma_{compressive}$ are the tensile and compressive strengths. However, the above criteria become insufficient when tangential, radial and axial stress become all compressive. Therefore, other failure mechanisms based on experiments were needed to determine the onset of failure. Following criteria was developed by Avram et al. to describe concrete fracture failure under triaxial stress in compliance with Mohr Coulomb's criterion (Avram 1981).

$$\frac{\sigma_1}{f_c} = 1 + 3{,}7\left(\frac{\sigma_3}{f_c}\right)^{0{,}86} \qquad 13.$$

f_c is compressive strength, σ_1 and σ_3 are the major and minor principal stress.

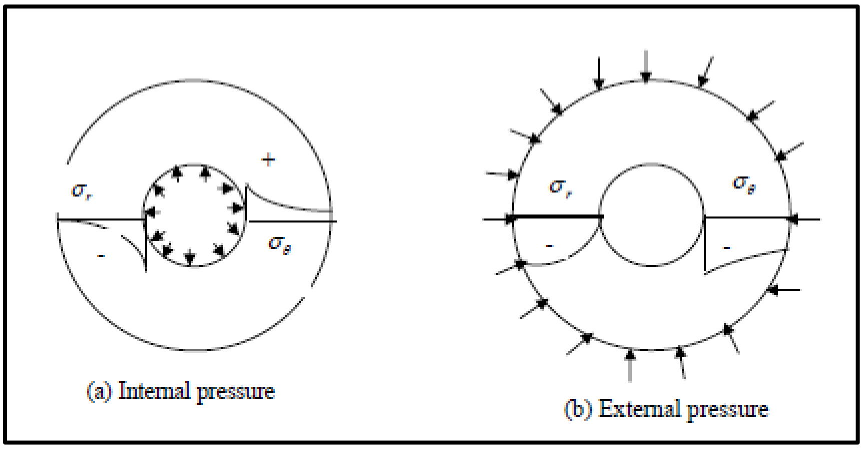

Figure 44: Hoop and radial stress profile on cylinders with different loading scenarios; Source: (Teodoriu et al. 2010)

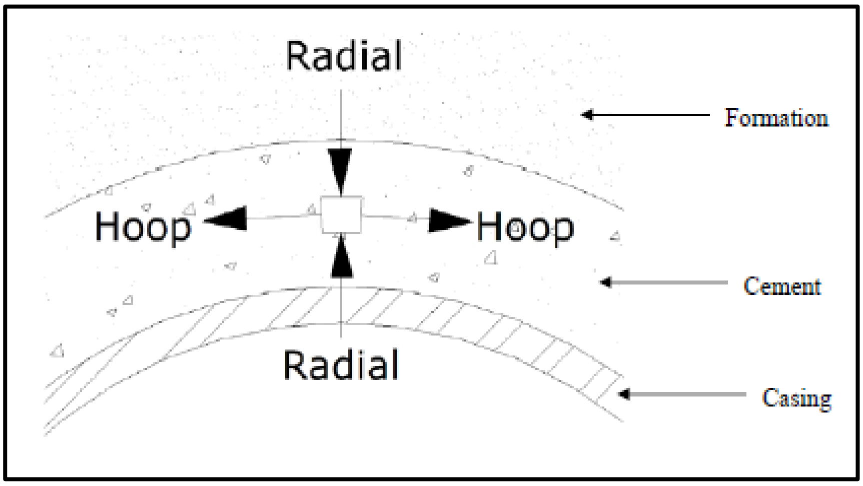

Figure 45: Stresses acting on an infinitesimal cement-sheat element; Source: (Teodoriu et al. 2010)

5.1 Analytical Model

Figure 46 shows a compound cylinder representing the casing and cement. p_i is an internal pressure acting on the casing (e.g., from LOT or casing pressure test), resulting in radial expansion of the casing. This expansion will translate to a contact pressure p_{c1} on the cement.

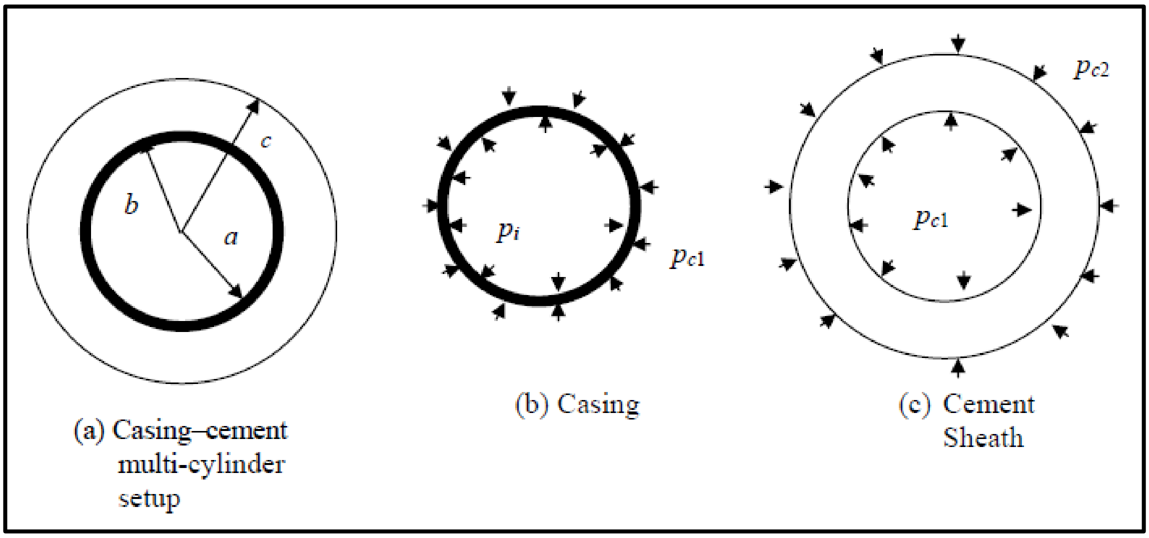

(a) Casing–cement multi-cylinder setup

(b) Casing

(c) Cement Sheath

Figure 46: Stresses acting on the casing-cement interface; Source: (Teodoriu et al. 2010)

Similarly, the cement-formation interface shown in Figure 47, p_{c2} is the contact pressure formed at the cement–formation boundary as a result of the confining pressure from the formation pressure, p_f.

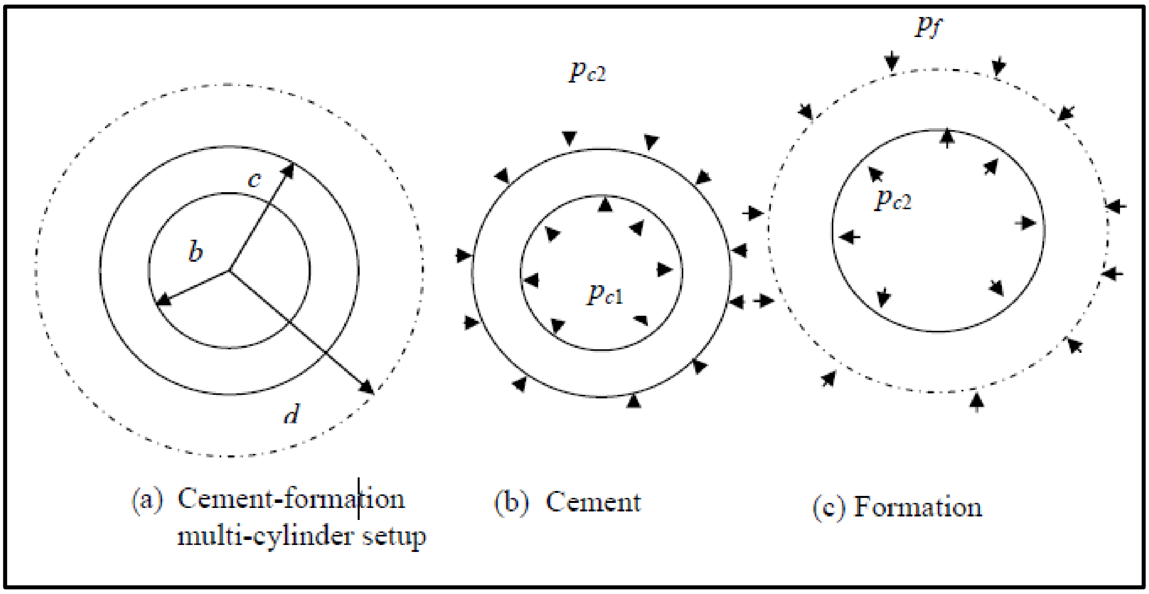

Figure 47: Stresses acting on the cement-formation interface; Source: (Teodoriu et al. 2010)

Considering the cement and the formation as a thick-walled cylinder, the tangential hoop stress and the radial stress in the cement sheath are related to Lamѐ's equations.

$$\sigma_{\theta cement} = \frac{p_{c1}b^2}{c^2-b^2}\left(1+\frac{c^2}{r^2}\right) - \frac{p_{c2}c^2}{c^2-b^2}\left(1+\frac{b^2}{r^2}\right) \tag{14.}$$

$$\sigma_{rcement} = \frac{p_{c1}b^2}{c^2-b^2}\left(1-\frac{c^2}{r^2}\right) - \frac{p_{c2}c^2}{c^2-b^2}\left(1-\frac{b^2}{r^2}\right) \tag{15.}$$

$$\sigma_{zcement} = \nu^2(\sigma_r + \sigma_\theta) - \alpha E \Delta T \tag{16.}$$

For the computation of the contact pressures p_{c1} *and* p_{c2} terms of A, B, C, D, K, and F are formed for simplification:

$$p_{c1} = \frac{FB-KC}{DB-AK} \tag{17.}$$

$$p_{c2} = \frac{C - \left[\frac{FB-KC}{DB-AK}\right]A}{B} \tag{18.}$$

Where,

$$A = \left\{\frac{b}{E_c}\left[(1-\nu_c^2)\left[\frac{b^2+c^2}{c^2-b^2}\right] + (\nu_c+\nu_c^2)\right] + \frac{a}{E_s}\left[\frac{r_m}{t_s}(1-\nu_s^2) + (\nu_s+\nu_s^2)\right]\right\} \tag{19.}$$

$$B = -\left[\frac{b}{E_c}\left(\frac{2c^2}{c^2-b^2}\right)(1-\nu_c^2)\right] \tag{20.}$$

$$C = \frac{p_i a}{E_s}\left[\frac{r_m}{t_s}(1-\nu_s^2) + (\nu_s+\nu_s^2)\right] + [(1+\nu_s)a\alpha_s\Delta T] - [(1+\nu_c)b\alpha_c\Delta T] \tag{21.}$$

$$D = -\left[\frac{c}{E_c}\left(\frac{2b^2}{c^2-b^2}\right)(1-\nu_c^2)\right] \tag{22.}$$

$$K = \Bigg\{\frac{c}{E_f}\bigg\{\left(1-\nu_f^2\right)\left[\frac{d^2+c^2}{d^2-c^2}\right]+\left(\nu_f+\nu_f^2\right)\bigg\}+\frac{c}{E_c}\left[1-\nu_c^2\right]\left(\frac{b^2+c^2}{c^2-b^2}\right)-\left(\nu_c+\nu_c^2\right)\Bigg\} \qquad 23.$$

$$F = \left\{\frac{p_f c}{E_f}\left(\frac{2d^2}{d^2-c^2}\right)\left(1-\nu_f^2\right)\right\}-\left[\left(1+\nu_f\right)c\alpha_f\Delta T\right]+\left[(1+\nu_c)c\alpha_c\Delta T\right] \qquad 24.$$

With,

Casing inner radius, a: 4,2675 in

Casing outer radius, b: 4,8125 in

Cement outer radius, c: 6,9375 in

Formation radius, d: 10 in

Casing thickness, t_s: 0,545 in

Casing mean radius, r_m: 4,54 in

Formation Young's Modulus, E_f: 3 x 10^6 psi

Formation Poisson ratio, ν_f: 0,42

Formation expansion coefficient, α_f: 3 x 10^-6 in/°F

Steel Young's Modulus, E_s: 29 x 10^6 psi

Steel Poisson ratio, ν_s: 0,3

Steel expansion coefficient, α_s: 7,2 x 10^-6 in/°F

Well internal pressure, p_i: 3000 psi

Formation pressure, p_f: 1000 psi

ΔT: 100 °F

Cement expansion coefficient, α_c: 6 x 10^-6 in/°F

The response of the model has been studied on three different cement cases, to show the influence of the cement properties on the stresses in the cement sheath, leading to a potential failure in the cement and loss of well integrity.

1. Cement case 1: A brittle cement with a compressive strength σ_c of 9500 psi, a tensile strength σ_t of 1000 psi, a Young's Modulus E_c of 3 x 10^6 psi, a Poisson ratio of 0,1 was used.
2. Cement case 2: A ductile cement with a compressive strength σ_c of 3000 psi, a tensile strength σ_t of 500 psi, a Young's Modulus E_c of 0,7 x 10^6 psi, a Poisson ratio of 0,4 was used.
3. Cement case 3: A ductile cement with a compressive strength σ_c of 2500 psi, a tensile strength σ_t of 300 psi, a Young's Modulus E_c of 1 x 10^6 psi, a Poisson ratio of 0,25 was used.

5.2 Discussion of Results

This analytical model has been used to understand the impact of static loads and temperature changes on the stresses in the cement sheath. Different cement systems have been used in the analysis to show the influence of ductility or brittleness on the acting stresses. To show the contribution of thermal effects and static loadings each, in the first part of the analysis only the contribution of the pressure is studied, and in the second part the contribution of both the pressure and the thermal effects are included.

Case Scenarios without consideration of thermal effects

With an inner pressure of 3000 psi and a formation pressure of 1000 psi, Figure 48 and Figure 49 show the trend of the tangential and radial stresses in the cement sheath. The results show that all three cement systems generate tensile (positive) tangential stresses, with cement system two being exposed to the lowest stress. Cement system one generates the highest tensile tangential stress. Also, there is a significant change in the tangential stress along the stress profile because there is a big difference between the Poisson ratio of the cement (0,1) and the formation (0,42). The cement system two generates the least amount of tangential stress. Cement system three also follows the pattern of cement system 2. The radial stresses for all three cement systems are mostly compressive (negative). Again, cement system one has steeper profile due to its material properties.

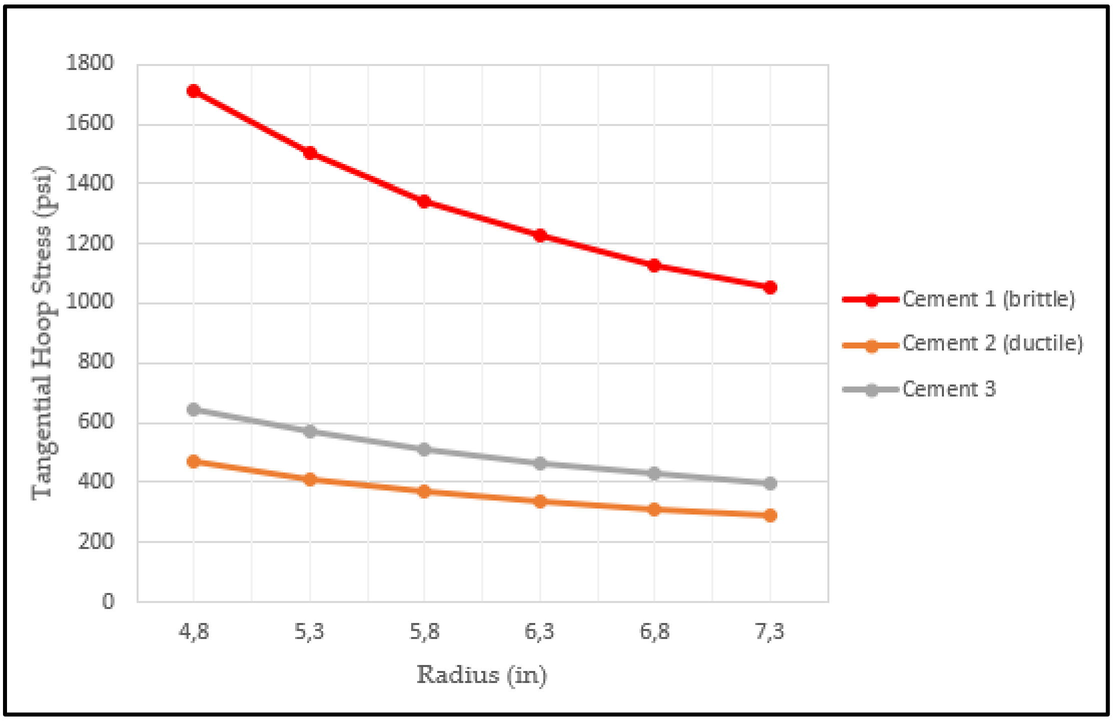

Figure 48: Tangential stress profile in the cement due to the static pressures in the formation and the internal part of the wellbore

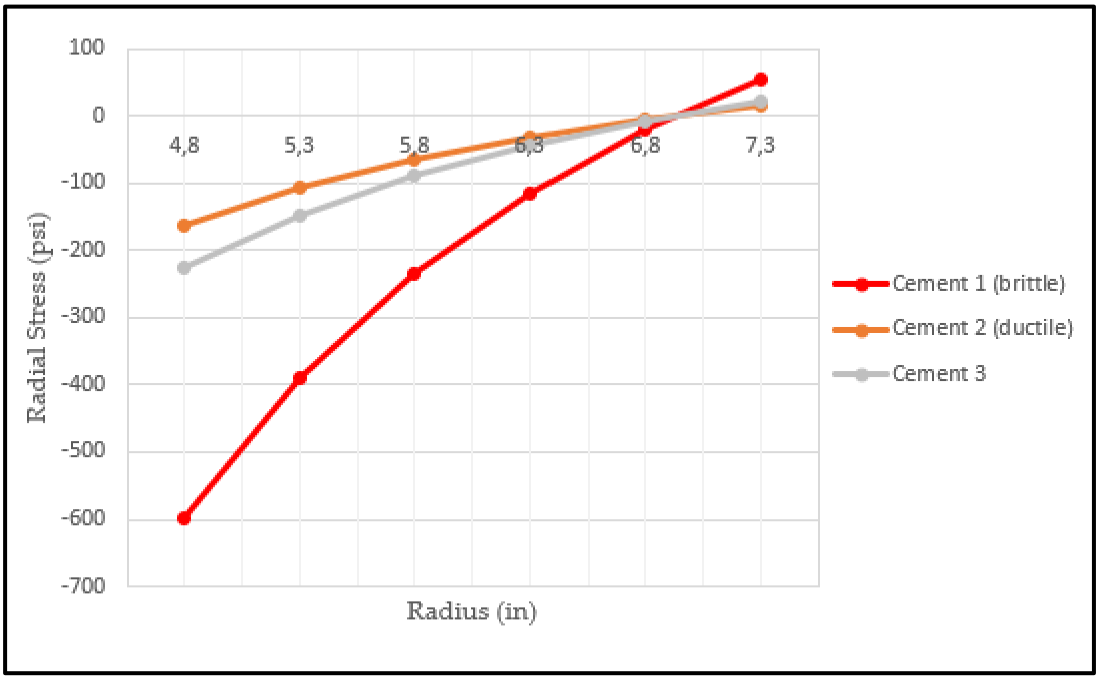

Figure 49: Radial stress profile in the cement sheath due to static pressures in the formation and the internal part of the wellbore

Case Scenarios with consideration of pressure and thermal effects

With all parameters unchanged, Figure 50 and Figure 51 show the stress profiles under consideration of both static pressures and temperature in the cement sheath. It shows that the highest part of the stresses is a product of static pressures in the wellbore and the formation. However, the influence of temperature to the total tangential stress is around 20 %. The trend of the tangential stress profile across the cement sheath remains somewhat similar, with the only difference that it is higher than without the consideration of thermal effects. This makes the tangential stress more tensile (positive). The radial stresses are also exhibiting a similar trend as they move from -736 psi (compressive) to 55 psi (tensile).

The analysis shows the importance of the cement's material properties and its ability to withstand certain stresses in the wellbore. Ductile cement systems, which was represented by cement system two in this case, with high Poisson ratio and low Young's modulus, perform more favorable under static loading conditions than brittle cement systems like cement system 1, which have a low Poisson ratio and high Young's modulus. Ductile systems also produce substantially lower values of tangential and radial stress, while brittle systems produce not only higher stress values but also exhibit a steep stress profile along the cement sheath, as seen in the figures above and below. The influence of other properties on the stress like formation material properties is rather low. However, a higher formation pressure counteracts high internal casing pressures reducing the stresses in the cement sheath. A formation that has a low Poisson ratio and is, therefore, more brittle will lead to the fact that more stresses are passed on to the cement sheath and the casing.

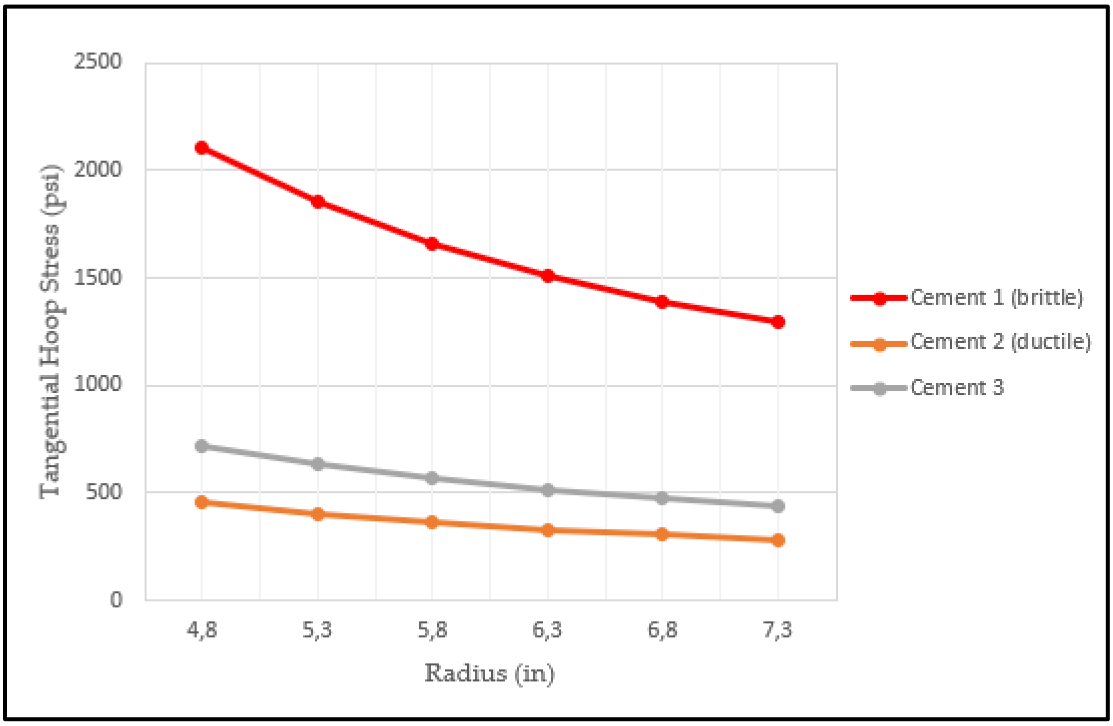

Figure 50: Tangential stress profile in the cement sheath due to pressures and thermal effects.

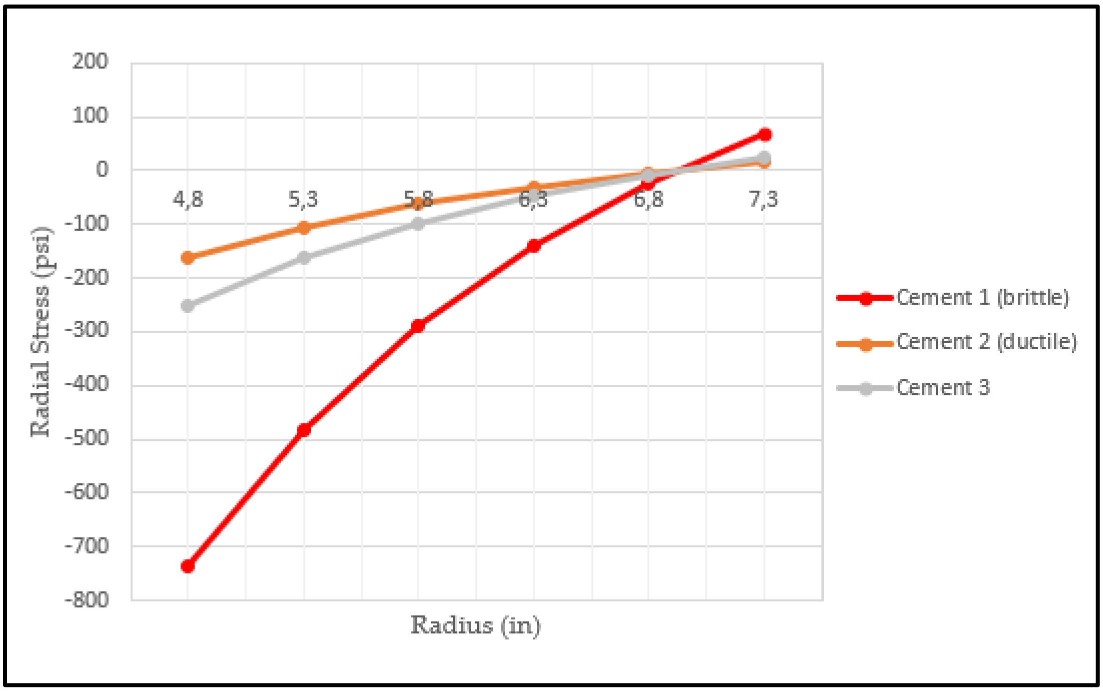

Figure 51: Radial stress profile in the cement sheath due to pressures and thermal effects.

Chapter 6 **Test Cell Design**

The basic cement stress model uses Lamè's equation to calculate the stresses in the cement sheath. For stress-model validation, a testing apparatus should help to verify the calculated stresses in the wellbore cement. Figure 52 and Figure 53 and Table 17 show a potential conceptual design of how such a testing cell could be assembled. The conceptual apparatus design is comprised of a base plate, a casing that is connected to the baseplate via a threaded connection, a top blind-flange with an inlet to produce the pressure needed. Spiral-wound gaskets were used as sealings between the casing, and the blind flange. Those gaskets are manufactured by spirally winding V-shaped metal strips as well as a piece of non-metallic filler material. The metal strip holds the filler, providing the gasket with mechanical resistance and resilience. The annulus between the casing and the Plexiglas should be filled with cement. Through CO_2-injection, the pressure inside the casing should be increased to a predefined value. As theoretically described in the previous chapter, through increasing internal pressure, the casing will expand and exert the pressure p_{c1} on the cement sheath, which will lead to stress in the cement sheath. These stresses will be measured with the help of sensors in the cement (see 6.1).

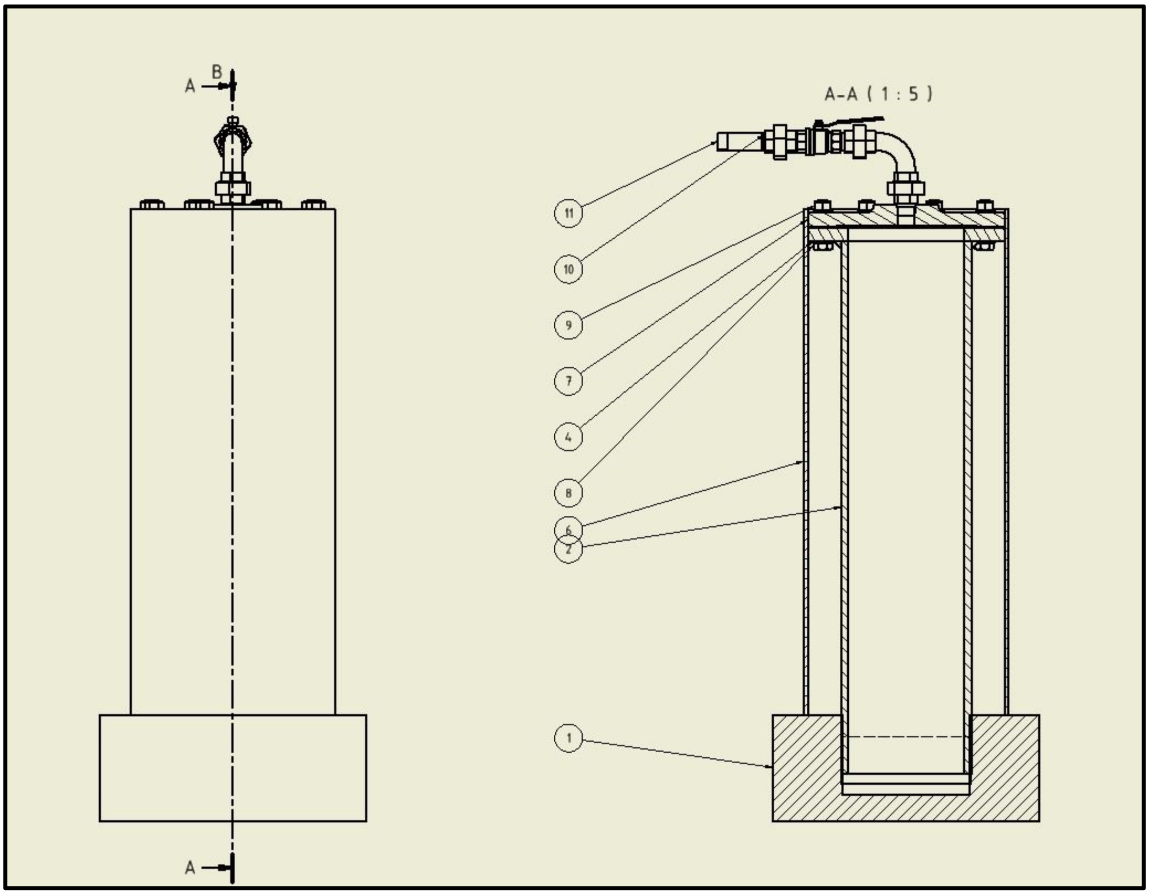

Figure 52: Front-and cross-sectional view of the test cell design

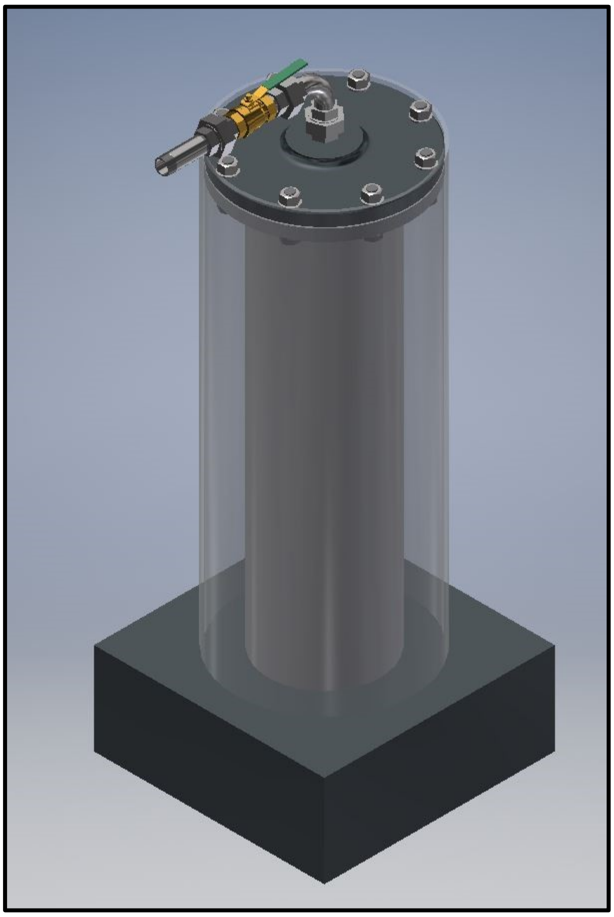

Figure 53: 3D-view of the test cell

Object no.	No. of pieces	Article/description
1	1	Baseplate
2	1	9 5/8″ casing with one flange and one threaded connection
3	1	Spiral wound gasket-ASME B16,5-Class 400-8
4	24	Washers-normal version-class A-ISO-7080-20
5	8	Hexagon screws-ISO 4018-M18 x 45
6	1	Plexiglas pipe ID 9 5/8″
7	1	Blind flange
8	8	Hexagon screws-ISO 4018-M20 x 80
9	8	Hexagon nuts-ISO 4032-M20
10	3	Malleable cast iron fittings ISO 49
10	1	90° angular fitting piece ISO 49
10	1	High-pressure two-way ball valve-XV520P-16
11	100,00mm	Threaded pipe ISO 7595 with DN 25-100 threads

Table 17: Part list for the test cell

6.1 Sensors

Designing the test cell in a way that it is easy to manufacture, set up, and also withstanding all the pressures applied, is a very crucial part. However, without sensors to measure the stresses and pressures, the testing cell would be useless. Various techniques have been applied to measure the stresses in concrete. Strain gauges are most commonly adhered to the outer surface of the specimen to measure pressure, force, and tension on the surface of the cement specimen. However, in the proposed testing apparatus, there is no outer surface available to place the gauges, and also the value and distribution of stress and strain inside of the cement specimen are needed to study the cement’s behavior during pressure testing and well operation. Therefore, strain gauges are not the optimal sensing devices for this setting. These types of sensors are primarily used to monitor strain in concrete structures for structural health monitoring in the construction industry. For the application proposed above, sensors that are embedded within the concentric cement annulus between the Plexiglas and the casing are necessary, to obtain data on the stress profile in the cement sheath. Fiber optic sensors (Deng 2007), ultrasonic sensors and magnetic microwires (Olivera et al. 2014) have been used to measure internal cement sheath stresses and deformations. Usually, mechanical stress/strain sensors are attached to the reinforcement. However, as there is no reinforcement in the concentric cement sheath, sensors that can be embedded in the liquid cement while it is hardening are the first choice for above application. Also, the sensors should have following requirements, accuracy, robustness, cost-effectiveness, immunity to magnetic interference, easy positioning, simplicity of operation, bonding between cement and sensor and possibility of remote operation (Olivera et al. 2014). Therefore, focus is put on fiber optics and magnetic microwires.

Magnetic Microwires

Magnetic microwires consist of a metallic nucleus (~10-80 micrometer diameter) covered by amorphous glass coating (~2-20 micrometer thickness) and have gained much attraction due to their small dimensions (Zhukov et al. 2004). The wires are manufactured by concurrently melting the metallic nucleus with the insulating coating, with subsequent sudden water cool down to achieve its amorphous characteristic, leading to a strong and unique internal stress distribution.

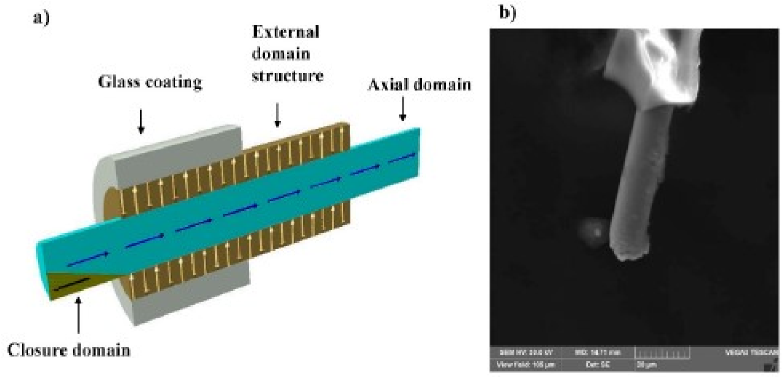

Figure 54: Schematic domain structure of a magnetic microwire and micrograph of the glass-coated microwire; Source: (Olivera et al. 2014)

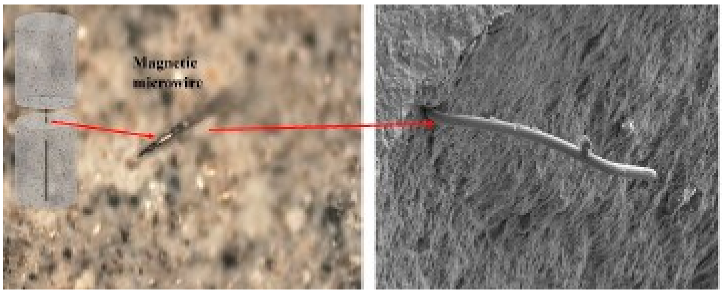

Figure 55: Optical and electronic micrograph of the concrete embedded microwire; Source: (Olivera et al. 2014)

Figure 54 and Figure 54 show the domain structure of amorphous microwires with one single axial domain in the inner part, surrounded by a radial domain, below the glass coating surface. Also, little closure domains are appearing at the end to decrease the stray fields. The glass-coated magnetic microwires exhibit exceptional magnetic properties such as magnetic bistability and a giant magneto impedance effect. The first one is characterized by the presence of rectangular hysteresis loops at a low applied magnetic field. The nature of the squared hysteresis loop is interpreted as a magnetization reversal process inside the inner core of a bistable microwire. The switching field in the microwire is susceptible to changes in the mechanical stress and the external magnetic field. Also, the wire is sensitive to temperature due to different thermal expansion coefficients of the glass coating and the metallic nucleus. The dynamics of domain wall propagation can be up to 18.000 km/s, making it easy to receive signals from a small number of microwires (Olivera et al. 2014). This makes the application of magnetic microwires very attractive for stress measurements in the cement sheath.

Fiber optics

Fiber optics measurements are used for smart sensing applications in structural health monitoring of civil engineering structures. They have numerous advantages compared to conventional electrical strain gauges. As magnetic microwires, they can be installed in the liquid cement, which makes these sensing technologies very interesting for strain and temperature measurements of the cemented annulus in a hydrocarbon well. In fiber optics, there is only one lead-in cable necessary to have numerous measurement points. Also, due to their relatively small size, impact on the cement through the sensor can be minimized, and a complete picture of the strain behavior with an adequate spatial resolution can be gathered. Challenges that have to be considered during these measurements, are glass fiber protection during installation and monitoring in harsh environments, and proper placement in the monitored cement without jeopardizing its integrity through the cable installation.

The measurement principle of a fiber cable is based on intensity losses and attenuation of optical light signals between input and output. Some components of these losses are backscattering effects with specific spectral characteristics, which carry information about geometrical, physical or chemical quantities. This information can be related to the fiber position by using the signal runtime. Various measurement principles are currently available on the market. Rayleigh backscattering systems provide a high spatial resolution of up to 10 mm with measurement precision of around 1 micrometer/m. However, the sensing range is almost always limited to 100 m or lower. Brillouin scattering is suitable for measurements along optical fibers with up to 100 km of length and measurement precision of around 4-10 micrometer/m (Monsberger and Moritz 2018).

Environmental conditions in the proposed in-situ test cell design would not be very harsh. However, in case of a field application, harsh conditions are prevalent for the optical fibers in well application. Therefore, sensor cables must be robust and protected. The challenge at this moment lies in the interlocking of all protective layers in the cable to ensure a reliable strain transfer from the outer layer to the sensitive glass-fiber core. However, as seen in Figure 56, there are different cable types. Usage of a special metal layer helps to protect the optical strain sensing fibre. Depending on the use of the cable, additional protecting layers are used, which are frictionally connected to the metal tube. The structured surface of the outer layer ensures that the cable bonds with the cement, preventing unwanted channels that might allow fluid passage (Monsberger and Moritz 2018).

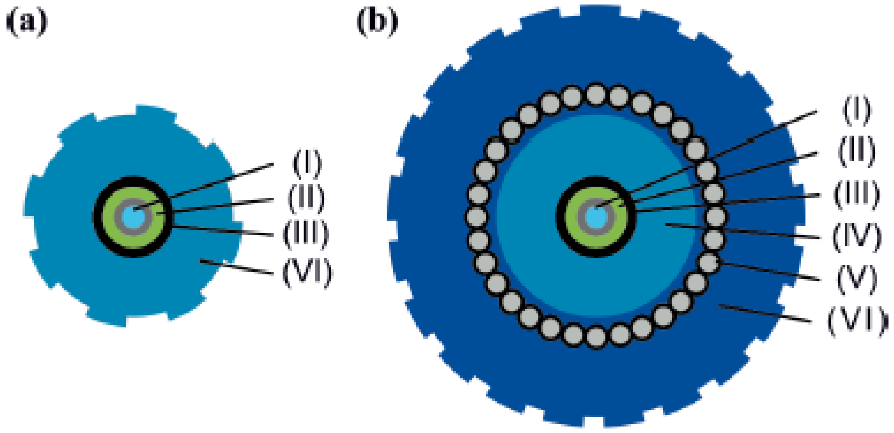

Figure 56: Structure of strain sensing cables from Solifos AG with (I) strain sensing single mode fiber (Ø 250 μm), (II) multi-layer buffer with strain transfer layer, (III) metal tube, (IV) polyamide protection layer, (V) special steel armouring and (VI) polyamide outer sheath: a) Type V9 (Ø 3.2 mm); b) type V3 (Ø 7.2 mm); Source: (Monsberger and Moritz 2018)

Chapter 7 **Summary, Conclusion, Discussion & Future Work**

This thesis is aimed to build a wellbore scorecard tool, to assess the performance of the well construction process on 29 casing/liner well sections in 11 wells on OMV's onshore Vienna Basing lease. The scorecard assigns each well section a score between 0 -100. A score of 100 means that the wellbore section is of "perfect" quality and drilling, final BHA pull-out-of-hole, casing-running and cementing was carried out "as per design" and according to industry-proven standards. A theoretical score of 0 assigns a "disastrous" wellbore quality. However, a score of 0 implies that crews were unable to bring the section to total depth due to stuck pipe or casing. The performance assessment applied in the scorecard is extremely valuable in detecting shortcomings in the well construction process to help determine root causes of well integrity events. The scorecard quickly identifies improper cement qualities and placement and shortcomings in the hydraulic/operational, well design and casing pressure testing parameters. Also, the influence of different cementing service providers can be compared.

Knowledge of the well construction process performance helps to avoid mistakes from the past, enhance overall wellbore quality, and avoid well integrity events in the future. It can be seen as a tool to help learning from the past. The scoring results of the analysed 29 well sections show a range between 51 and 83 and are already part of the "proof of concept" of the scorecard. The two lowest-performing well sections fail their respective pressure test, and also, the third-and fourth worst-performing sections have a proven lack of zonal isolation. Furthermore, the scorecard's ability to point out problematic well sections has been proved with actual and expected/calculated casing pressure test bleed-off volumes.

Up to now, studies and research on well integrity incidents have focused firmly on constraints and shortcomings in the well operation phase and how the stresses in the casing/cement/rock-interface are developing and potentially threatening well integrity. In contradiction to that, the wellbore scorecard tool is the perfect and unique gadget of choice to determine the root causes of well integrity events due to shortcomings in the well construction process. After all, the aim is to make well construction and operation safer for the environment and humans involved and make the process more efficient to save costs and this tool is undoubtedly contributing to that goal.

However, the tool only covers the well construction process and not what is going on during well operation, including production, injection, and abandonment. In case a well section scores between 90 and 100, indicating perfect wellbore quality, this does not imply that there will never occur any well integrity event. Sure, it can be ruled out that this event is occurring due to mistakes in the well construction process. However, the tool does not capture what is happening in the later life stages of the well. Therefore, a more holistic approach to study and understand well integrity issues is necessary. To cover the whole life cycle of the well, the stress model should help to understand what is happening to the cement sheath during well operations. Understanding these in-situ tangential, radial and axial stresses in a wellbore helps to give recommendations on pressure thresholds, that should not be exceeded during pressure testing for example. The proposed design for an in-situ test cell should help to verify the stress model and complete the holistic approach to help understand, predict and avoid well integrity events.

As always the case, there are some limitations of this holistic approach that may affect the validity of the results. One might be that that the tool has only been applied and approved in OMV's Vienna Basin area lease, which consists of relatively conventional onshore wells. It would be exciting to see how the tool behaves in different areas like high-pressure high-temperature, offshore or shale/unconventional environment. Also, another significant role in determining the stress distribution in the cement sheath is its material properties, especially the cement's Young's modulus. All the perfect cement lab testing in the world cannot help in determining these in-situ properties in the hole at any point during the life of the well. Therefore, many assumptions would have to be made to do these calculations. Another original goal of the thesis was to use the scorecard tool as a prescription tool to prescribe or avoid the execution of a lengthy and expensive negative pressure test based on the scoring result. However, as OMV Austria is conducting these negative pressure tests only on liner laps, bridge plugs and cement plugs and only limited tests were conducted in the last years, the tools ability to prescribe the negative pressure test is still unsure and needs further testing.

One valuable way to expand this thesis could include the establishment of a finite element analysis (FEA) stress model to enhance the stress prediction in the casing/cement/formation interface, with particular focus on the bond strength. Furthermore, manufacturing and first tests of the proposed in-situ test cell design could be subject for a new Master's or Ph.D. Thesis, for which the work proposed here could be the basis. The thesis can be expanded to experiment with different kind of sensors to make the necessary strain measurements in the cement sheath. Among other parameters, statistical comparison of the measured cement-flow rate and density could also be included in the scorecard but were not fully considered for time reasons.

Avoiding well integrity events in the future requires a holistic approach to the topic. While the oil industry is slow in adopting new technologies a lot of other disciplines like metallurgy, material science or measurement systems engineering might have already found solutions to our problems. We need to look outside our discipline and also industry to learn, adopt and adapt these technologies to our challenges quickly and effectively. This thesis offers a valuable input in covering the well construction process, to capture what can be done better in the future to positively impact the environment, humans involved and costs.

Appendix A Stresses and Deformations of cylinders

When talking about pressurization effects on cylinders, a distinction has to be made between thin-walled cylinders and thick-walled cylinders. Generally, when a concentric cylinder's inner diameter d_i is 40 times larger than its thickness t_h, thin-wall analysis can be safely used. For ratios smaller than 40, the thick-wall analysis should be used (refer to Table 18)

$\frac{d_i}{t_h} > 40$	→	thin-walled cylinders	25.
$\frac{d_i}{t_h} < 40$	→	thick-walled cylinders	26.

Table 18: Criteria for the usage of thin-or thick-walled cylinder analysis

The thin-wall analysis becomes more accurate as the ratio increases. Equation 25 must be fulfilled, but 26 may be valid for a larger range than stated here.

For oilfield casing only the thick-walled cylinder analysis is applicable. This is demonstrated by the following example:

Consider a typical, rather thin 7 in OD production casing with the following specifications:

- $d_i = 6.456\ in$
- $t_h = 0.272\ in$

Therefore, the ratio is:

$$\frac{6.456}{0.272} = 23.74$$

Consequently, thick wall analysis should be applied for all other 7 in casings, as this is the thinnest. Out of the 90 different casing configurations available according to the drilling data handbook, only 3 have a ratio that is greater than 40:

1. $d_i = 15.25\ in;\ t_h = 0.375\ in;\ \frac{d_i}{t_h} = 40.67$
2. $d_i = 17.755\ in;\ t_h = 0.435\ in;\ \frac{d_i}{t_h} = 40.82$
3. $d_i = 19.124\ in;\ t_h = 0.438\ in;\ \frac{d_i}{t_h} = 43.66$

This makes the thick-walled cylinder analysis preferred choice for stress and deformation calculation in most oilfield casings. However, for the sake of completeness thin-walled cylinder analysis is also covered at this point.

A.1 Thin-Walled Cylinders

Figure 57 shows a thin-walled cylinder, which is subject to internal pressure p_i. In thin-walled cylinders, it is assumed, that the stress distribution is uniform throughout the cross-section. The radial stress is small relative to the circumferential (hoop) stress because $t_h/d_i \ll 1$. Therefore, a small element can be considered to be in plane stress with principal stresses, σ_r in radial direction, σ_θ in circumferential direction (hoop stress) and σ_z in longitudinal direction, shown in Figure 59. Figure 58 shows the forces acting on a small element due to internal pressure. This element as well has a length dl coming out of the paper. Summing forces in radial direction gives

$$p_i r_i d\theta dl = 2\sigma_{avg} \sin\left(\frac{d\theta}{2}\right) t_h dl$$

As $d\theta/2$ is very small, sin $(d\theta/2)$= $d\theta/2$ and

$$\sigma_{\theta,avg} = \frac{p_i r_i}{t_h} \qquad 27.$$

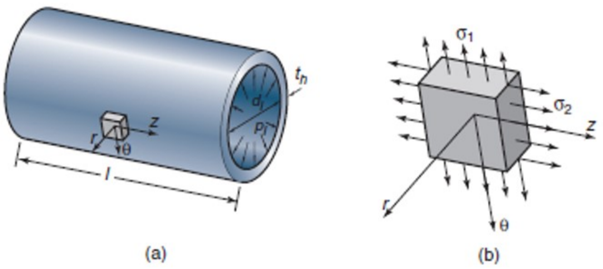

Figure 57: (a) Internally pressurized, thin-walled cylinder; (b) stresses acting on a small cylinder element; Source: (Schmid, S.R.; Hamrock, B. J.; Jacobson 2014)

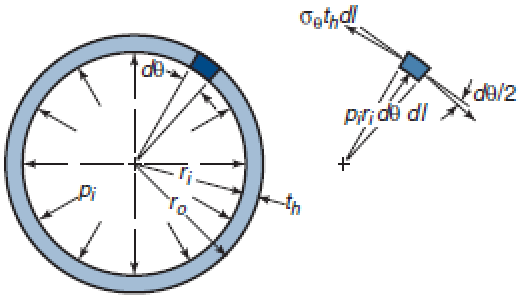

Figure 58: Front view of an internally pressurized thin-walled cylinder; Source: (Schmid, S.R.; Hamrock, B. J.; Jacobson 2014)

The θ component of the stress is called tangential or hoop stress. The maximum hoop stress can be obtained by modifying Equation 27 in a way that r_i is displaced with r_{avg}

$$r_{avg} = r_i + \frac{t_h}{2} = \frac{d_i + t_h}{2} \qquad 28.$$

$$\sigma_{\theta,max} = \frac{p_i r_{avg}}{t_h} = \frac{p_i(d_i + t_h)}{2t_h} \qquad 29.$$

The area exposed to axial stress is

$$A = \pi\left(r_o^2 - r_i^2\right) = 2\pi r_{avg} t_h \tag{30.}$$

Therefore, the axial stress is

$$\sigma_{z,avg} = \frac{p_i r_i^2}{r_o^2 - r_i^2} = \frac{p_i r_i^2}{2 r_{avg} t_h} \tag{31.}$$

With consideration of $r_i \approx r_{avg} \approx r$ and Equations 29 and 31, the stresses in thin-walled cylinders are

$$\sigma_r = 0 \tag{32.}$$

$$\sigma_\theta = \frac{p_i r}{t_h} \tag{33.}$$

$$\sigma_z = \frac{p_i r}{2 t_h} \tag{34.}$$

Note that the circumferential (hoop) stress is twice the axial stress.

A.2 Thick Walled Cylinders

As mentioned in the previous section, for thin-walled cylinders, the axial and circumferential stresses are assumed to be uniformly distributed over the cross-section. This assumption cannot be made for thick-walled cylinders.

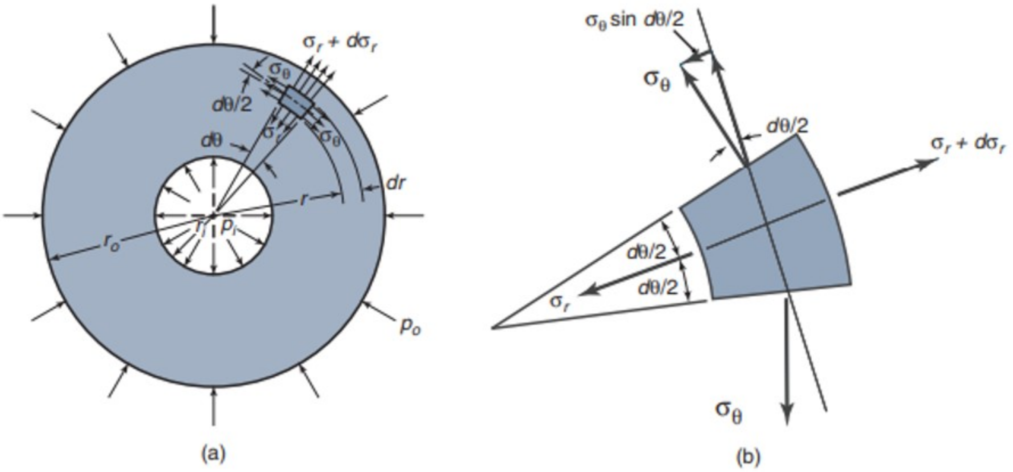

Figure 59: Cross-sectional view of a cylinder (a), with stresses acting on the element (b); Source: (Schmid, S.R.; Hamrock, B. J.; Jacobson 2014)

Figure 59 (a) shows a thick-walled cylinder, that is pressurized both internally and externally. Shear stresses in the circumferential and radial direction are not present due to the symmetry of the cylinder and the loading. Therefore, only normal stresses in the radial σ_r and circumferential direction σ_θ are present.

Figure 59 (b) shows a polar element of the cylinder before and after deformation. δ_r and δ_θ represent the radial and circumferential displacement. The strain is given by the change in the thickness, divided by the element thickness.

Stresses and Deformations of cylinders

$$\epsilon_r = \frac{\delta_r + (\partial\delta_r/\partial r)dr - \delta_r}{dr} = \frac{\partial\delta_r}{\partial_r} \quad 35.$$

$$\epsilon_\theta = \frac{(r+\delta_r)d\theta - rd\theta}{rd\theta} = \frac{\delta_r}{r} \quad 36.$$

Making use of Equations 35 and 36 together with Hooke's law, the stress-strain relation for the biaxial stress state gives

$$\epsilon_r = \frac{\partial\delta_r}{\partial r} = \frac{1}{E}(\sigma_r - \nu\sigma_\theta) \quad 37.$$

$$\epsilon_\theta = \frac{\delta_r}{r} = \frac{1}{E}(\sigma_\theta - \nu\sigma_r) \quad 38.$$

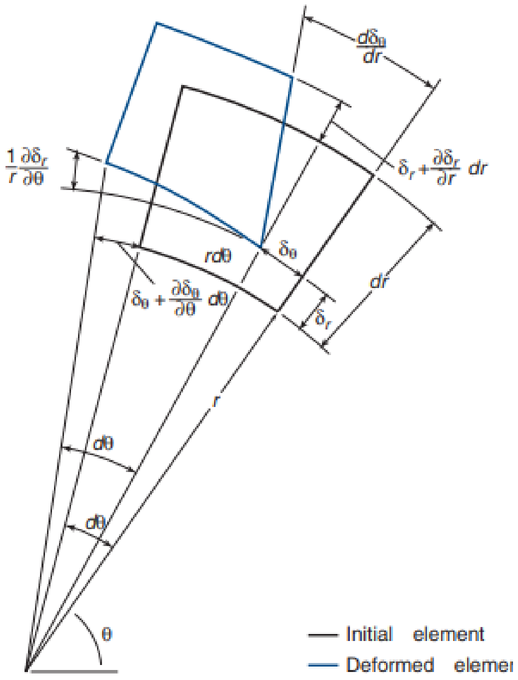
$\frac{d\delta_\theta}{dr}$
$\delta_r + \frac{\partial\delta_r}{\partial r}dr$
$\frac{1}{r}\frac{\partial\delta_r}{\partial\theta}$
$rd\theta$
δ_θ
$\delta_\theta + \frac{\partial\delta_\theta}{\partial\theta}d\theta$
dr
δ_r
r
$d\theta$
$d\theta$
θ
Initial element
Deformed elemei

Figure 60: Cylinder element before and after deformation; Source: (Schmid, S.R.; Hamrock, B. J.; Jacobson 2014)

Summation of all forces gives

$$(\sigma_r + d\sigma_r)(r+dr)d\theta dz - \sigma_r rd\theta dz - 2\sigma_\theta \sin\left(\frac{d\theta}{2}\right)drdz = 0 \quad 39.$$

For small $d\theta$, sin $(d\theta/2)$= $d\theta/2$ and when neglecting higher-order terms, Equation 39 reduces to

$$\sigma_\theta = r\frac{d\sigma_r}{dr} + \sigma_r \quad 40.$$

Substituting Equation 40 into 37 and 38, differentiating Equation 38 concerning r and then equalize 37 and 38 gives

$$0 = 2\frac{d\sigma_r}{dr} + \frac{d}{dr}\left(r\frac{d\sigma_r}{dr}\right) \quad 41.$$

Integrating and solving for the boundary equations for thick-walled cylinders pressurized both internally and externally:

1. $\sigma_r = -p_o$ at $r = r_o$
2. $\sigma_r = -p_i\ at\ r = r_i$

Gives

$$\sigma_r = \frac{p_i r_i^2 - p_o r_o^2 + (p_o - p_i)(r_o r_i/r)^2}{r_o^2 - r_i^2} \tag{42.}$$

$$\frac{d\sigma_r}{dr} = -\frac{2(p_o - p_i)(r_o r_i)^2}{r^3\left(r_o^2 - r_i^2\right)} \tag{43.}$$

Substituting Equations 42 and 43 into 40 gives

$$\sigma_\theta = \frac{p_i r_i^2 - p_o r_o^2 - \left(\frac{r_i r_o}{r}\right)^2 (p_o - p_i)}{r_o^2 - r_i^2} \tag{44.}$$

Equations 42 and 44 are also known as Lamé's equations.

Inserting Equations 42 and 44 in 38 gives the radial displacement δ_r of the cylinder

$$\epsilon_\theta = \frac{\delta_r}{r_i} = \frac{p_i}{E}\left(\frac{r_o^2 + r_i^2 - 2\left(\frac{p_o}{p_i}\right) r_o^2}{r_o^2 - r_i^2} + \nu\right) \tag{45.}$$

$$\delta_r = \frac{p_i r_i}{E}\left(\frac{r_o^2 + r_i^2 - 2\left(\frac{p_o}{p_i}\right) r_o^2}{r_o^2 - r_i^2} + \nu\right) \tag{46.}$$

With the help of the displacement due to the pressure differential, it is relatively easy to calculate the additional volume needed to compensate for casing expansion to fill the casing

$$\Delta V = \pi L_{csg}\left((r_i + \delta_r)^2 - r_i^2\right) \tag{47.}$$

$$\delta_r = \epsilon_\theta r_i \tag{48.}$$

$$\Delta V = \pi L_{csg}\left((r_i + \epsilon_\theta r_i)^2 - r_i^2\right) \tag{49.}$$

$$\Delta V = \pi L_{csg} r_i^2\left(2\epsilon_\theta + \epsilon_\theta^2\right) \tag{50.}$$

As ϵ_θ is already rather small, ϵ_θ^2 is even smaller and will, therefore, be neglected. Inserting Equation 45 into 50 will give the differential volume due to the casing expansion

$$\Delta V = 2\pi L_{csg} r_i^2 \frac{p_i}{E}\left(\frac{r_o^2 + r_i^2 - 2\left(\frac{p_o}{p_i}\right) r_o^2}{r_o^2 - r_i^2} + \nu\right) \tag{51.}$$

Internally Pressurized

In many applications, the external pressure p_o is zero, in that case, Equations 42 and 44 reduce to

$$\sigma_r = \frac{p_i r_i^2 \left(1 - \frac{r_o^2}{r^2}\right)}{r_o^2 - r_i^2} \tag{52.}$$

$$\sigma_\theta = \frac{p_i r_i^2 (1 + r_o^2/r^2)}{r_o^2 - r_i^2} \tag{53.}$$

Figure 61 shows that the circumferential stress is tensile, and the radial stress is compressive in an internally pressurized cylinder. Both stress maxima occur at $r = r_i$.

$$\sigma_{r,max} = -p_i \tag{54.}$$

$$\sigma_{\theta,max} = p_i \left(\frac{r_o^2 - r_i^2}{r_o^2 - r_i^2}\right) \tag{55.}$$

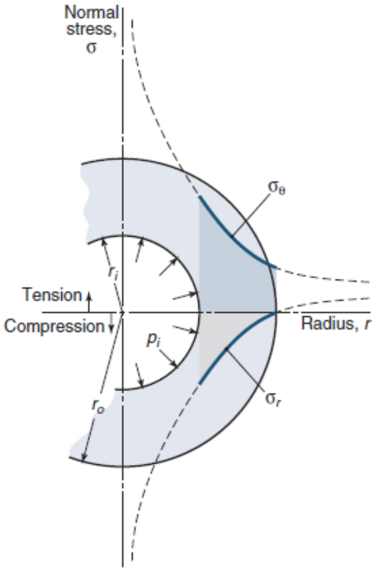

Figure 61: Radial and circumferential stress behavior for different radii for an internally pressurized, thick-walled cylinder; Source: (Schmid, S.R.; Hamrock, B. J.; Jacobson 2014)

The circumferential strain at the maximum stress location $r = r_i$ and the outward radial displacement, from Equation 36 gives

$$\epsilon_\theta = \frac{\delta_r}{r_i} = \frac{p_i}{E}\left(\frac{r_o^2 + r_i^2}{r_o^2 - r_i^2} + \nu\right) \tag{56.}$$

$$\delta_r = \frac{p_i r_i}{E}\left(\frac{r_o^2 + r_i^2}{r_o^2 - r_i^2} + \nu\right) \tag{57.}$$

Externally Pressurized

If only external pressure is present, and p_i is zero, Equations 42 and 44 reduce to

$$\sigma_r = \frac{p_o r_o^2}{r_o^2 - r_i^2}\left(\frac{r_i^2}{r^2} - 1\right) \tag{58.}$$

$$\sigma_\theta = -\frac{p_o r_o^2}{r_o^2 - r_i^2}\left(\frac{r_i^2}{r^2} + 1\right) \qquad 59.$$

Figure 62 shows that the in an externally pressurized cylinder, both the radial and circumferential stress are in the compressive area and the maximal radial stress occurs at $r = r_o$ moreover, the maximum circumferential stress occurs at $r = r_i$

$$\sigma_{r,max} = -p_o \qquad 60.$$

$$\sigma_{\theta,max} = -\frac{2p_o r_o^2}{r_o^2 - r_i^2} \qquad 61.$$

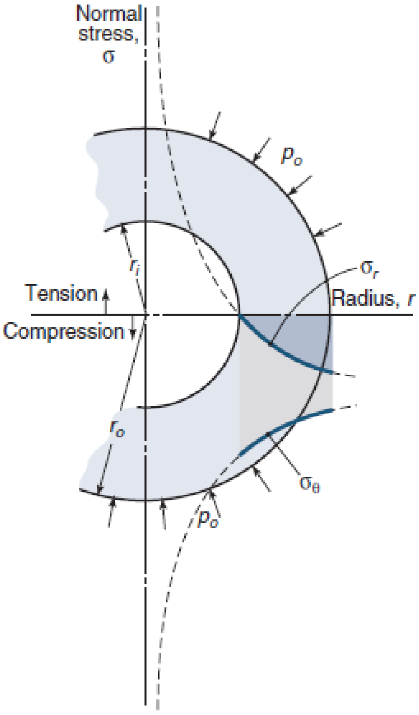
Normal
stress,
σ
p_o
σ_r
r_i
Radius, r
Tension
Compression
r_o
σ_θ
p_o

Figure 62: Radial and circumferential stress behavior for different radii for an externally pressurized, thick-walled cylinder; Source: (Schmid, S.R.; Hamrock, B. J.; Jacobson 2014)

Appendix B Approximate Solution of Compressibility Equation

The part is determined to the derivation of the differential volume ΔV due to compressibility and thermal expansion of the testing fluid used during a casing pressure test.

$$c_{mud} = \left(-\frac{1}{V}\frac{\partial V}{\partial P}\right) \tag{62.}$$

$$\alpha_{mud} = \left(\frac{1}{V}\frac{\Delta V}{\Delta \mathrm{T}}\right) \tag{63.}$$

The minus sign can be omitted in case of a positive pressure test, as the volume decrease is compensated by pumping more fluid.

$$c_{mud} = \left(\frac{1}{V}\frac{\partial V}{\partial P}\right) \tag{64.}$$

Integration will lead to the exact solution

$$c_{mud}\int \partial P = \int \frac{\partial V}{V} \tag{65.}$$

$$c_{mud}\Delta P = \ln(V) + C \tag{66.}$$

For Boundary condition $V(\Delta P = 0) = V_0$:

$$0 = \ln(V_0) + C \rightarrow K = -\ln(V_0) \tag{67.}$$

$c_{mud}\Delta P = \ln\left(\frac{V}{V_0}\right)$, with $V = V_0 + \Delta V$

$$c_{mud}\Delta P = \ln\left(1 + \frac{\Delta V}{V_0}\right) \tag{68.}$$

This can be simplified using series expansion

$$c_{mud}\Delta P = \ln\left(1 + \frac{\Delta V}{V_0}\right) = \frac{\Delta V}{V_0} - \frac{1}{2}\left(\frac{\Delta V}{V_0}\right)^2 + \frac{1}{3}\left(\frac{\Delta V}{V_0}\right)^3 - \frac{1}{4}\left(\frac{\Delta V}{V_0}\right)^4 + \cdots \tag{69.}$$

As the differential volume is already small compared to the original volume, all the following potential terms can be neglected, and the approximate solution for the compressibility equations can be reduced to the following

$$\Delta V = c_{mud} V_0 \Delta P \tag{70.}$$

$$\Delta V = \alpha_{mud} V_0 \Delta \mathrm{T} \tag{71.}$$

Appendix C Green Cement Pressure Test Data

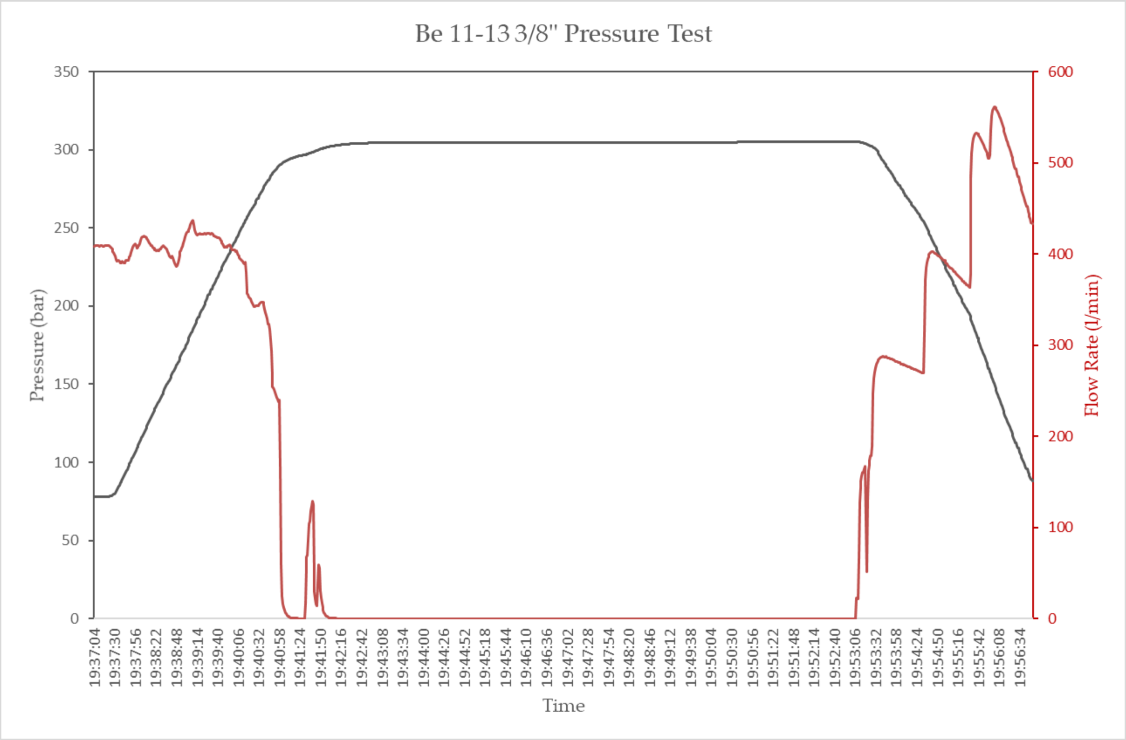

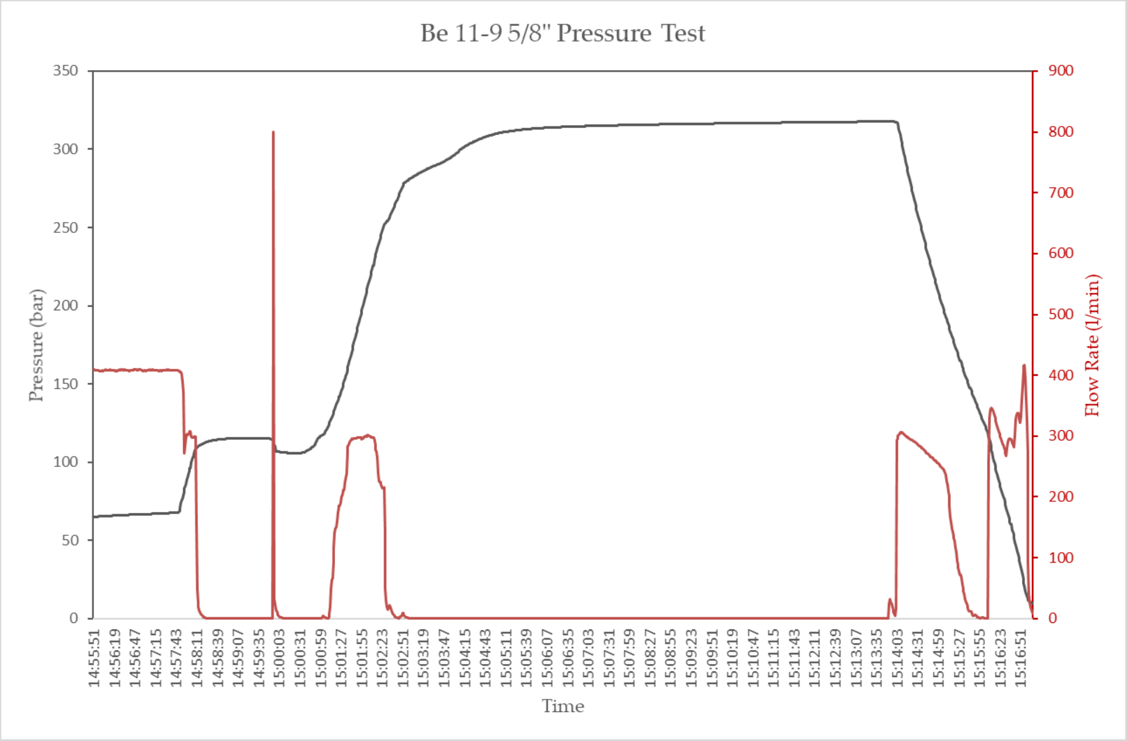

Green Cement Pressure Test Data

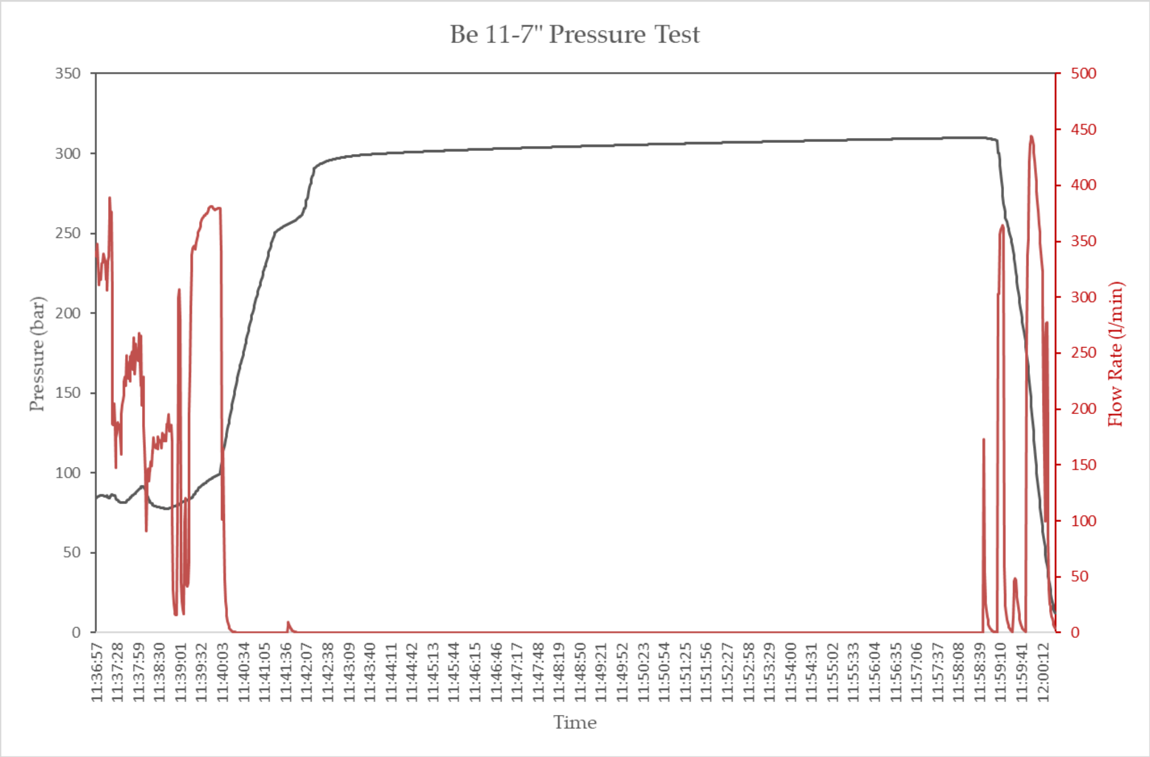

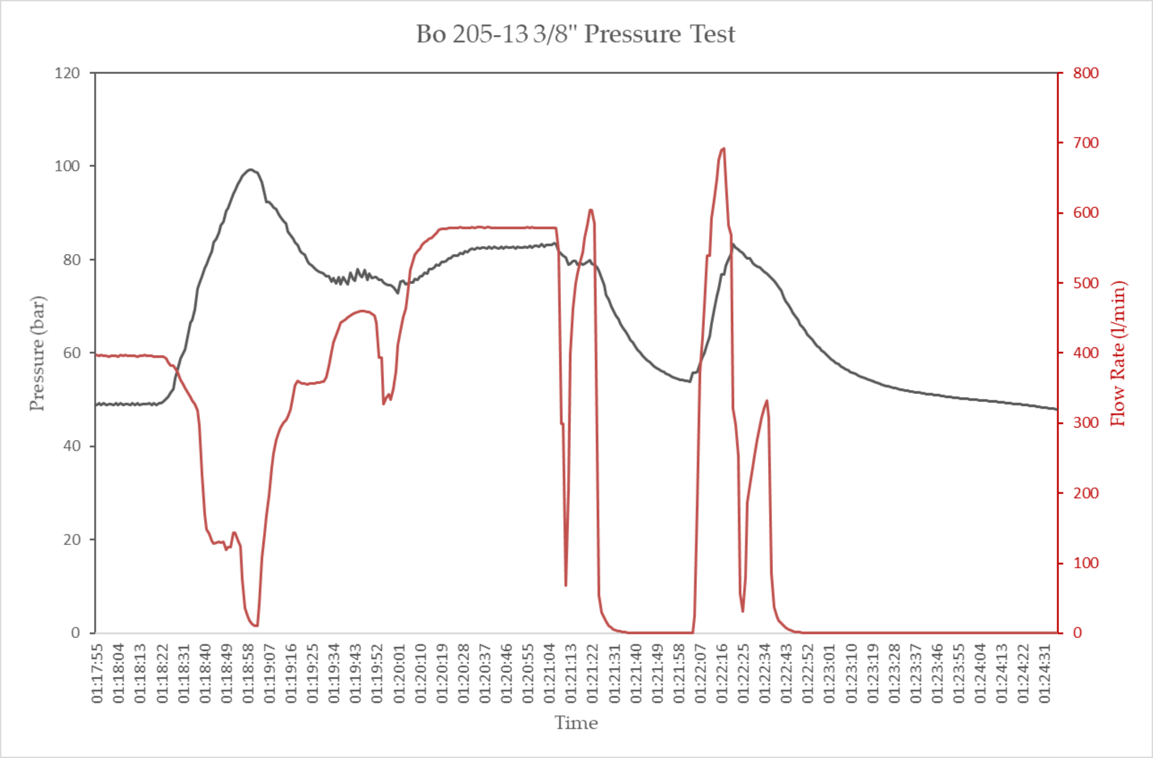

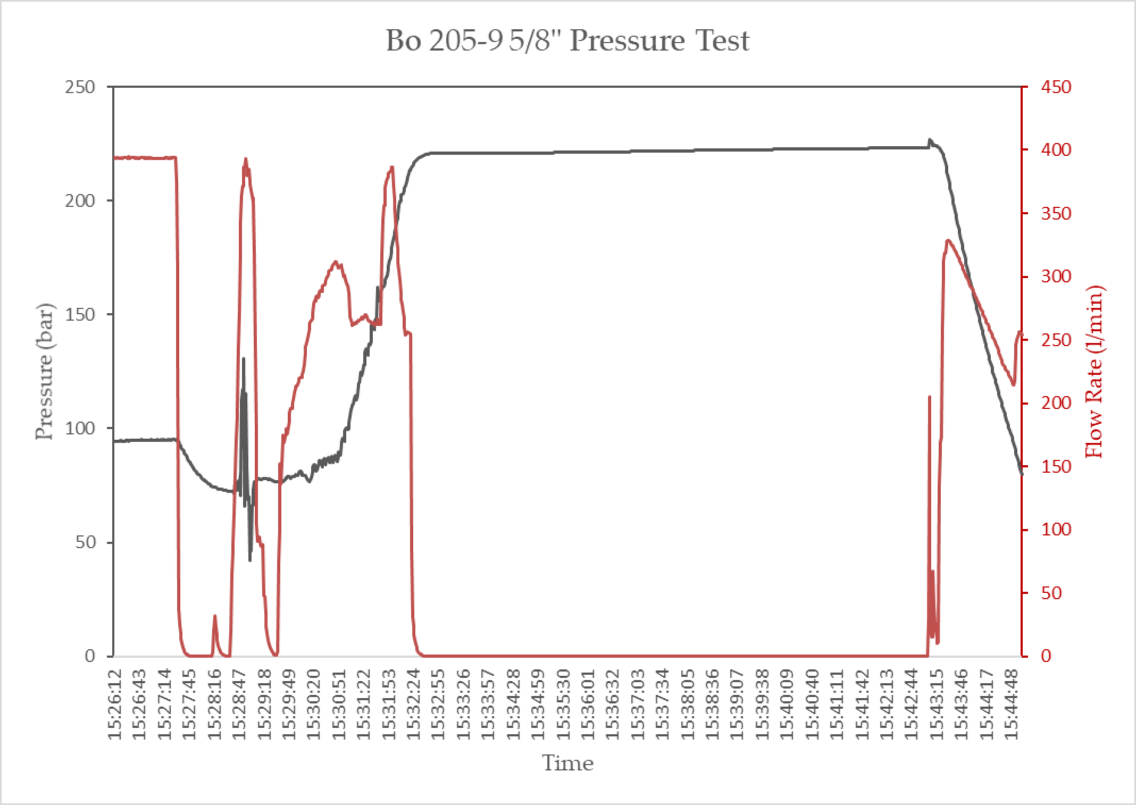
Bo 205-9 5/8" Pressure Test
Pressure (bar)
0
50
100
150
200
250
Flow Rate (l/min)
0
50
100
150
200
250
300
350
400
450
Time
15:26:12
15:26:43
15:27:14
15:27:45
15:28:16
15:28:47
15:29:18
15:29:49
15:30:20
15:30:51
15:31:22
15:31:53
15:32:24
15:32:55
15:33:26
15:33:57
15:34:28
15:34:59
15:35:30
15:36:01
15:36:32
15:37:03
15:37:34
15:38:05
15:38:36
15:39:07
15:39:38
15:40:09
15:40:40
15:41:11
15:41:42
15:42:13
15:42:44
15:43:15
15:43:46
15:44:17
15:44:48

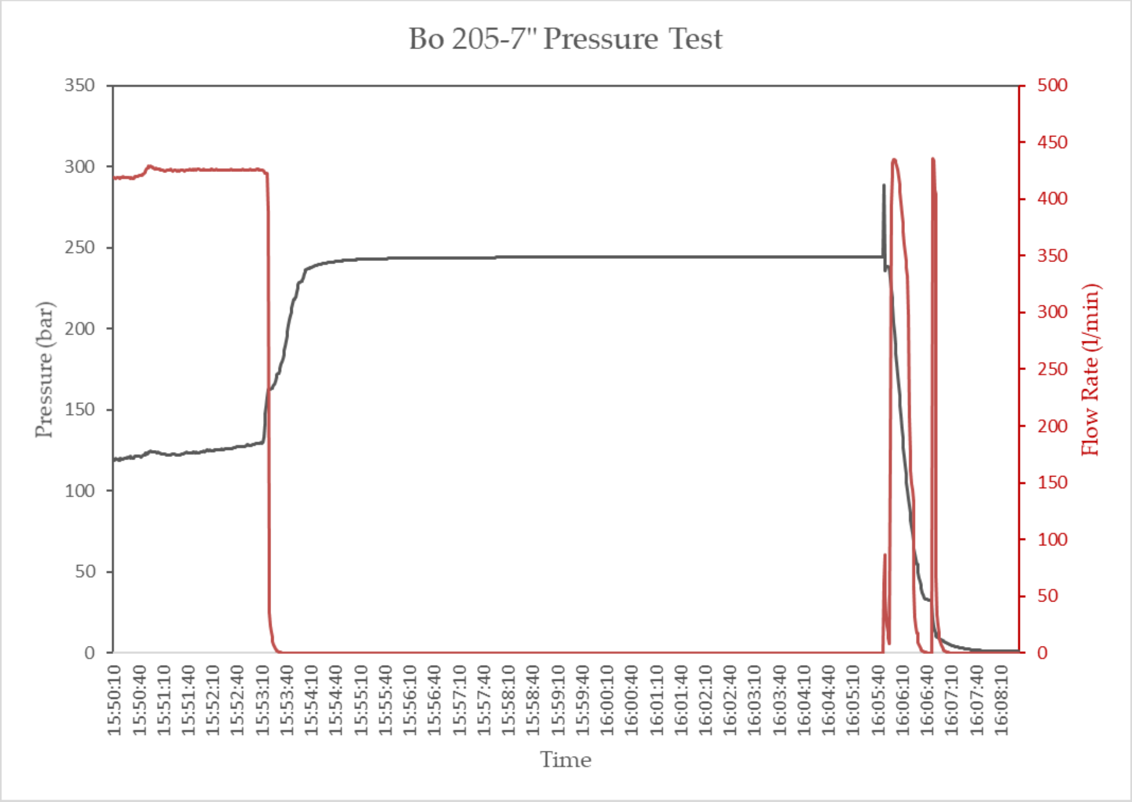
Bo 205-7" Pressure Test
Pressure (bar)
0
50
100
150
200
250
300
350
Flow Rate (l/min)
0
50
100
150
200
250
300
350
400
450
500
Time
15:50:10
15:50:40
15:51:10
15:51:40
15:52:10
15:52:40
15:53:10
15:53:40
15:54:10
15:54:40
15:55:10
15:55:40
15:56:10
15:56:40
15:57:10
15:57:40
15:58:10
15:58:40
15:59:10
15:59:40
16:00:10
16:00:40
16:01:10
16:01:40
16:02:10
16:02:40
16:03:10
16:03:40
16:04:10
16:04:40
16:05:10
16:05:40
16:06:10
16:06:40
16:07:10
16:07:40
16:08:10

Green Cement Pressure Test Data

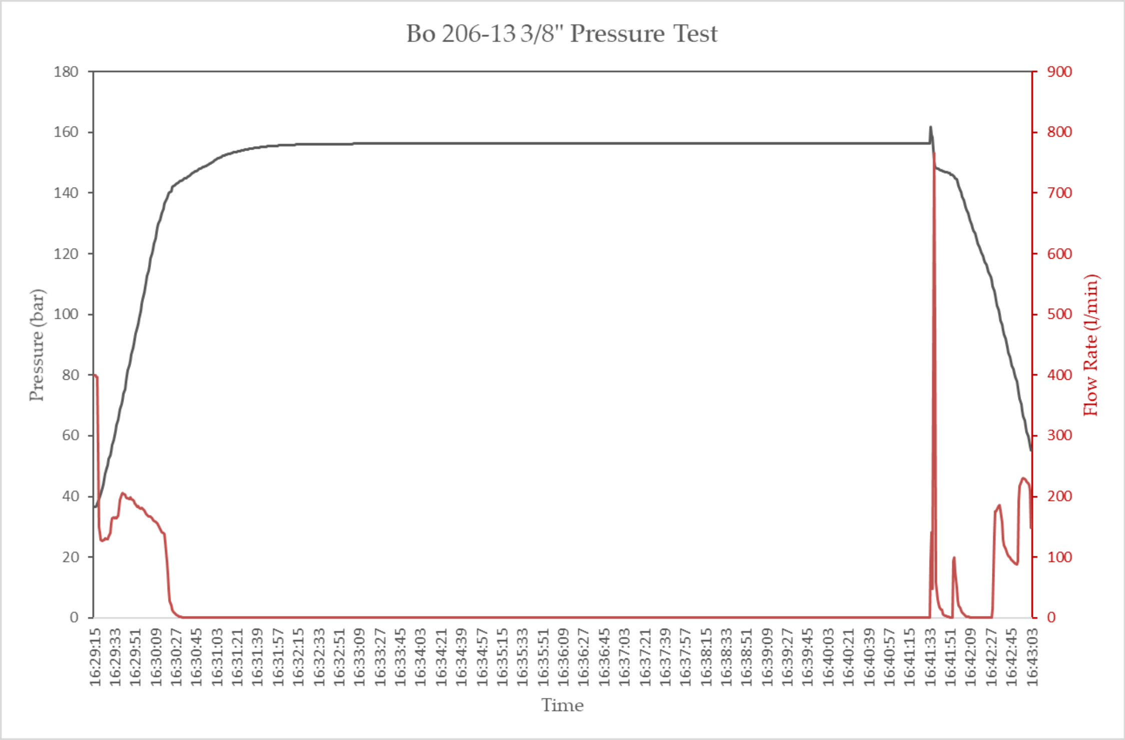

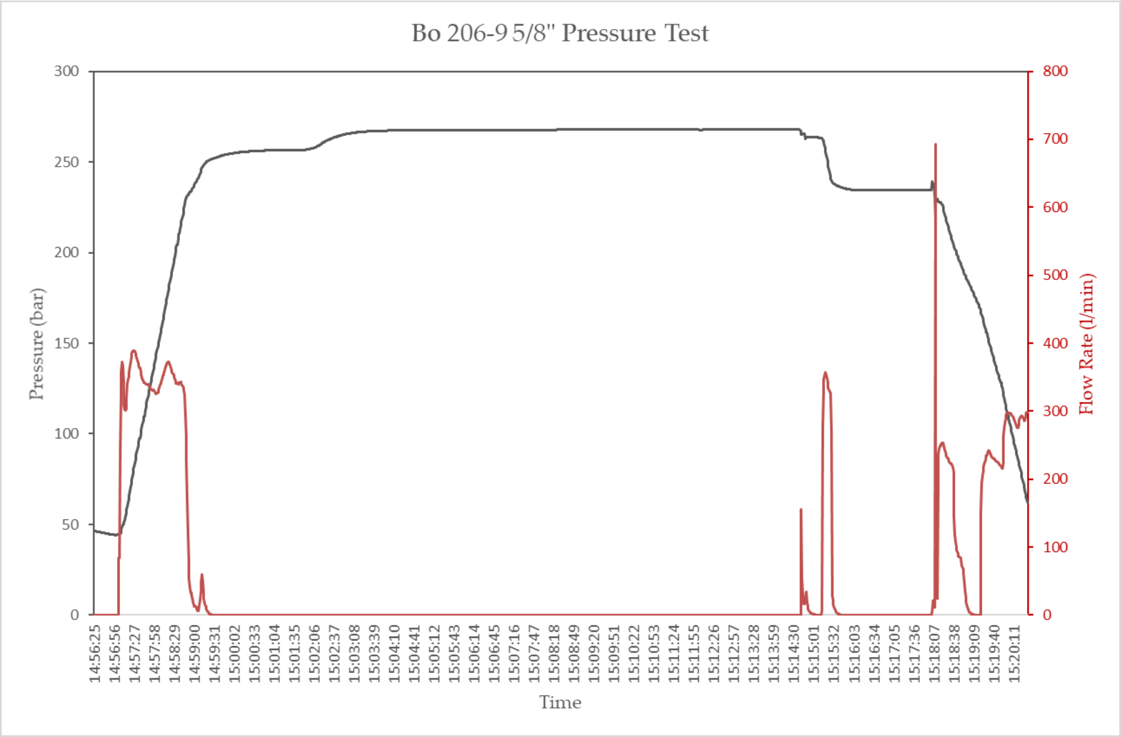

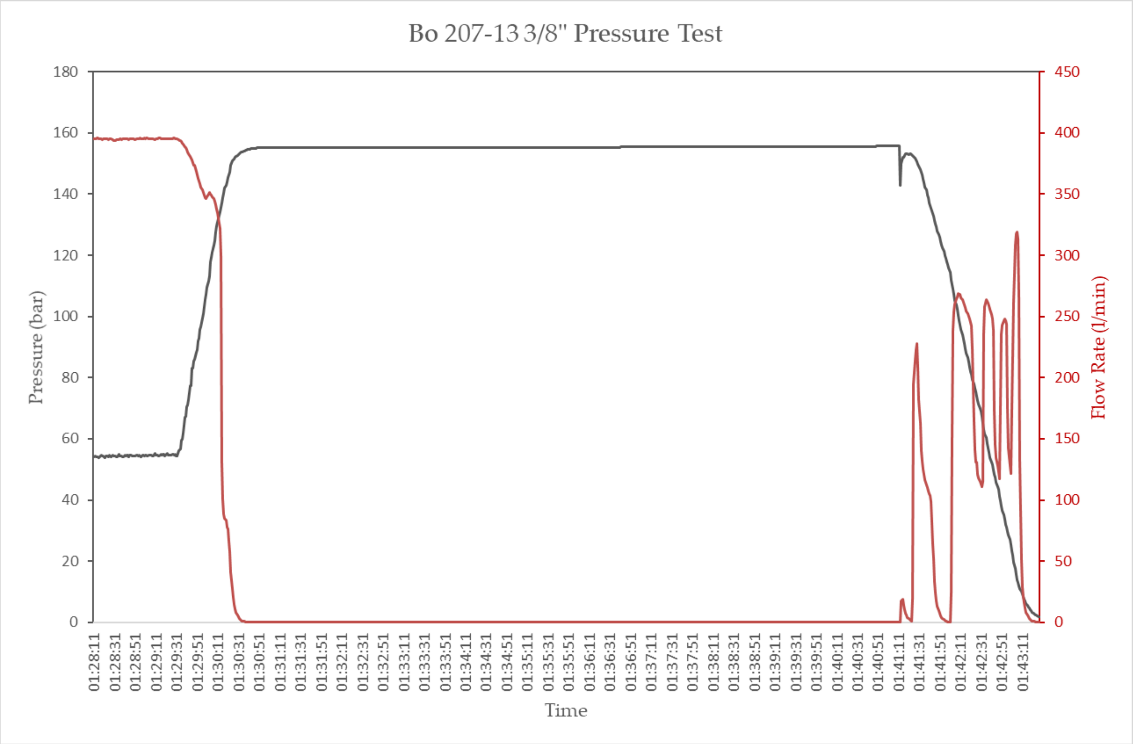
Bo 207-13 3/8" Pressure Test
Pressure (bar)
180
160
140
120
100
80
60
40
20
0
Flow Rate (l/min)
450
400
350
300
250
200
150
100
50
0
Time
01:28:11
01:28:31
01:28:51
01:29:11
01:29:31
01:29:51
01:30:11
01:30:31
01:30:51
01:31:11
01:31:31
01:31:51
01:32:11
01:32:31
01:32:51
01:33:11
01:33:31
01:33:51
01:34:11
01:34:31
01:34:51
01:35:11
01:35:31
01:35:51
01:36:11
01:36:31
01:36:51
01:37:11
01:37:31
01:37:51
01:38:11
01:38:31
01:38:51
01:39:11
01:39:31
01:39:51
01:40:11
01:40:31
01:40:51
01:41:11
01:41:31
01:41:51
01:42:11
01:42:31
01:42:51
01:43:11

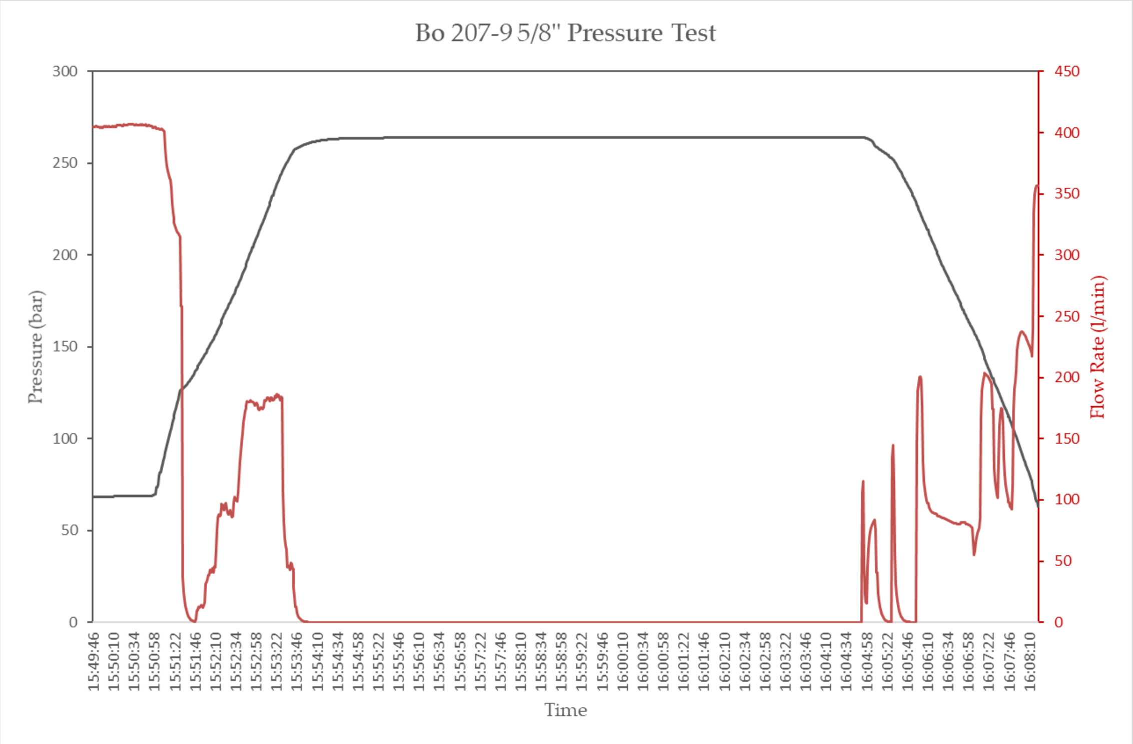
Bo 207-9 5/8" Pressure Test
Pressure (bar)
300
250
200
150
100
50
0
Flow Rate (l/min)
450
400
350
300
250
200
150
100
50
0
Time
15:49:46
15:50:10
15:50:34
15:50:58
15:51:22
15:51:46
15:52:10
15:52:34
15:52:58
15:53:22
15:53:46
15:54:10
15:54:34
15:54:58
15:55:22
15:55:46
15:56:10
15:56:34
15:56:58
15:57:22
15:57:46
15:58:10
15:58:34
15:58:58
15:59:22
15:59:46
16:00:10
16:00:34
16:00:58
16:01:22
16:01:46
16:02:10
16:02:34
16:02:58
16:03:22
16:03:46
16:04:10
16:04:34
16:04:58
16:05:22
16:05:46
16:06:10
16:06:34
16:06:58
16:07:22
16:07:46
16:08:10

Green Cement Pressure Test Data

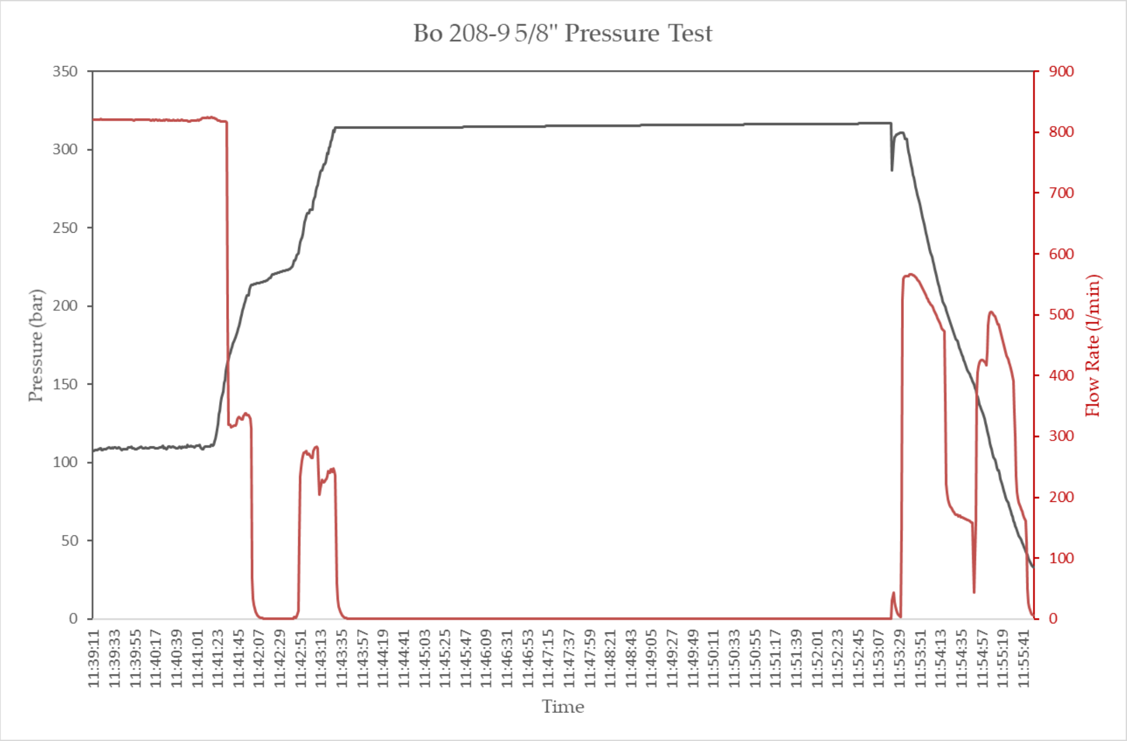

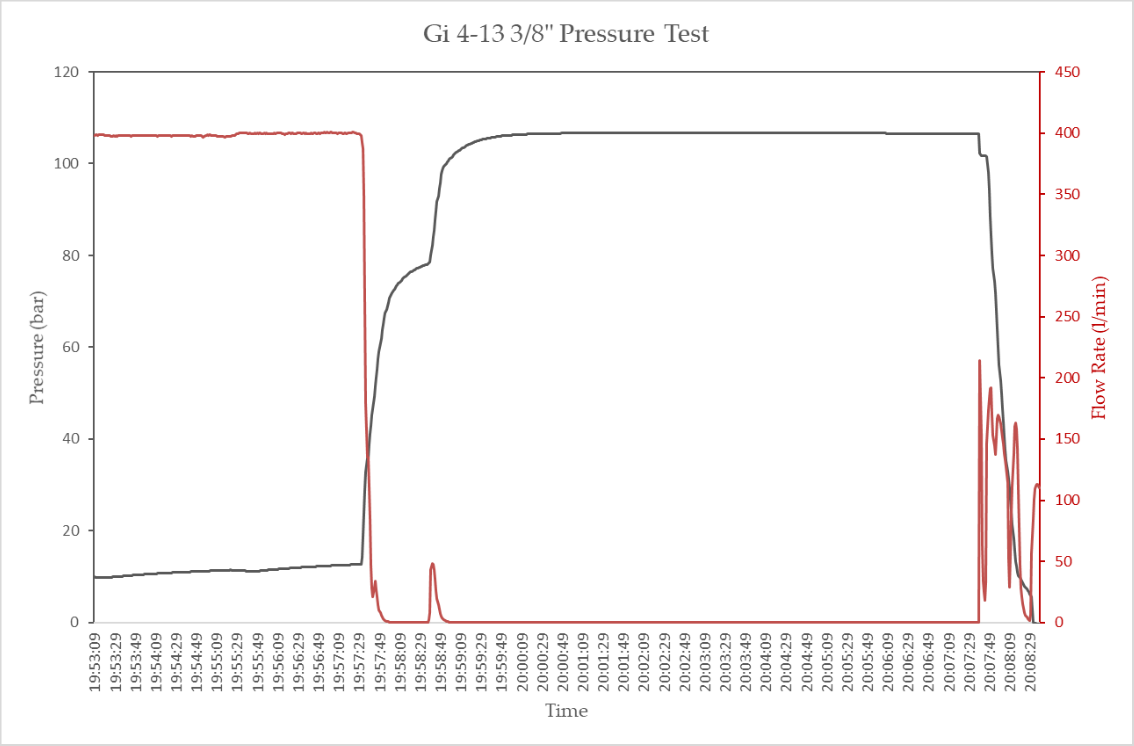

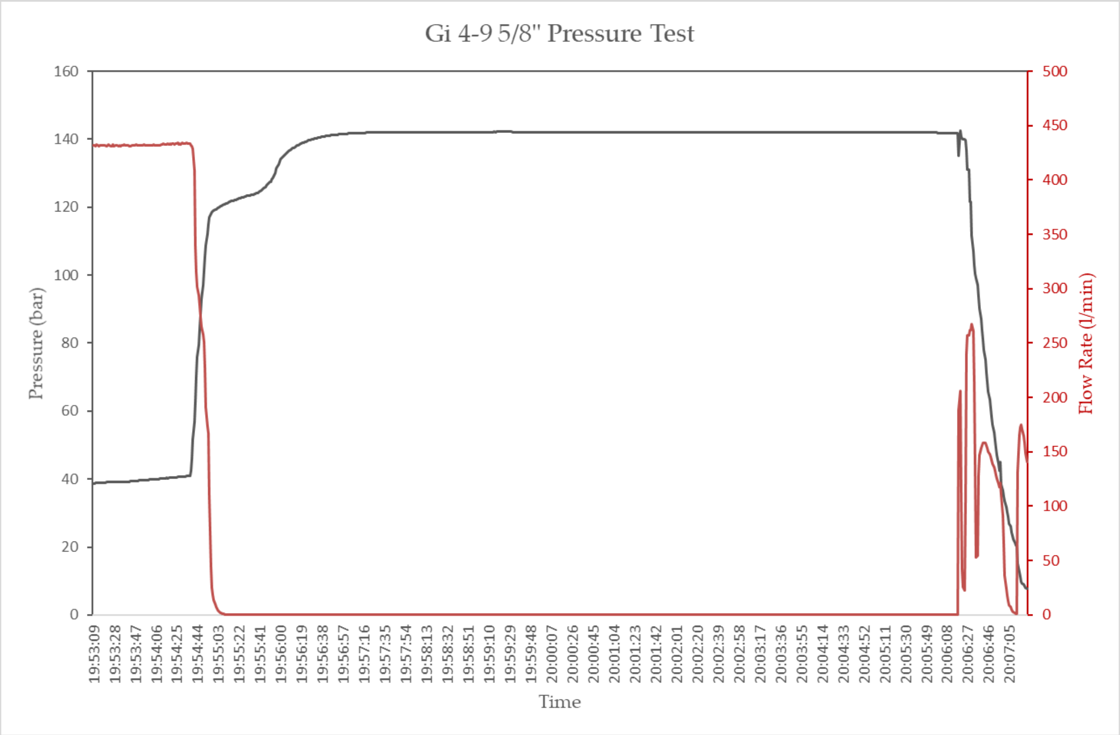
Gi 4-9 5/8" Pressure Test
Pressure (bar)
0
20
40
60
80
100
120
140
160
Flow Rate (l/min)
0
50
100
150
200
250
300
350
400
450
500
Time
19:53:09
19:53:28
19:53:47
19:54:06
19:54:25
19:54:44
19:55:03
19:55:22
19:55:41
19:56:00
19:56:19
19:56:38
19:56:57
19:57:16
19:57:35
19:57:54
19:58:13
19:58:32
19:58:51
19:59:10
19:59:29
19:59:48
20:00:07
20:00:26
20:00:45
20:01:04
20:01:23
20:01:42
20:02:01
20:02:20
20:02:39
20:02:58
20:03:17
20:03:36
20:03:55
20:04:14
20:04:33
20:04:52
20:05:11
20:05:30
20:05:49
20:06:08
20:06:27
20:06:46
20:07:05

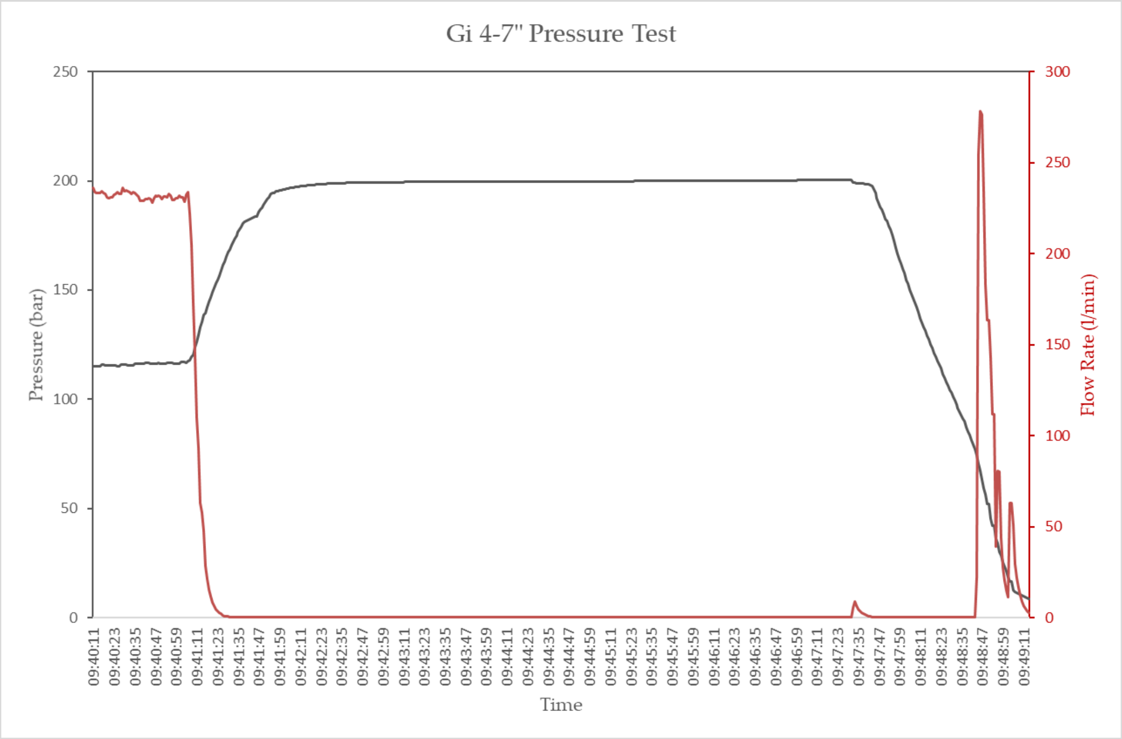
Gi 4-7" Pressure Test
Pressure (bar)
0
50
100
150
200
250
Flow Rate (l/min)
0
50
100
150
200
250
300
Time
09:40:11
09:40:23
09:40:35
09:40:47
09:40:59
09:41:11
09:41:23
09:41:35
09:41:47
09:41:59
09:42:11
09:42:23
09:42:35
09:42:47
09:42:59
09:43:11
09:43:23
09:43:35
09:43:47
09:43:59
09:44:11
09:44:23
09:44:35
09:44:47
09:44:59
09:45:11
09:45:23
09:45:35
09:45:47
09:45:59
09:46:11
09:46:23
09:46:35
09:46:47
09:46:59
09:47:11
09:47:23
09:47:35
09:47:47
09:47:59
09:48:11
09:48:23
09:48:35
09:48:47
09:48:59
09:49:11

Green Cement Pressure Test Data

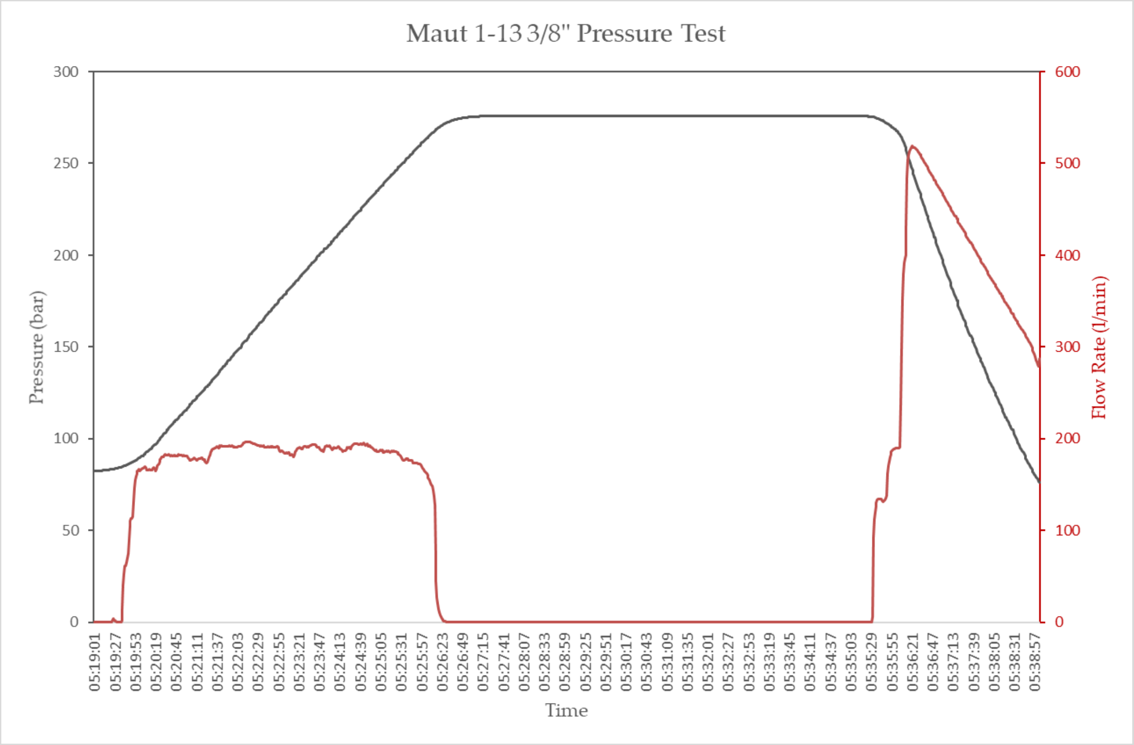

Maut 1-13 3/8" Pressure Test

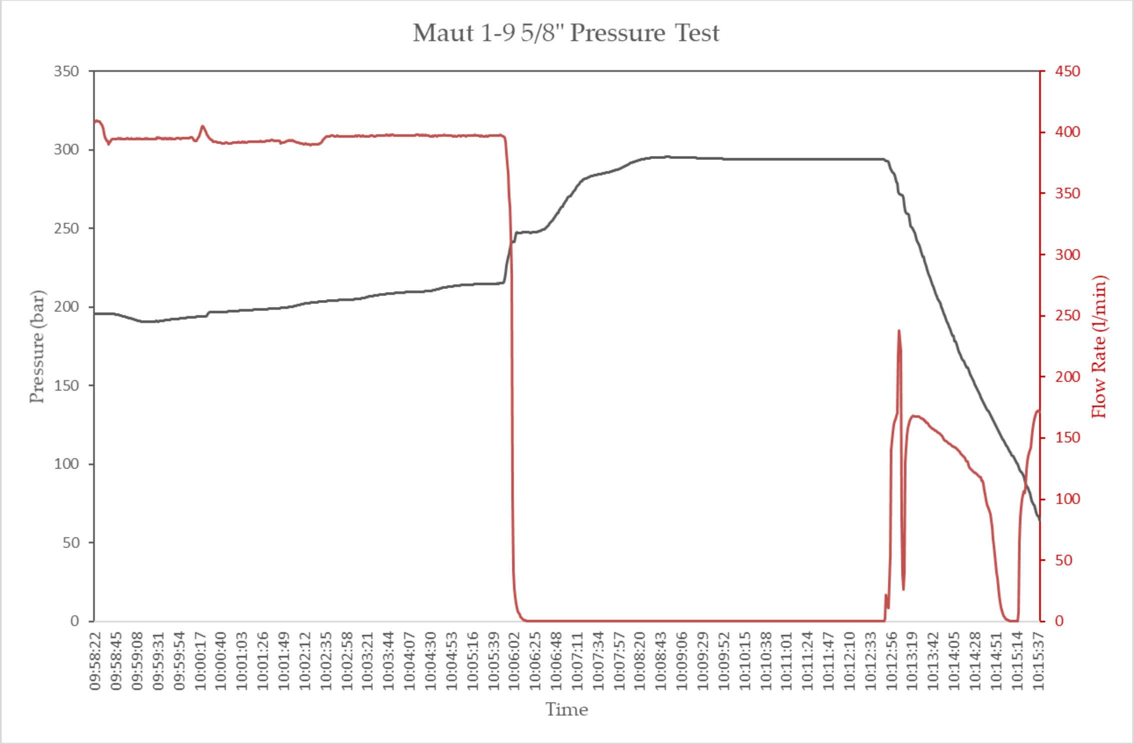

Maut 1-9 5/8" Pressure Test

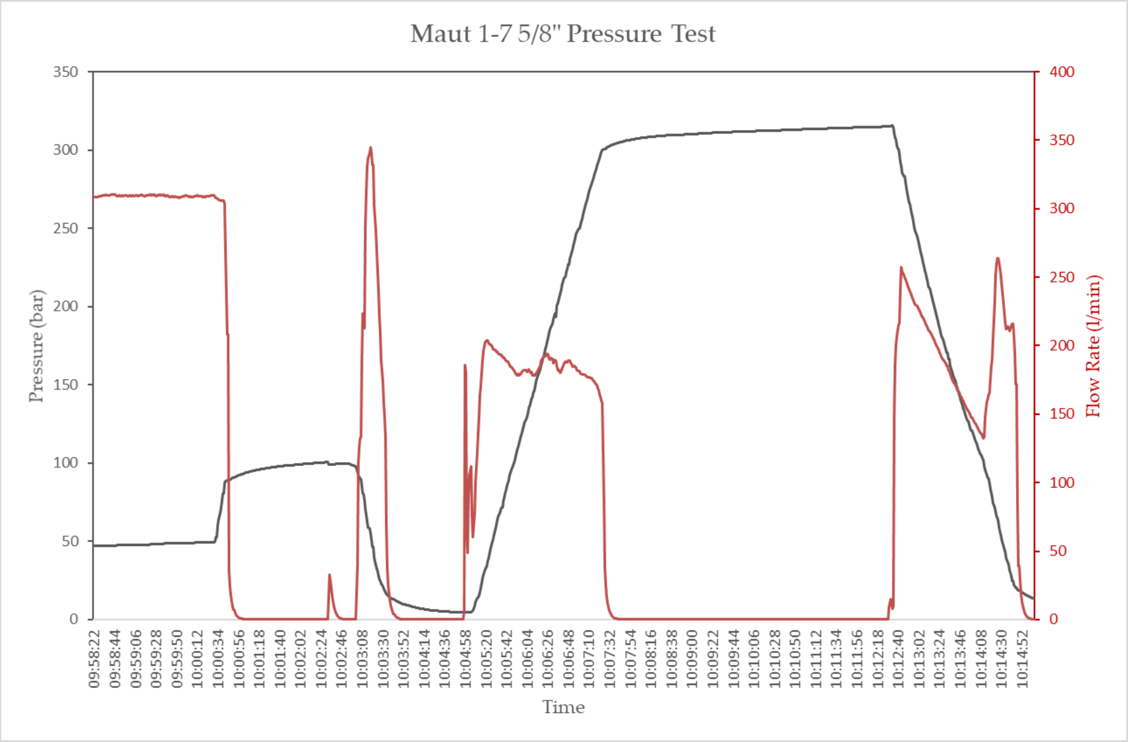
Maut 1-7 5/8" Pressure Test
Pressure (bar)
0
50
100
150
200
250
300
350
Flow Rate (l/min)
0
50
100
150
200
250
300
350
400
Time
09:58:22
09:58:44
09:59:06
09:59:28
09:59:50
10:00:12
10:00:34
10:00:56
10:01:18
10:01:40
10:02:02
10:02:24
10:02:46
10:03:08
10:03:30
10:03:52
10:04:14
10:04:36
10:04:58
10:05:20
10:05:42
10:06:04
10:06:26
10:06:48
10:07:10
10:07:32
10:07:54
10:08:16
10:08:38
10:09:00
10:09:22
10:09:44
10:10:06
10:10:28
10:10:50
10:11:12
10:11:34
10:11:56
10:12:18
10:12:40
10:13:02
10:13:24
10:13:46
10:14:08
10:14:30
10:14:52

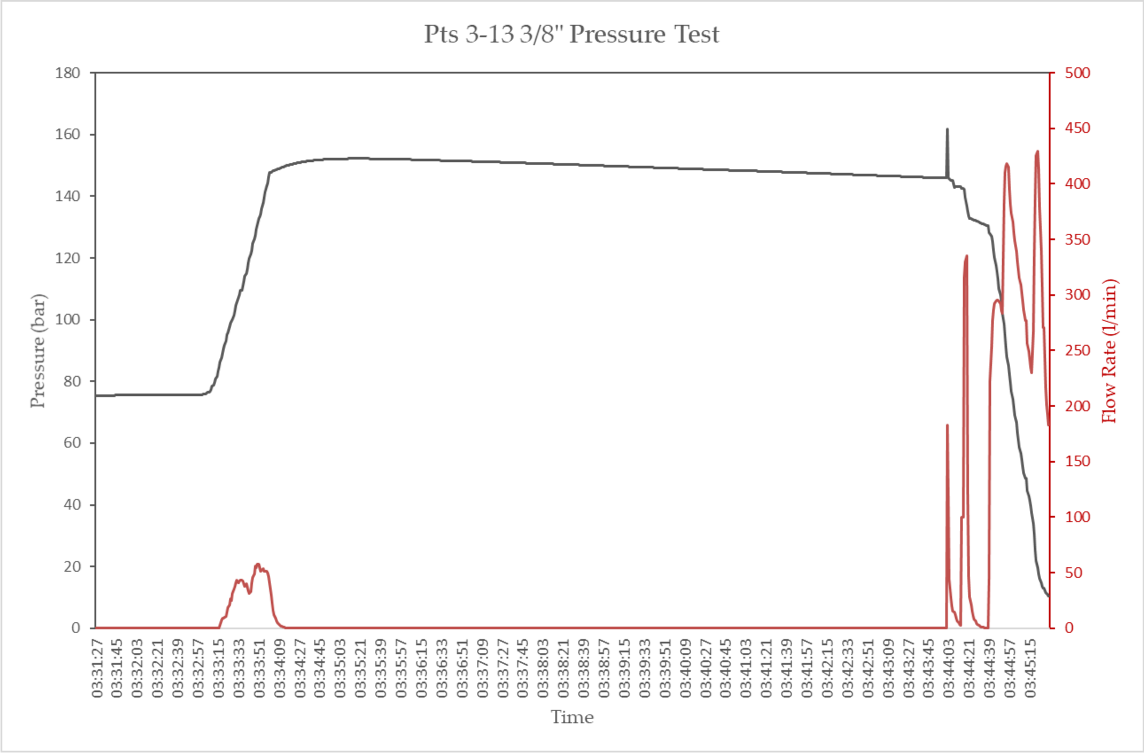
Pts 3-13 3/8" Pressure Test
Pressure (bar)
0
20
40
60
80
100
120
140
160
180
Flow Rate (l/min)
0
50
100
150
200
250
300
350
400
450
500
Time
03:31:27
03:31:45
03:32:03
03:32:21
03:32:39
03:32:57
03:33:15
03:33:33
03:33:51
03:34:09
03:34:27
03:34:45
03:35:03
03:35:21
03:35:39
03:35:57
03:36:15
03:36:33
03:36:51
03:37:09
03:37:27
03:37:45
03:38:03
03:38:21
03:38:39
03:38:57
03:39:15
03:39:33
03:39:51
03:40:09
03:40:27
03:40:45
03:41:03
03:41:21
03:41:39
03:41:57
03:42:15
03:42:33
03:42:51
03:43:09
03:43:27
03:43:45
03:44:03
03:44:21
03:44:39
03:44:57
03:45:15

Green Cement Pressure Test Data

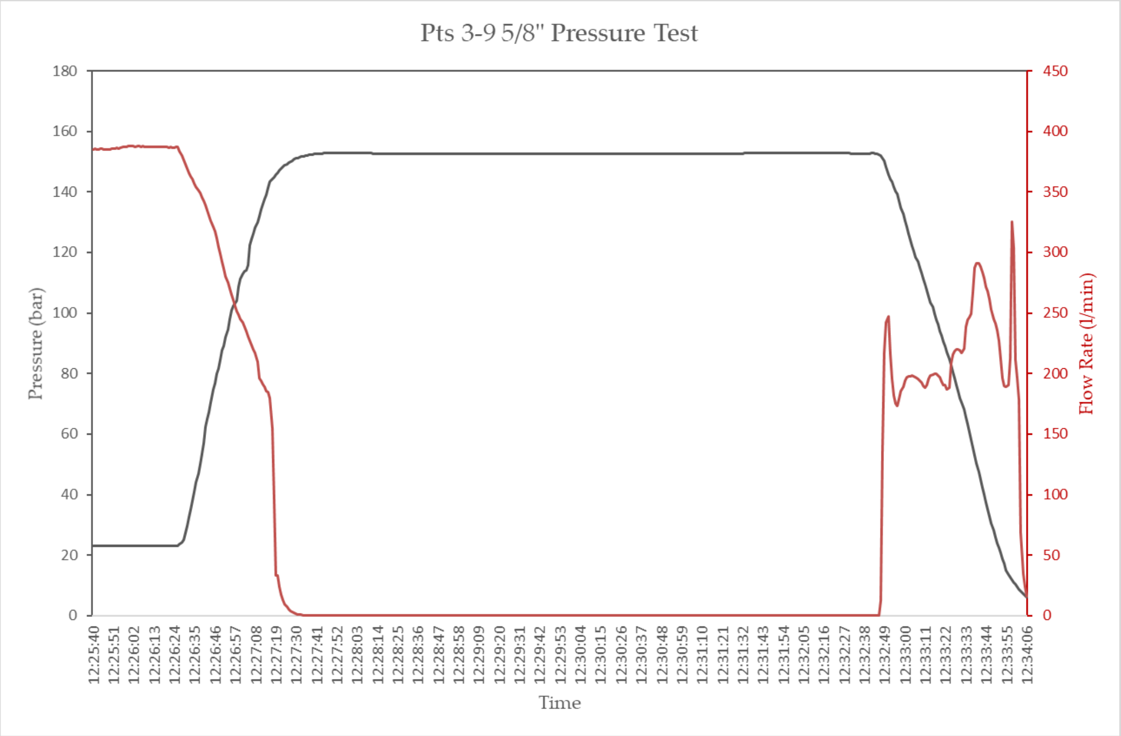

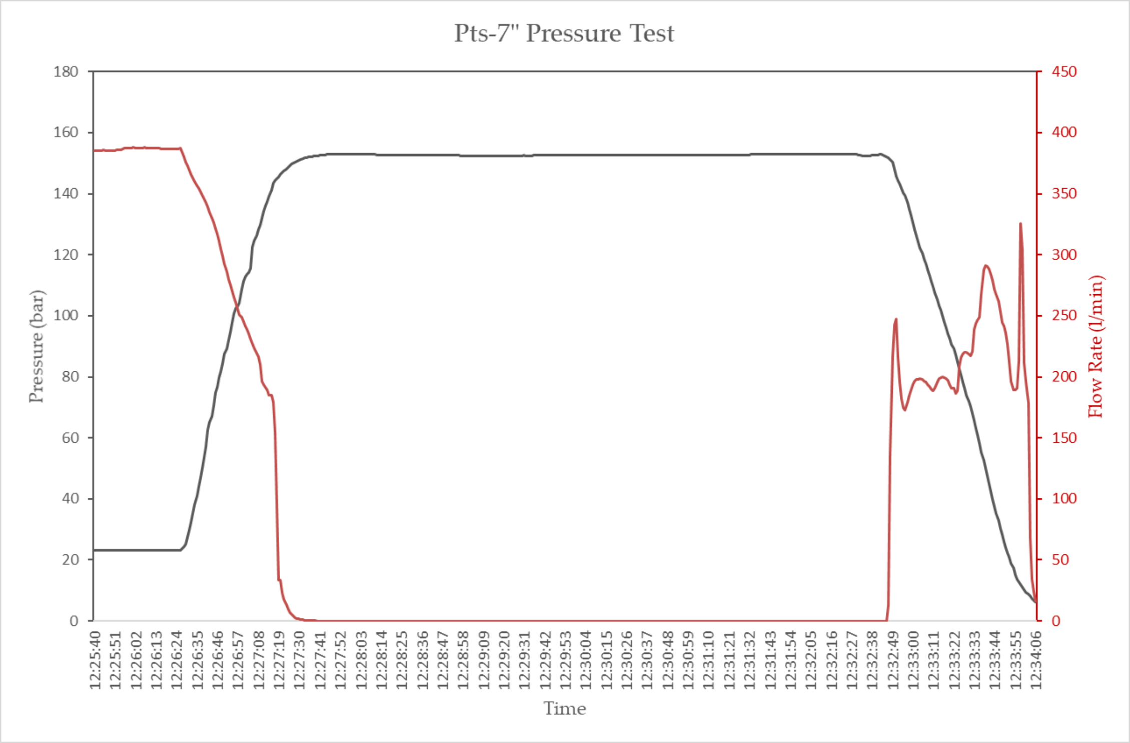

Bibliography

Al-buraik, Khalid, Khalid Al-abdulqader, Saudi Aramco, Riad Bsaibes, and Schlumberger Dowell. 1998. "IADC / SPE 47775 Prevention of Shallow Gas Migration Through Cement."

Avram, C. et al. 1981. *Concrete Strength and Strains*. Amsterdam, Holland: Elsevier Scientific Publishing Co.

Baltes, Andrew, Yu Liang, Darrin Moe, Richard Newman, and Gabrielle Stuckenschneider. 2017. "Post Macondo Negative Pressure Testing for Offshore Drilling." University of Wyoming.

Brechan, Bjorn, Sigbjorn Sangesland, Stein Inge, Dale Ntnu, Christoffer Naaden, and Kjetil Borgersen. 2018. "Well Integrity - Next Developments."

British Petroleum. 2010. "Deepwater Horizon Accident Investigation Report." *Internal BP Report*, 1–192. http://www.bp.com/liveassets/bp_internet/globalbp/globalbp_uk_english/incident_response/STAGING/local_assets/downloads_pdfs/Deepwater_Horizon_Accident_Investigation_Report.pdf.

Crook, Ron, and James Heathman. 1998. "Predicting Potential Gas-Flow Rates to Help Determine the Best Cementing Practices," no. December: 40–43.

Deng, Lu. 2007. "Applications of Fiber Optic Sensors in Civil Engineering" 25 (5).

Drillingcourse.com. 2015. "Cementing Job Types." 2015. http://www.drillingcourse.com/2015/12/cementing-job-types.html.

DrillingForGas.com. 2019. "Inflow Testing Procedure." 2019. http://www.drillingforgas.com/well-control/primary-control/inflow-testing-procedure.html.

Economides, Michael J. 1998. *Petroleum Well Construcion*. Wiley.

Franklin, C M, I P T Global, T L Sargent, Noble Energy, C R Brown, Hamilton Engineering, G W Owen, et al. 2011. "SPE / IADC 140086 Thermally Compensated Leak Detection Results in Significant Blow Out Preventer (BOP) Testing Efficiencies," no. 2004: 1–11.

Global CCS Institute. 2019. "Generic Failure Modes for Well Integrity under Exposure to CO2." 2019. https://hub.globalccsinstitute.com/publications/guideline-risk-management-existing-wells-co2-geological-storage-sites/appendix-b#tbl_011.

Heu, Tieng Soon, Anson Wee, Caroline Combe, Razif Mohd-radzi, Ting-ting Zhang, and Sarawak Shell Berhad. 2018. "Cementing Scorecard and Post-Job Execution Data."

IPT Global. 2019. "Onshore Pressure Testing." Pressure Testing. 2019. https://www.iptglobal.com/solutions/onshore.

Lahann, R. W., J. A. Rupp, and and C. R. Medina. 2016. "State of Stress in the Illinois Basin and Constraints on Inducing Failure." *Indiana Geological Survey*.

Mair, Stephen. 2015. “Inflow (Negative) Testing – Why & How?-ODFJELL Well Services.” 2015. https://blog.odfjellwellservices.com/inflow-negative-testing-why-and-how.

Mason, C J, B P Exploration, D C Chen, Halliburton Sperry, and Drilling Services. 2006. “IADC / SPE 98893 The Wellbore Quality Scorecard (WQS),” 1–14.

MI-Swaco. 2017. “Extended Reach/Horizontal Drilling Solutions.” https://slideplayer.com/slide/7246860/.

Monsberger, Christoph M, and Bernd Moritz. 2018. “In-Situ Assessment of Strain Behaviour inside Tunnel Linings Using Distributed Fibre Optic Sensors” 11 (6): 701–9. https://doi.org/10.1002/geot.201800050.

Moroni, N, K Ravi, T Hemphill, and P Sairam. 2009. “SPE 124726 Pipe Rotation Improves Hole Cleaning and Cement-Slurry Placement : Mathematical Modeling and Field Validation,” no. 1996.

Nelson, Erik; Guillot, Dominique. 2006. *Well Cementing*. Edited by Jennifer Smith. Second. Sugar Land, TX, USA: Schlumberger.

NORSOK D-010. 2004. “Well Integrity in Drilling and Well Operations.” *NORSOK Standard D-010*, no. August: 157.

Office of the Federal Register. 2018. *Code of Federal Regulation-Title 30-Chapter II-Subchapter B-Part 250.423*. US Department of the Interior. https://www.federalregister.gov/documents/2011/10/18/2011-22675/reorganization-of-title-30-bureaus-of-safety-and-environmental-enforcement-and-ocean-energy#sectno-citation- 250.423.

Olivera, Jesús, Margarita González, José Vicente Fuente, Rastislav Varga, Arkady Zhukov, and José Javier Anaya. 2014. “An Embedded Stress Sensor for Concrete SHM Based on Amorphous Ferromagnetic Microwires.” https://doi.org/10.3390/s141119963.

Oort, Eric van, and Richard Vargo. 2007. “SPE / IADC 105193 Improving Formation Strength Tests and Their Interpretation.” *Stress: The International Journal on the Biology of Stress*.

Pegasus Vertex. 2015. “Eccentric Annulus in a Cement Job.” 2015. http://www.pvisoftware.com/blog/tag/casing-standoff/.

Prabhakar, Abhinav, Namkon Lee, Building Technology, Khim Chye, Gary Ong, Minhong Zhang, Juhyuk Moon, Arthur Cheng, and Kian Hau Kong. 2019. “IPTC-19224-MS Enhancing the Gel Transition Time and Right-Angle-Set Property of Oil Well Cement Slurries by Incorporating CSA Cement and Gypsum.”

Prohaska, Michael. 2017. “Well Integrity Definitions.” Leoben. https://wip.dpe.ac.at/docs/knowledge/well-integrity-definitions.pdf.

Ravi, K., M. Bosma, and O. Gastebled. 2007. “Safe and Economic Gas Wells through Cement Design for Life of the Well-SPE 75700.” https://doi.org/10.2118/75700-ms.

Ravi, K, M Fukuzawa, W J Hunter, A Isvan Noerdin, and Star Energy. 2009. “SPE 115638

Advanced Cement Systems Used to Improve Geothermal Well Reliability in Java" 2007.

Ravi, Kris. 2019. "Well Integrity-Class Notes 2019."

Schlumberger Oilfield Glossary. 2018. "Keyseat." In .

———. 2019a. "Non-Newtonian Fluid." In *Schlumberger Oilfield Glossary*. https://www.glossary.oilfield.slb.com/en/Terms/n/non-newtonian_fluid.aspx#.

———. 2019b. "Wiper Plug." 2019. https://www.glossary.oilfield.slb.com/en/Terms/w/wiper_plug.aspx.

Schmid, S.R.; Hamrock, B. J.; Jacobson, B. O. 2014. *Fundamentals of Machine Elements*. *Mechanical Design Engineering Handbook*. https://doi.org/10.1016/B978-0-08-097759-1.00004-6.

Teodoriu, Catalin, T U Clausthal, Ignatius Ugwu, and Jerome Schubert Texas A. 2010. "SPE 131335 Estimation of Casing-Cement-Formation Interaction Using a New Analytical Model."

Zhukov, A., J. González, J.M. Blanco, M. Vazquez, and V Larin. 2004. "Amorphous Magnetic Microwires." In *Encyclopedia of Nanoscience and Nanotechnology*, 365–87. American Scientific Publishers.

List of Figures

Figure 1: Well Integrity must be implemented through the life cycle of a well; Source: (Prohaska 2017) ... 5
Figure 2: Different fluid migration pathways in an abandoned well; Source: (Global CCS Institute 2019) ... 6
Figure 3: Multiple fluid migration paths leading to potential well integrity failure; Source: (Brechan et al. 2018) ... 7
Figure 4: "Boycott" settling of barite and cuttings in an inclined well; Source: (MI-Swaco 2017). 8
Figure 5: Proper drilling fluid removal and mud displacement might be jeopardized by gelled-up, low mobility mud around the filter cake; Source: (Moroni et al. 2009) ... 9
Figure 6: Velocity profile for different casing standoff values. Low standoff leads to a high velocity-wide side, and low velocity-narrow side; Source: (Pegasus Vertex 2015) ... 9
Figure 7: Low casing standoff is increasingly appearing in horizontal wellbores and might lead to missing zonal isolation between zone A and zone B; Source: (Moroni et al. 2009) ... 10
Figure 8: In case of low standoff value and highly gelled up mud, the narrow side of the annulus might remain uncemented, leading to various well integrity issues; Source: (Moroni et al. 2009) ... 10
Figure 9: For non-Newtonian fluids the viscosity decreases with increasing shear rate, resulting in the desired shear thinning behavior; Source: edited after (Schlumberger Oilfield Glossary 2019a) ... 11
Figure 10: Conventional cement slurry with progressive gelation tendency, tested by Halliburton's Celle, Germany-lab, for OMV Austria's Bockfließ-204 13 3/8" lead section cement slurry ... 13
Figure 11: Quick-setting cement, tested by Halliburton's Celle, Germany-lab, for OMV Austria's Bockfließ-204 9 5/8" lead section cement slurry ... 14
Figure 12a & 12b: Potential equipment in an onshore (a) and offshore (b) well construction operation, that can be pressure tested; Source: edited from (IPT Global 2019) ... 18
Figure 13: Typical Shoe Track; Source: (British Petroleum 2010) ... 19
Figure 14: Float Collar Conversion; Source: (British Petroleum 2010) ... 20
Figure 15: Cementing plugs crucial for the Placement of the uncontaminated Slurry; Source: (Schlumberger Oilfield Glossary 2019b) ... 21
Figure 16: Single-Stage Cementing Job Sequences; Source: (Drillingcourse.com 2015) ... 21
Figure 17: "Successful/Passed" Positive-Pressure Test of the 9 7/8 in. X 7 in. production casing of BP's Macondo Well conducted approximately 11 hours before the explosion of Transocean's Deepwater Horizon Platform; Source: edited from (British Petroleum 2010)23
Figure 18: Typical negative-pressure test pressure chart; Source: (Nelson, Erik; Guillot 2006)... 24
Figure 19: FIT and LOT pressure curves; Source: (Lahann, Rupp, and Medina 2016) ... 26
Figure 20: Pressures and stresses acting on a casing during expansion; Source: (Schmid, S.R.; Hamrock, B. J.; Jacobson 2014) ... 31
Figure 21: Radial displacement due to internal pressure marked by maximum internal yield pressure of K55, C90 and P110 casing grades with zero outside pressure ... 32
Figure 22: Volumetric expansion due to internal pressure, marked by yield pressure limits of K55, C90 and P110 casing grades with constant 1000 psi outside pressure ... 33
Figure 23: Volumetric expansion as a percentage of the original volume, marked by yield pressure limits of K55, C90 and P110 casing grades with constant 1000 psi outside pressure ... 33
Figure 24: Key seats and ledges occur when drilling in sequential formations; Source: (Schlumberger Oilfield Glossary 2018) ... 46

Figure 25: The gas flow potential factor represents the severity of gas flow that can be expected from a formation; Source: (Crook and Heathman 1998) 51
Figure 26: Scoring results show the tool's ability to score the well construction processes very accurately, as the worst-performing sections fail their green cement pressure test........ 56
Figure 27: BO-205's 13 3/8" section green cement pressure test fails to deliver a stabilized pressure........ 56
Figure 28: During the green cement test of PTS 3's 13 3/8" section the pressure is dropping by 9 bar........ 57
Figure 29: Average scores for production section (7") are higher than those of surface and intermediate sections........ 57
Figure 30: Casing drilling sections score particularly bad 58
Figure 31: % Variation between expected and actual backflow shows a correlation between a low score and a high backflow variation........ 60
Figure 32: Assumption of channel communication; Source: OMV 62
Figure 33: Schlumberger cement evaluation falsely indicates a completely guaranteed zonal isolation; Source: OMV 62
Figure 34: Tracer experiment proved that there is communication behind the casing; Source: edited from OMV 63
Figure 35: Calliper log shows tight spots; Source: OMV 63
Figure 36: Summary of scores of every well section and the driving factor behind the low score 64
Figure 37: Equipment arrangement during a positive pressure test (green cement pressure test) 65
Figure 38: *Halliburton* Cementing unit used to displace cement and conduct a green cement test 66
Figure 39: A 1-minute contingency after pumps were shut down was used to account for dynamic effects 67
Figure 40: Results show that low scoring well sections have higher negative pressure decline rates, possibly indicating a leak........ 68
Figure 41: Sensor arrangement between the cementing unit and the wellbore 68
Figure 42: Recording unit of the cementing unit 69
Figure 43: Tank/Container, where the backflow is bled-off and measured 69
Figure 44: Hoop and radial stress profile on cylinders with different loading scenarios; Source: (Teodoriu et al. 2010)........ 72
Figure 45: Stresses acting on an infinitesimal cement-sheat element; Source: (Teodoriu et al. 2010)........ 73
Figure 46: Stresses acting on the casing-cement interface; Source: (Teodoriu et al. 2010) 73
Figure 47: Stresses acting on the cement-formation interface; Source: (Teodoriu et al. 2010)........ 74
Figure 48: Tangential stress profile in the cement due to the static pressures in the formation and the internal part of the wellbore 76
Figure 49: Radial stress profile in the cement sheath due to static pressures in the formation and the internal part of the wellbore 77
Figure 50: Tangential stress profile in the cement sheath due to pressures and thermal effects. 78
Figure 51: Radial stress profile in the cement sheath due to pressures and thermal effects........ 78
Figure 52: Front-and cross-sectional view of the test cell design 79
Figure 53: 3D-view of the test cell........ 80
Figure 54: Schematic domain structure of a magnetic microwire and micrograph of the glass-coated microwire; Source: (Olivera et al. 2014) 82
Figure 55: Optical and electronic micrograph of the concrete embedded microwire; Source: (Olivera et al. 2014)........ 82

Figure 56: Structure of strain sensing cables from Solifos AG with (I) strain sensing single mode fiber (Ø 250 µm), (II) multi-layer buffer with strain transfer layer, (III) metal tube, (IV) polyamide protection layer, (V) special steel armouring and (VI) polyamide outer sheath: a) Type V9 (Ø 3.2 mm); b) type V3 (Ø 7.2 mm); Source: (Monsberger and Moritz 2018)..... 84
Figure 57: (a) Internally pressurized, thin-walled cylinder; (b) stresses acting on a small cylinder element; Source: (Schmid, S.R.; Hamrock, B. J.; Jacobson 2014)... 88
Figure 58: Front view of an internally pressurized thin-walled cylinder; Source: (Schmid, S.R.; Hamrock, B. J.; Jacobson 2014).. 88
Figure 59: Cross-sectional view of a cylinder (a), with stresses acting on the element (b); Source: (Schmid, S.R.; Hamrock, B. J.; Jacobson 2014) 89
Figure 60: Cylinder element before and after deformation; Source: (Schmid, S.R.; Hamrock, B. J.; Jacobson 2014)... 90
Figure 61: Radial and circumferential stress behavior for different radii for an internally pressurized, thick-walled cylinder; Source: (Schmid, S.R.; Hamrock, B. J.; Jacobson 2014) 92
Figure 62: Radial and circumferential stress behavior for different radii for an externally pressurized, thick-walled cylinder; Source: (Schmid, S.R.; Hamrock, B. J.; Jacobson 2014) 93

List of Tables

Table 1: Fluid compressibility calculation for the lighter fluid part (water in this case) of a negative pressure test 36
Table 2: Fluid compressibility calculation for the heavier fluid part (Synthetic-oil based mud in this case) of a negative pressure test 37
Table 3: Total fluid compressibility of a negative pressure test 37
Table 4: Fluid compressibility calculation for a green cement test on OMV's Bernhardsthal Süd 10 well 38
Table 5: Thermal expansivity calculation for the Bernhardsthal Süd 10 well 39
Table 6: Calculated versus actual returns 39
Table 7: Scoring ranges define the wellbore quality 44
Table 8: The drilling responses are ranked from most severe to most favorable. The most severe response is determining the total drilling score for the section, high/erratic torque and drag in this case 45
Table 9: The final BHA POOH responses are ranked from severe to favourable. The most severe response is determining the total final BHA POOH-score for the section, tight spots in this case 47
Table 10: The casing running responses are ranked from severe to favourable. The most severe response is determining the total casing running score for the section. In this case, the drag level measured was as expected 48
Table 11: Parameters representing the mechanical/well design factors 50
Table 12: Parameters representing the cement slurry aspects 52
Table 13: Parameters representing the hydraulic/operational aspects 54
Table 14: Parameters representing the casing pressure testing aspects 55
Table 15: Fluid compressibility calculation; for this 3480 psi (240 bar) green cement test, the expected backflow due to the fluid's compression is 1,7 barrels 59
Table 16: The expected expansion due to the fluid's thermal expansion during the green cement test is 0,8 barrels. 59
Table 17: Part list for the test cell 81
Table 18: Criteria for the usage of thin-or thick-walled cylinder analysis 87